TECHNICAL SUPPORT FOR THE HYDROGEN CONTROL REQUIREMENT FOR THE EPRI ADVANCED LIGHT WATER REACTOR REQUIREMENTS DOCUMENT

January 1990

Fauske and Associates, Inc.
Burr Ridge, Illinois 60521

Prepared for EG&G Idaho, Inc.
Under Subcontract No. C85-100740
and the U.S. Department of Energy
Under Contract No. DE-AC07-76ID01570

ABSTRACT

Hydrogen can be a significant contributor to severe accident risk if hydrogen generation and combustion were to lead to containment failure and a resulting high release of fission products. To eliminate hydrogen as a significant risk contributor for advanced light water reactors (ALWRs), the Electric Power Research Institute (EPRI) ALWR Requirements Document has established a hydrogen control requirement as an element of the licensing design basis. This requirement considers hydrogen generation during severe accidents and specifies a design basis level hydrogen generation equal to the amount resulting from oxidation of 75% of the active fuel cladding. Evaluation of experiments and analytical models substantiates the required level as appropriate for ALWR design. In part, hydrogen generation for a range of recovered core-damage sequences is well below 75% MWR equivalent. Required control of the generated hydrogen involves design to accommodate the combustion of hydrogen in the containment and design to limit the hydrogen concentration to 13% hydrogen by volume in dry conditions. It is shown that when combustion is considered at this hydrogen concentration the resulting overpressure is within the capability of large, dry ALWR containment designs. Furthermore, for concentrations up to this limit the potential for detonation in ALWR containments is extremely remote. Finally, representative more severe accidents which progress beyond vessel failure are evaluated to demonstrate that ALWRs designed for 75% and 13% include design features with sufficient margin to mitigate total hydrogen generation (in-vessel and ex-vessel) as required for the risk evaluation basis.

CONTENTS

CONTENTS (Continued)

TABLES

FIGURES

FIGURES (Continued)

ACRONYMS AND ABBREVIATIONS

ADS	Automatic depressurization system
AICC	Adiabatic, isochoric, complete combustion
ALWR	Advanced light water reactor
APWR	Advanced pressurized water
BWR	Boiling water reactor
CCI	Core concrete interaction
DDT	Deflagration to detonation transition
ECCS	Emergency core cooling system
EPRI	Electric Power Research Institute
FLHT	Full-length heat transfer
HDT	Heated detonation tube
IDCOR	Industry Degraded Core Rulemaking Program
IRWST	In-containment refueling water storage tank
LDB	Licensing Design Basis
LOCA	Loss-of-coolant accident
LOFT	Loss-of-Fluid Test
MWR	Metal-water reaction
NTS	Nevada Test Site
PBF	Power Burst Facility
PORV	Power-operated relief valve
PRA	Probabilists risk assessment
PWR	Pressurized water reactor
REB	Risk Evaluation Basis
SBO	Station blackout
SFD	Severe fuel damage
TMI-2	Three Mile Island - Unit 2
VF	Vessel failure
ZND	Zeldovich-Von Neumann-Doring

1.0 INTRODUCTION

1.1 ALWR Hydrogen Control Requirements

The Electric Power Research Institute (EPRI) has formulated a set of design requirements for advanced light water reactors (ALWRs).[1] The EPRI ALWR design requirement for hydrogen control to mitigate severe accidents is presented in Table 1-1. Two parameter values are defined as the basis for this requirement: an amount of hydrogen production equivalent to that generated by oxidizing 75% of the active fuel cladding (commonly stated as 75% metal-water reaction, or 75% MWR) and a hydrogen concentration of less than 13% by volume in dry air within the containment. Maintaining the overall concentration below 13% provides margin to avoid hydrogen detonation, and requiring the accommodation of 75% MWR limits the risk of an overpressure challenge to the containment from a severe accident. The technical basis for selection of these parameter values is the principal subject of this report.

EPRI has established additional, more-detailed performance requirements to ensure that the engineered safety features designed for hydrogen control ensure compliance with the requirement in Table 1.1 and are effective for mitigating severe accidents. These more-detailed requirements address such considerations as the capability of critical equipment to perform its intended function after a hydrogen burn, design to ensure a mixed atmosphere, monitoring of hydrogen concentration, residual hydrogen removal, and analyses of hydrogen generation to be performed by the plant designer (see reference 1, Section 6.5). These more detailed requirements are generally outside the scope of this report except as they affect the acceptability of the 75% and 13% parameters.

1.1.1 Licensing Design Basis

The requirement in Table 1-1 establishes the minimum acceptable capability for hydrogen control to mitigate severe accidents in an ALWR. EPRI has proposed to include this requirement in one of the multiple design

Table 1-1
EPRI ALWR PERFORMANCE REQUIREMENT

2.4.1.7	The plant design shall provide control of hydrogen so as to assure that necessary accident prevention mitigation functions can be performed during and after events in which hydrogen is produced. The approach for control of hydrogen shall assure that the uniformly distributed hydrogen gas concentration in containment does not exceed 13 percent under dry conditions for an amount of hydrogen equivalent to that generated by oxidation of 75 percent of the fuel cladding surrounding the active fuel. This approach includes sizing of containment and combustible gas control systems as appropriate. Analyses shall be completed to assure containment integrity and critical equipment performance under the above conditions.

bases for the ALWR designated as the Licensing Design Basis (LDB). With this designation, the plant design to accommodate 75% hydrogen will involve conservative design practices traditionally applied for licensing requirements. Hydrogen burns, for example, are to be addressed through bounding analyses of an adiabatic burn in order to demonstrate that containment loads are within applicable ASME Code limits as discussed in Section 1.2.1.

EPRI has identified an optimization issue (see Appendix C of reference 1) regarding the suitability of the proposed parameter values for licensing. As noted in the rationale for this mitigation requirement, the 75% MWR value was chosen as "a conservative upper limit on the amount of hydrogen generated in a degraded core situation with recovery." The selection of this value can be viewed as a deterministic process, intended to envelop the range of severe accidents for which the ALWR is designed to achieve recovery and terminate the accident without vessel failure. ALWR designs that meet all of the ALWR requirements will afford margins affecting the generation and accommodation of hydrogen for more severe core damage accidents as well. Such severe accidents are addressed probabilistically in the risk evaluation basis to confirm the acceptability of the overall plant design as discussed in the following section.

1.1.2 Risk Evaluation Basis

The top-level safety design requirements for the ALWR[2] establish multiple design bases to achieve defense-in-depth as illustrated in Figure 1-1. The Risk Evaluation Basis (REB) contributes to assuring the mitigation capability of the ALWR and thus is applicable to hydrogen control. The corresponding requirement for ALWRs is established in Chapter 1 of the Requirements Document[3] under the heading "Public Safety and Plant Protection." This requirement specifies:

> In the event of a severe accident, the dose beyond a half mile radius from the reactor shall not exceed 25 Rem. The expected frequency of occurrence for higher off-site doses shall be less than once per million reactor years, considering both internal and external events.

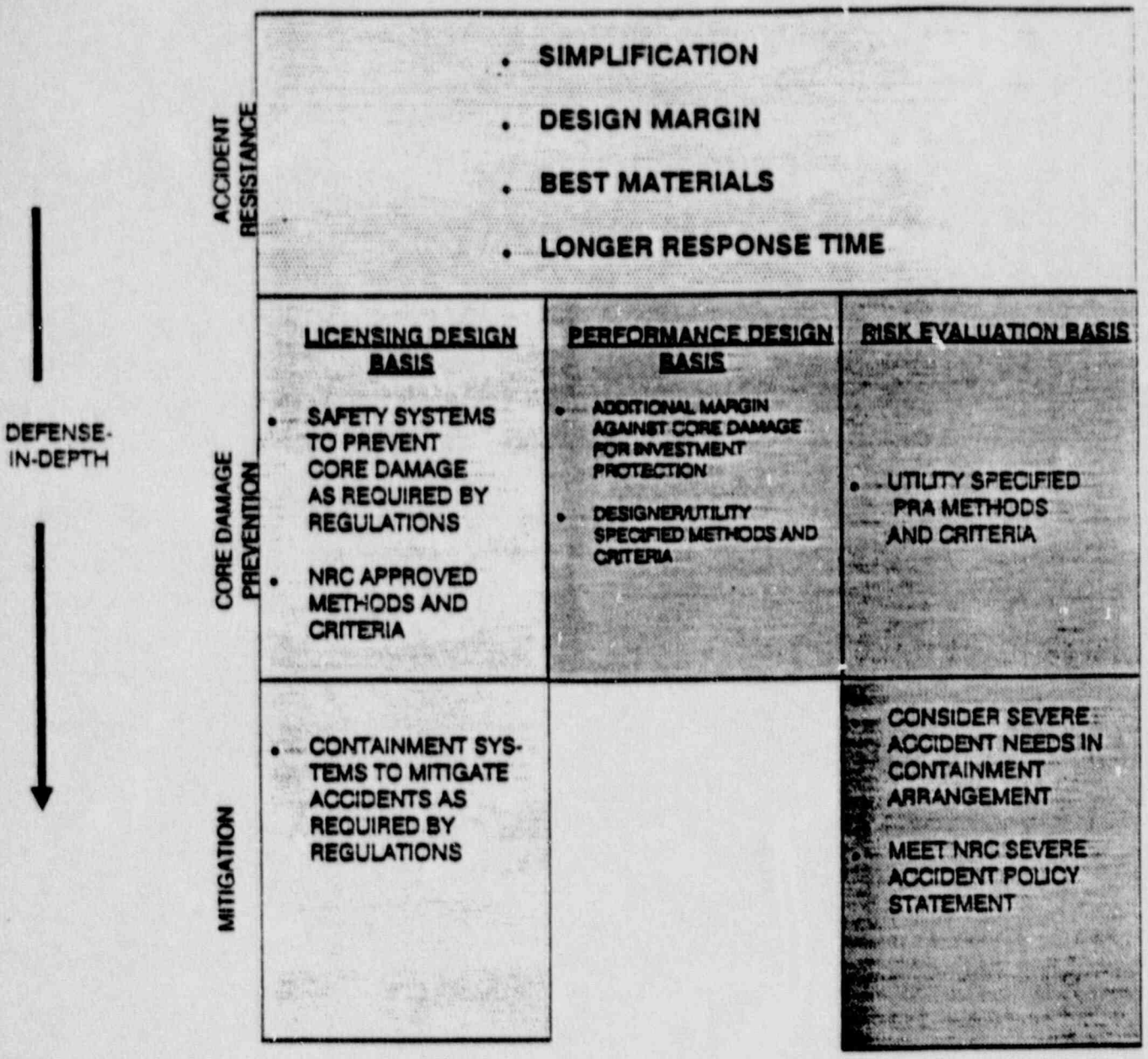

Figure 1-1 ALWR safety with relationship of defense-in-depth and design bases.

In order to meet this requirement, containment failure must be prevented for the risk-relevant sequences (i.e. those sequences potentially contributing to the once-per-million-year cumulative dose at one-half mile). Containment success for these sequences requires the accommodation of expected hydrogen generation, and combustion, considering both in-vessel and ex-vessel phenomena.

ALWR designers are thus required to address severe accidents that are outside the range underlying the licensing design basis (such as sequences without recovery and with vessel failure) but are included in the risk evaluation basis. Both ex-vessel hydrogen generation and the potential for total hydrogen generation in excess of 75% MWR must be included in these analyses for the risk-relevant severe accident sequences in order to demonstrate through best-estimate probabilistic risk assessment that the above requirement is met. These risk evaluation basis analyses are permitted to utilize margins afforded by the more conservative licensing design basis as long as the potential for containment failure is addressed. Thus, containment loads above code allowables but within ultimate capabilities could be acceptable.

This approach differs from the regulatory approach in the CP/ML rule which raised the licensing design basis value to 100% MWR in order to consider "potential accidents that are more severe than those considered in the interim rule [i.e. more severe than 'a class of accidents which produce a large amount of hydrogen but hold promise of being recoverable']."[4] The ALWR approach requires probabilistic treatment of such sequences instead. Each design meeting the full set of ALWR requirements is expected to include design features that ensure acceptable hydrogen mitigation capability for the risk-relevant sequences and to confirm that capability through the required analyses.

1.2 ALWR Approach to Satisfy Requirements

The EPRI Requirements Document envisions two fundamentally different approaches to satisfying the hydrogen control requirement (see reference 1,

Appendix B). Containments for advanced pressurized water reactors (APWRs) are expected to be large dry containments with sufficient volume, mixing, and pressure-retaining capacity to permit the hydrogen that is generated to accumulate and possibly burn without global detonation or containment failure. Containments for advanced boiling water reactors are expected to be too small to accommodate 75% MWR hydrogen generation without exceeding the 13% concentration limits. For these containments, igniters are the preferred means of hydrogen control for simplicity, but inerting is an alternative approach. The balance of this report emphasizes the technical basis for providing hydrogen control via large dry containment designs for APWRs.

1.2.1 Licensing Design Basis

To demonstrate that APWRs satisfy the LDB requirement for hydrogen control, it must be shown that the selected parameter values are appropriate and that an APWR whose design is based on these parameters will accommodate hydrogen generation and combustion both at the design limit and for representative severe accident sequences with in-vessel recovery.

Hydrogen generation (all in-vessel for these recovery sequences) is addressed first (see Section 2.1 below). The available experimental evidence is reviewed to confirm that 75% MWR is an appropriate upper limit on hydrogen generation for recovered severe accident sequences provided that differences between test and prototypical reactor conditions are taken into account (Section 2.1.3). Analyses are then performed for a specific APWR representative of an APWR designed to the EPRI requirements. The analyzed design includes such ALWR features as a representative core design and zirconium content, an in-containment refueling water storage tank (IRWST), core flood tanks, a safety-grade depressurization system with corresponding procedures for its utilization in severe accidents, and a containment sized to meet applicable requirements. These analyses (Section 2.1.4) demonstrate that hydrogen generation is less than 75% for actual LDB event sequences.

The information in Section 2.1 is sufficient to demonstrate the generic suitability of the 75% MWR parameter value as the licensing design basis for

LWRs. Specific designs should be analyzed for LDB hydrogen generation by their designers (EPRI requirement 6.5.2.7, see reference 1) and these results should be considered in certification review. While hydrogen generation in excess of 75% is not expected for any such ALWR design, a design found to be subject to atypically large hydrogen generation would require plant specific design features or administrative controls to establish acceptable hydrogen control. For example, design refinements to control reflood rates and timing might be pursued until the LDB limit could be shown to envelop the design recovery sequences. Mitigation improvements, if required, would be developed without compromising prevention capabilities.

Hydrogen deflagration must then be addressed (Section 2.2) in order to demonstrate that a specific design accommodates deflagrations that may occur, up to the limiting case for rapid burning of 75%-MWR-equivalent hydrogen generation. Applicable limits for the ALWR include containment loads within ASME Service Level C.[5] Section 2.2 provides an evaluation of experimental data on combustion followed by a generic, idealized analysis of containment pressurization from deflagration with a 13% hydrogen concentration in dry air to demonstrate that ALWR containments will meet these limits. Plant specific analyses are necessary to demonstrate that bounding case deflagration is acceptable for each ALWR. It is expected, based on the generic evaluation, that these requirements will not be limiting in the determination of required containment size and strength.

Finally, experimental evidence and analyses are provided (Section 2.4) to demonstrate that the 13% parameter value ensures that the potential for a detonation which could threaten containment integrity is remote for an ALWR. Plant specific analyses will demonstrate that the 13% limit is met for each ALWR design considering mixing, etc.

1.2.2 Risk Evaluation Basis

The evaluation of hydrogen control provisions for event sequences more severe than the recovery sequences underlying the licensing design basis begins with the identification and modelling of the potential sources of

additional hydrogen generation as an accident progresses. The REB analyses are to be performed (see Reference 2) using the applicant's best-estimate models that have been selected for use in the required probabilistic risk assessment (PRA). The potential sources of additional hydrogen generation include zirconium oxidation during: the final stage of the in-vessel core melt progression, co-dispersal of debris and water from the vessel, core-concrete interaction that may occur in the cavity, debris falling in a steam environment, and quenching of either the initial melt or subsequent molten material. Oxidation of other metals must be considered, whenever the contribution is potentially significant.

Best-estimate modelling must also consider the potential for combustion that might limit the amount of hydrogen present in the containment at any given time. Combustion modelling requires the identification of ignition sources (e.g. operating electrical equipment, hot debris, or local igniters) and the evaluation of the surrounding atmosphere for flammability based on the content of hydrogen, oxygen, steam, other combustible gasses, etc.

The analyses are carried out until a bound on the quantity of hydrogen that may be present in the containment at any given time can be established. Such a bound requires consideration of the available zirconium inventory (typically zirconium is used for structures other than active cladding that may be involved in a severe accident), but credit is taken for zirconium that reaches a permanently coolable configuration while in an unoxidized state. Any burned hydrogen can also be credited. The design capability to accommodate the bounding quantity must then be addressed. If accommodation can not be demonstrated (through means that are discussed below), then containment failure must be modelled and the resulting consequences included in the evaluation of the capability of the design to meet the REB risk goal in Section 1.1.2. If the goal is not met, design refinements that would resolve the risk outliers are to be considered by the designer.

Accommodation of the bounding hydrogen generation, including both in-vessel and ex-vessel sources, is covered by the licensing design basis for

sequences that never exceed 75% MWR equivalent. Should risk-relevant sequences result in hydrogen generation above 75%, additional evaluations for pressurization, deflagration, and detonation as challenges to containment are required. Such evaluations may utilize certain margins in the original design. For example, the containment size may be above the minimum required (as it is for the Combustion Engineering's System 80+), loads may exceed Service Level C yet it may still be possible to preclude failure, or the minimum steam content may adequately limit the risk of detonation even though the hydrogen present would exceed a 13% concentration in dry air.

An REB evaluation for one particular ALWR design is provided in Section 3 to illustrate this process. For the case studied however, total hydrogen generation never exceeded 75% and thus the design's marginal capability to accommodate additional hydrogen generation while assuring containment integrity did not require a separate evaluation for the severe accident sequences considered. Each ALWR would provide its own evaluation for conditions of hydrogen generation above 75% should such cases arise as part of a plant-specific PRA.

2. LICENSING DESIGN BASIS TECHNICAL EVALUATION

Technical evaluation for the Licensing Design Basis (LDB) for the EPRI ALWR hydrogen requirement is discussed here in three subsections. Cases considered within the LDB are those accidents which are recoverable by design with the reactor vessel intact; accomodation of the required 75% MWR hydrogen generation is also addressed. Any sequence more severe than those underlying the licensing design basis, including those which progress to reactor vessel failure, are considered in the Risk Evaluation Basis in Section 3.

2.1 In-Vessel Hydrogen Generation Evaluation

2.1.1 Introduction

The purpose of this section is to demonstrate that the source of hydrogen will not exceed 75% MWR for a credible in-vessel recoverable accident for a plant designed to the ALWR requirements and subject to appropriate emergency operating procedures. The basic phenomena of in-vessel hydrogen generation are treated in section 2.1.2. Evidence of these phenomena is provided by the experimental database for core melt progression and hydrogen generation presented in section 2.1.3. Models which incorporate the understanding of these phenomena are discussed in section 2.1.4 and are used to provide an evaluation of hydrogen generation for ALWR cases. Results of this evaluation confirm that the EPRI ALWR hydrogen requirement of 75% envelops core damage events with recovery for ALWRs.

2.1.2 Hydrogen Generation by Zirconium Oxidation

Hydrogen is generated during a severe accident primarily through the in-vessel process of zirconium oxidation by steam from overheated coolant and through the ex-vessel processes of zirconium oxidation which may be by steam from concrete

decomposition. Only the in-vessel source of hydrogen need be considered in licensing design basis evaluation since it focuses on in-vessel recoverable sequences. The kinetics of the zircaloy cladding-steam reaction have been extensively studied[6,7] and there is good agreement upon the appropriate equations. A parabolic rate law is used, characteristic of a solid-state diffusion limitation in the oxidized material; with such a law, the oxidation rate varies inversely with the square root of time. In addition, there is a rapid increase in the rate at the cubic-tetragonal phase transition of the oxide which occurs at 1580°C.

In ALWR designs, oxidation of cladding is not only limited by the rate of the process, but also by the local availability of steam and the local deformation of core geometry. Oxidation of zirconium is highly exothermic, and because the rate increases with temperature, it is a positive-feedback process. During oxidation of cladding, local energy deposition rates from the chemical reaction can exceed decay power by more than an order of magnitude. This tremendous power input can lead rather quickly to melting of core material with the implication that this molten debris progresses to lower regions of the core. This melting-slumping process has several mitigating effects on the oxidation rate. First, solid state diffusion of oxygen and hydrogen in core regions containing relocated material must take place over longer distances than in intact regions. Second, the cladding plus fuel surface to volume ratio decreases, lowering the surface area for the reaction. Third, the gas natural circulation flow is impeded by increasingly restricted geometry, reducing the local supply of oxidant (steam). Finally, a region of the core may become completely blocked by molten and refrozen material, diverting steam to other regions and effectively cutting off the oxidant supply to some core regions.

Consequently, core thermal-hydraulics and the core melt process tend to control hydrogen generation. For direct applicability to reactor conditions, experiments must match the prototypical boundary conditions and geometry as closely as possible to account for these effects. Models must mechanistically account for the mechanisms which restrict and redistribute

the supply of steam in order to correctly reproduce experimental data and extrapolate to the prototypical ALWR case.

As defined in Section 1, in-vessel hydrogen generation is quantified throughout this report in terms of an effective fraction of active fuel cladding reacted, or percent metal-water reaction (% MWR). This definition is used for consistency with existing hydrogen generation terminology. The corresponding models recognize that zircaloy and other metals outside the active fuel cladding region may oxidize as well, but total hydrogen production is normalized according to this definition.

2.1.3 Experimental Basis for 75% MWR Upper Limit

2.1.3.1 Hydrogen Generation During the Severe Fuel Damage Tests A series of in-pile tests were conducted at the Power Burst Facility (PBF) to examine LWR fuel assembly behavior under high temperature and limited steam flow conditions.[8,9,10,11] These severe fuel damage (SFD) tests involved substantial hydrogen generation and fuel damage, and are useful for both understanding phenomena and benchmarking. All of these tests were performed with 32 fuel rods (a 6 x 6 array with corners removed) of 0.91 m active length and guide tubes placed in an isolated shroud with a zircaloy liner. Water flow outside the shroud provided a heat sink for the test bundle and prevented damage to the rest of the in-pile test apparatus. A nearly constant inlet water flow of 0.6 g/sec was maintained by a positive displacement pump. The scoping test, SFD-ST, used a higher steam supply rate and was steam-rich, while the subsequent tests were steam starved.

The procedure in all of the tests was similar. Water in the test bundle was boiled down to an elevation between 0.2 and 0.25 m, and nuclear power was ramped up to about 35 kW and held constant for about 4 minutes. Cladding temperatures in excess of 2200°K were obtained during this period. Tests were terminated by lowering the power to decay levels, and flushing the assembly with argon to purge and cool it. Test SFD-ST was cooled by a water reflood.

In test SFD 1-1, 64 ∓ 7 grams of hydrogen were measured, corresponding to an equivalent of about 27% MWR. In test SFD 1-3, 59 ∓ 30 grams were measured, or about 22% MWR, and in test SFD 1-4 86 ∓ 12 grams or 32% MWR was measured. (These particular oxidation percentages are based on the total zircaloy mass of the active fuel cladding and inner shroud liner. Oxidation of material outside the test bundle bounders cannot be ruled out.) In test SFD-ST, which was steam-rich, 190 ∓ 40 grams or 79% MWR was measured based on post-irradiation examination of the zircaloy (additional oxidation of fuel occurred). Differences between the tests can be attributed to the amount of steam available and differences in absolute power level, test duration, and initial conditions.

The SFD tests served to confirm in an integral sense the current understanding of core heatup, melt progression, and hydrogen generation.

2.1.3.2 Hydrogen Generation During the Three Mile Island - Unit 2 Accident The events which occurred during the Three Mile Island Unit 2 (TMI-2) Accident in March, 1979 progressed to the point of core degradation and substantial hydrogen production.[12,13,14] The circumstances of the accident need not be repeated here aside from a brief account of the availability of coolant. Briefly, about 73 minutes from the start of the accident, with the pressurizer relief valve stuck open, the A loop main coolant pumps were shut off, and at about 100 minutes the B loop pumps were shut off, allowing the core to slowly boil away coolant leading to partial core uncovery and heat up. At about 140 minutes, the pressurizer relief block valve was closed, allowing the system to pressurize. At about 174 minutes (2.9 hours) the main coolant pump 2B was restarted and then shut off, reflooding the core temporarily. This undoubtedly caused a large amount of hydrogen production. At about 203 minutes, high-pressure water injection was initiated, resulting in a complete submergence of the core. At about 225 minutes, a failure in crust that surrounded a large volume of still-molten material in the lower core region resulted in relocation of about 20-30 tones of molten material into the core bypass region and the lower head. Between 110 minutes and 174 minutes some makeup flow was also available which is hypothesized to have had an impact on hydrogen production.

Analyses of this accident, considering a combination of recorded plant data and modeling, have concluded that about 450 kg of hydrogen were produced, corresponding to 50% MWR.[15] Further analysis has lead to the hypothesis that most of this hydrogen was generated during and after the 2B pump restart.[16] Hypotheses aside, TMI-2 provides an example of an accident with a substantial amount of steam available for conversion to hydrogen and gross core damage, and yet significantly less hydrogen was produced than the limit established in the EPRI ALWR requirement.

2.1.3.3 The LOFT LP-FP-2 Test On July 9, 1985, the Loss-of-fluid Test (LOFT) Facility was used for its last test, which involved severe fuel damage to the central test bundle of the core.[17]

The LOFT LP-FP-2 experiment simulated a containment bypass accident, known as a V sequence. A single intact loop with one steam generator and two parallel coolant pumps was connected to the reactor vessel, and the bypass break was located in a separate hot leg. A single 11 x 11 fuel bundle with 100 fuel rods and 21 control and guide tubes was subjected to the transient. The test began with scram, shutdown of the coolant pumps, and opening of a break in the single loop. The bypass break was opened when high quality two-phase flow was expected. System pressure was reduced by cycling the loop break and the power-operated relief valve (PORV). The experiment was terminated by closing the breaks and reflooding the core.

High temperatures, hydrogen generation, and fuel melting were observed. Details of the results will be presented later as part of model validation, Section 2.1.4.1. The essential result is that the majority of the hydrogen is believed to have been generated during reflood.

2.1.3.4 Summary of Hydrogen Generation Database A summary of the experimental database for melt progression and hydrogen generation is presented in Table 2-1. Cases with and without reflood appear in the table. Clearly those cases with reflood exhibit greater cladding oxidation. The

Table 2-1. HYDROGEN GENERATION:
EXPERIMENTAL DATABASE SUMMARY

Test	% Zr Oxidized	Reflood	Reference	Reactor Prototypicality
SFD-ST	79%	Yes	8	Partial (3)
SFD 1-1	27%	Yes/Slowly	9	Partial (3)
SFD 1-3	22%	No	10	Partial (3)
SFD 1-4	32%	No	11	Partial (3)
LOFT LP-FP-2	58%	Yes	17	Partial (3)
TMI-2	50%	Yes	15	Yes
NRU-FLHT-1	5% (1)	No (2)	18	Partial
NRU-FLHT-2	15% (1)	No (2)	18	Partial
NRU-FLHT-4	75% (1)	No (2)	18	Partial (4)
NRU-FLHT-5	100% (1)	No (2)	18	Partial (4)

∴ Experiments with reflood show range of 27-79% MWR
Experiments without reflood show range of 5-100% MWR

(1) Degree of zirconium oxidation directly related to test duration.
(2) No reflood but continuous water flow per experimental procedure to produce high chemical heat rate.
(3) Positive displacement pump sustained high steam flow even with distorted geometry.
(4) High radial heat loss relative to test power and chemical energy suppressed relocation and thus sustained oxidation.

amount of oxidation depends on many factors such as test duration, water injection rate, boundary conditions, etc.

The amount of oxidation and hydrogen production in these experiments does not directly support or contradict the EPRI ALWR requirement. Such conclusions can only be reached by careful and critical analysis of the experiments and model application to a prototypical reactor case.

For example, in the SFD tests (and typical of similarly small-scale integral fuel damage experiments) the zirconium oxidation power was a low fraction of the total test bundle power and the radial heat loss was a large fraction of that power. In the full-length heat transfer (FLHT) tests, heat losses were large and limited the maximum temperature of the test bundle so that substantial oxidation could occur without relocation.[18] In anticipated reactor cases, the zirconium power dominates decay power and radial losses (except in peripheral core nodes) are relatively small. Therefore, the melt progression and hydrogen production in experiments is not directly representative of a reactor. Furthermore, these factors indicate that more oxidation can occur in such experiments than in a reactor because of the lower heatup rate and consequently delayed geometric deformation.

2.1.4 Analytical Basis for 75% MWR Upper Limit

The ALWR requirement for hydrogen generation is supported analytically by computer simulation of core meltdown accidents with models which have been benchmarked against experimental data. Application of these models has consistently shown the difficulty in achieving a hydrogen source corresponding to the ALWR limit equivalent to 75% MWR. The MAAP severe accident integrated analysis code [19,20,21] has been employed in modeling the accident at TMI-2,[20,21], LOFT LP-FP-2,[20,21] and the SFD tests[22]. Results of these applications are briefly presented below.

2.1.4.1 Model Validation Prediction of hydrogen production for TMI-2 is restricted currently to the time period before the 2B main coolant pump restart, which reflooded the core. Based upon numerous estimates, as much as 450 kg of hydrogen were produced during the entire sequence, with about 350 kg in the containment at the time of the burn (about 10 hours into the accident) and 100 kg remaining in the reactor vessel (see Reference 15). This corresponds to just under 50% MWR.

The MAAP-DOE prediction for hydrogen generation prior to 174 minutes is 382 kg[20]. This is believed to be an overestimate because of the reflood contribution to total hydrogen. The MAAP-DOE prediction for reflood is 180 kg[21], leading to a total of 562 kg hydrogen, which is probably an overestimate of the total hydrogen production.

The TMI-2 data is being used in an international standard problem exercise for severe accident codes. Figure 2-1 represents the results presented for several severe accident codes[23] for the first 174 minutes of the TMI-2 event. The MAAP-DOE result is conservative since it appears to overpredict hydrogen generation during the core melt progression stage of the event.

This interpretation of TMI leads to two conclusions regarding extrapolation to other accidents. First, less hydrogen can be produced under realistic assumptions for a case with no recovery than for a case with core reflood. Second, the TMI case provides one reasonable estimate of expectations during recovery sequences. In any event, the ALWR requirement of 75% lies above the 50% oxidation credited at TMI.

Comparisons of MAAP have been made with the LOFT LP-FP-2 experiment.[20, 21] MAAP-DOE was used to simulate the experiment in two steps, prior to reflood and during reflood. This allowed independent testing of the melt progression and core recovery models. 340 grams of hydrogen were predicted during the core heatup, and 210 grams of hydrogen were predicted during the

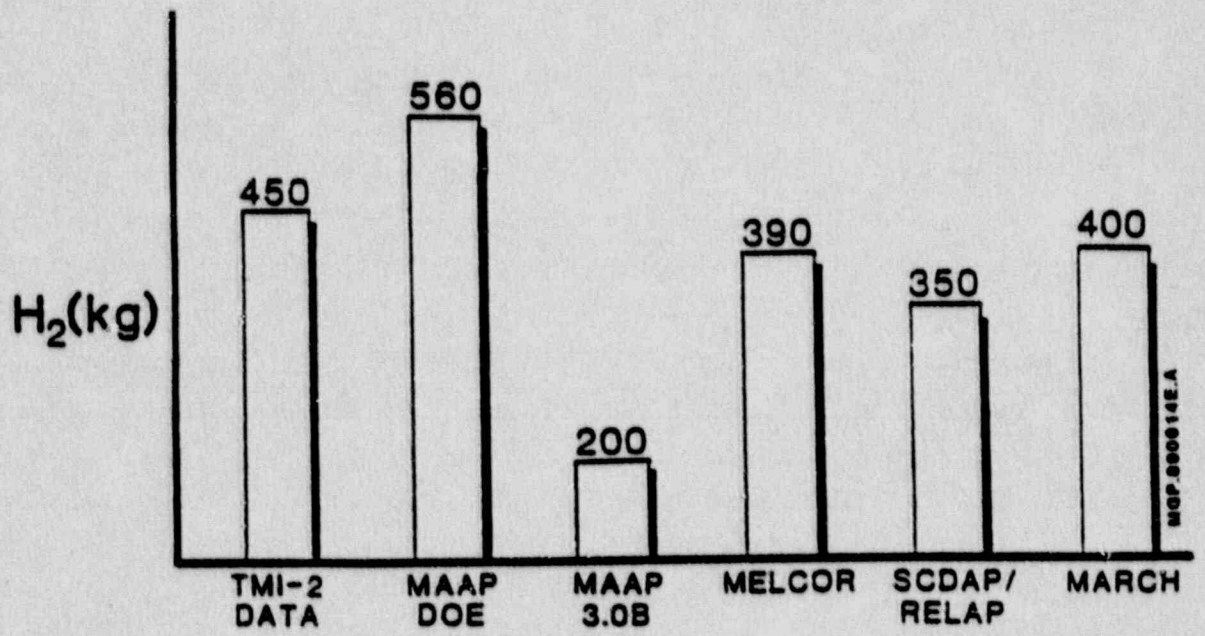

Figure 2-1 Comparison of TMI-2 hydrogen generation data with model predictions.

reflood, or a total of 510 grams. This falls within the range of 240 g to 1000 g which may have been produced.

2.1.4.2 MAAP-DOE Comparisons with SCDAP/RELAP5

An advanced version of the Modular Accident Analysis Program, MAAP-DOE, was used to simulate the response of the Surry nuclear power plant during a station blackout transient. Results of this analyses appear in Table 2-2 together with the results from a SCDAP/RELAP5[24] simulation of the same transient.

Modeling assumptions used in the MAAP-DOE simulation are consistent with those used in the SCDAP/RELAP5 Scoping Case 3 calculation. In-vessel natural circulation, hot leg counter current flow and primary loop natural circulation are all accounted for by models in both codes. Input data required by the MAAP-DOE code simulations is consistent with that used in the SCDAP/RELAP5 analyses.

The timing of events as calculated by the MAAP-DOE analysis and the SCDAP/RELAP5 analysis are in very good agreement up to the point of core uncovery and the start of core heatup. The time predicted for core uncovery and the start of core heat are essentially identical. The steam generator dryout times are also in good agreement. The difference in the reported dryout times appears to reflect different definitions for this event. The numbers appear to represent the difference between linearly extrapolating the falling steam generator water level to zero rather than defining a dry steam generator based upon a minimum mass of liquid in a steam generator.

The MAAP-DOE analysis predicts fuel rod relocation 15 minutes later than the SCDAP/RELAP5 analysis. MAAP-DOE appears to have calculated a more uniform core heatup than was predicted by the SCDAP/RELAP5 analysis. This may be a consequence of different treatment of radiation heat transfer within the core. The higher maximum middle channel fuel cladding temperature calculated by MAAP-DOE at the time of fuel rod relocation is consistent with

Table 2-2. MAAP-DOE COMPARISON WITH SCDAP/RELAP FOR SURRY STATION BLACKOUT SEQUENCE

Sequence of Events	SCDAP/RELAP Scoping (Case 3)	MAAP-DOE
Transient starts (min)	0.0	0.0
Steam generator dryout (min)	(75.4-77.2)	115.9
Core uncovery heatup starts (min)	129.7	130.4
Cladding oxidation starts (core @ 1000°K) (min)	148.0	156.8
Fuel relocation starts (core @ 2500°K) (min)	178.3	193.6
Conditions when fuel rod relocation begins:		
Hydrogen generated by start of fuel relocation (Kg)	33.7	67.8
Hot leg natural circulation outlet flow Kg/s	11	10
Upper plenum recirculating flow Kg/s	49	12.6
Maximum middle channel fuel cladding temperature °K	1546	1723 (@ 192.3 min)
Maximum upper plenum structure temperature °K	1153	997
Maximum hot leg temperature °K	829	991
Maximum surge line temperature °K	1001	886
Maximum S/G tube temperature °K	731	685

a more uniformly heated core. Thus, a difference in the event timing and hydrogen generation predicted by the different codes is observed.

Hot leg counter-current natural circulation flow rates predicted by the MAAP-DOE analysis are in good agreement with those calculated by the SCDAP/RELAP5 analysis.

Primary system structure temperatures at the time of fuel rod relocation are consistent within the various analyses. At the time of fuel rod relocation the MAAP-DOE code predicts somewhat lower temperatures than the SCDAP/RELAP5 analysis. This is consistent with the smaller in-vessel natural circulation rate predicted by MAAP-DOE which would cause heat to be retained in the core.

In conclusion, the results of the MAAP-DOE analysis for the Surry station blackout are in good agreement with the result of a more detailed analysis using SCDAP/RELAP5. The observed differences are within the phenomenological uncertainty of the current knowledge base. The MAAP-DOE prediction of the thermal-hydraulic behavior of the Surry primary system agrees with the similar SCDAP/RELAP5 prediction such that a significant degree of consistency is demonstrated between the two simulations.

2.1.4.3 ALWR Predictions Given the comparisons of the MAAP-DOE model with experimental results and SCDAP/RELAP, it is reasonable to apply MAAP-DOE to several types of ALWR accident sequences. A set of hydrogen generation predictions using the MAAP-DOE melt progression model[20] is presented here for an ALWR design. Table 2-3 is a key to the cases which fall into two categories: Licensing Design Basis (LDB) and Risk Evaluation Basis (REB). The licensing design basis cases are all accidents recovered without vessel failure, while risk evaluation basis cases extend beyond vessel failure. The latter cases are discussed further in Section 3.1.

The matrix of cases was defined to include a range of sequence types (initiators) and a range of operator actions that could be expected anticipating emergency procedures for such sequences. All the simulated

Table 2-3. MAAP-DOE ALWR APPLICATION MATRIX
SUMMARY OF CASES ANALYZED

Sequence Type (Basis)[1][2]	Operator Initiated Depressurization[3]		Recovery of Core Injection[4][5][6][7]				
	Yes	No	t_1	t_2	t_3	t_4	No
1. Large LOCA (REB)		X					X
2. Large LOCA (LDB)		X	X				
3. Large LOCA (LDB)		X		X			
4. Medium LOCA (REB)		X					X
5. Small LOCA (REB)		X					X
6. Small LOCA (LDB)		X			X		
7. Small LOCA (REB)	X						X
8. Small LOCA (LDB)	X		X				
9. Small LOCA (LDB)	X			X			
10. Small LOCA (LDB)	X				X		
11. Small LOCA (LDB)	X					X	
12. SBO (REB)		X					X
13. SBO (LDB)		X	X				
14. SBO (REB)		X			X		
15. SBO (REB)	X						X
16. SBO (LDB)	X		X				
17. SBO (LDB)	X				X		
18. SBO (LDB)	X					X	

Notes: 1) Basis: Licensing design basis (LDB) or Risk Evaluation Basis (REB)
2) All LOCA cases include loss of all injection
3) Depressurization by operator action at steam generator dryout
4) t_1 recovery at core uncovery
5) t_2 recovery within 1/2 hour of core uncovery
6) t_3 recovery at approximately 1 hour after core uncovery
7) t_4 recovery at approximately 2 hours after core uncovery

sequences considered the initiating event plus failure of injection and feedwater. The principal operator actions include primary system depressurization to permit water injection from low pressure sources and recovery of primary system injection capability. A time suitable for initiating depressurization by operator action and consistent with the guidance expected to be provided by emergency procedures was selected for these MAAP-DOE simulations. Depressurization was initiated at steam generator dryout as reported in these predictions unless stated otherwise. Furthermore, the depressurization rate is dependent upon the valve capacity, which has been taken as 100% of the full capacity value for the chosen currently under consideration in the ALWR conceptual design. This represents the expected (i.e. best-estimate) capacity of the depressurization system. A sensitivity study has been performed (see Appendix C) for depressurization capacity. In that study, the predicted hydrogen generation (% MWR) for cases ranging from 0 to 100% of depressurization capacity is presented and discussed.

Recovery and water injection could occur over a range of times. To represent those recovery times assumed to be between sequence initiation and core uncovery, the injection recovery time was simulated to be core uncovery. To represent those recovery times assumed to be between core uncovery and ve sel failure, the injection recovery time was simulated to be the core uncovery time plus about one or two hours. The recovery time was delayed as close to vessel failure as possible without preventing recovery of the damaged core in-vessel. This delay increased the time available for core heatup and enhanced the potential for hydrogen generation. A few cases of recovery time between these two extremes were tested to investigate the sensitivity of hydrogen generation over this range of recovery time. The recovery flow rate was governed by the pump curves for each of the recovered ECCS system pumps given the primary system pressure following the systems' recovery. Furthermore, each sequence type was run without any recovery for both a depressurized and a pressurized case. All the non-recovered cases resulted in reactor vessel failure. The associated ex-vessel hydrogen production mechanisms were quantified and are reported as part of this study under the Risk Evaluation Basis discussion (Section 3.1). The non-recovery cases also provided the timing of the key events, i.e., core uncovery, steam generator dryout, and vessel failure, such that the delayed recovery cases could be defined as discussed above.

The cases analyzed include large, medium, and small break loss-of-coolant (LOCAs) and blackout sequences (SBOs). Conventional hot leg breaks of 0.0929, 0.011, and 0.00156 M^2 for large, medium and small break LOCAs respectively, were selected for the analyses.

The results for the Licensing Design Basis cases appear in Table 2-4. It can be seen that insignificant clad oxidation occurred in all but three of these cases because recovery occurred prior to widespread core damage. In case 6 which was a small LOCA with delayed recovery 43% cladding oxidation occurred. While case 14 (SBO), which recovered injection at approximately the same time after core uncovery as case 6, did not recover the core in-vessel. The depressurization provided by the break in the small break LOCA (case 6) allowed the accumulator water to enter the core before the safety injection was recovered and became effective. In the similar SBO sequence (case 14) the primary system pressure remained high (near the safety relief valve set point) before vessel failure occurred and depressurized the system. The vessel failure occurred prior to the recovery of safety injection for this case (a case with earlier recovery would need to be run for recovery success for this sequence). The primary system in cases 8, 9, and 10 was depressurized (through the break and depressurization system) fast enough such that the water from the accumulator quenched the core before the core became degraded, and then the safety injection water followed the depressurization to keep the core flooded and cooled.

In cases 6, 11, and 18 the recovery of safety injection was delayed to prolong core damage but still prevent vessel failure. The hydrogen production in these three cases was 43%, 46%, and 49%, respectively. Comparing these cases with case 5, 7, and 15, respectively (see Table 3-1), it is observed that delayed recovery increases the hydrogen production by about 10 - 17%. The REB cases with no recovery (5, 7, and 15) produce less hydrogen in-vessel than their corresponding LDB cases (6, 11, and 18).

The possibility that another reactor accident sequence with recovery in-vessel would yield near (or perhaps even greater than) 75% reacted cladding remains to be addressed. For example, Chambers, et al[25] calculated 73% Zr oxidation for a station blackout sequence with a selected depressurization rate for Surry (which is not an ALWR).

Table 2-4 Licensing Design Basis: MAAP-DOE Results Summary for In-Vessel (Recovery Cases)

Sequence Number	Sequence Type	Time (Sec) of S/G Dryout[1]	Time (Sec) of Core Uncovery	% Active[2] Cladding Oxidized
2	Large LOCA	NA	119	0.0%
3	Large LOCA	NA	115	1.3%
6	Small LOCA	3620	4767	42.9%
8	Small LOCA	3620	4246	0%
9	Small LOCA	3620	4246	0%
10	Small LOCA	3620	4246	0%
11	Small LOCA	3620	4246	46.4%
13	SBO	4765	6688	0%
16	SBO	4774	5892	0%
17	SBO	4774	5892	0%
18	SBO	4774	5892	49.1%

(1) S/G = Steam generator
(2) Active clad defined as zirconium inventory in cladding within core boundary. Calculation utilizes total zirconium inventory.

However, this Surry calculation was performed for the purpose of assessing system behavior when the fuel rods stayed essentially intact through the time when the accumulators had emptied, thus maximizing cladding oxidation and heat transfer to the coolant and minimizing the rate of fuel rod temperature increase. As reported in reference 25 this calculation did not include improved models for UO_2 dissolution and fragmentation of oxidized cladding by quenching. Later calculations in reference 25 with these improved models predicted a maximum of 45% Zr oxidation. From such evaluations it is concluded that it is necessary to maintain a low water level in the core plus the optimum water supply rate to obtain high oxidation sequences with realistic models. These conditions would allow a low fuel rod temperature increase and buildup of a thick ZrO_2 layer, thus limiting cladding melting, dissolution of UO_2, and relocation of the eutectic[26]. Based on the MAAP-DOE calculations performed, such water level and water supply conditions for an ALWR are extremely unlikely given the required depressurization capability, the ECCS design flow rates, and representative guidelines for emergency operation.

The cases presented here are not an exhaustive set of possible accident scenarios. However, cases 6, 11, and 18 were defined to approximately maximize the hydrogen production for LDB cases. The number of fundamental sequence types investigated and the range of recovery times are illustrative of realistic cases for examination in a PRA. The EPRI ALWR requirement is shown to be limiting with margin for these cases. As analyzed, these cases confirm the suitability of 75% MWR hydrogen generation as the ALWR requirement.

2.1.5 LDB Hydrogen Generation Summary

Evaluation of severe fuel damage experience and analysis of ALWR cases supports the EPRI ALWR requirement for hydrogen generation. The experiments have provided a foundation for model development and validation. Analysis of ALWR cases shows that operator actions can be taken to terminate a severe accident without vessel failure and that the resulting hydrogen source is considerably less than the 75% MWR limit imposed by the ALWR Design Requirements.

2.2 Hydrogen Deflagration Evaluation

2.2.1 Introduction

The purpose of this evaluation is to demonstrate that deflagration of hydrogen will not threaten containment integrity for concentrations up to 13%on a dry air basis. Combustion processes are described in Section 2.2.2 to provide a distinction between deflagration and detonation, which is discussed in section 2.3. Experimental data and deflagration phenomena are presented in section 2.2.3. The analytical basis for the deflagration technical evaluation follows in section 2.2.4. The ideal thermodynamic results demonstrate that the EPRI ALWR requirement provides margin for containment integrity.

2.2.2 Combustion Processes

Two types of hydrogen combustion reactions are pertinent to the design requirement: deflagration and detonation. Deflagration is a combustion process in which the combustion front moves at subsonic velocity with respect to the unburned gas, while detonation is defined as sonic or supersonic propagation of the combustion front. This distinction is important because the transient pressure in a deflagration cannot exceed the adiabatic constant volume process value (adiabatic, isochoric, complete combustion, or AICC). In a detonation, transient overpressures can exceed this value by a factor of two or more, and pressure can vary significantly across the detonation front. However, pressure is uniformly distributed during a deflagration because the flame moves slowly with respect to pressure waves. The transient overpressure associated with a detonation lasts only briefly, so structures may be able to withstand detonations when the impulse is not excessive.

Factors which determine the type of combustion reaction are concentrations of fuel (hydrogen), oxidant (oxygen in air), and inertant (nitrogen or steam in air), initial temperature and pressure, containment

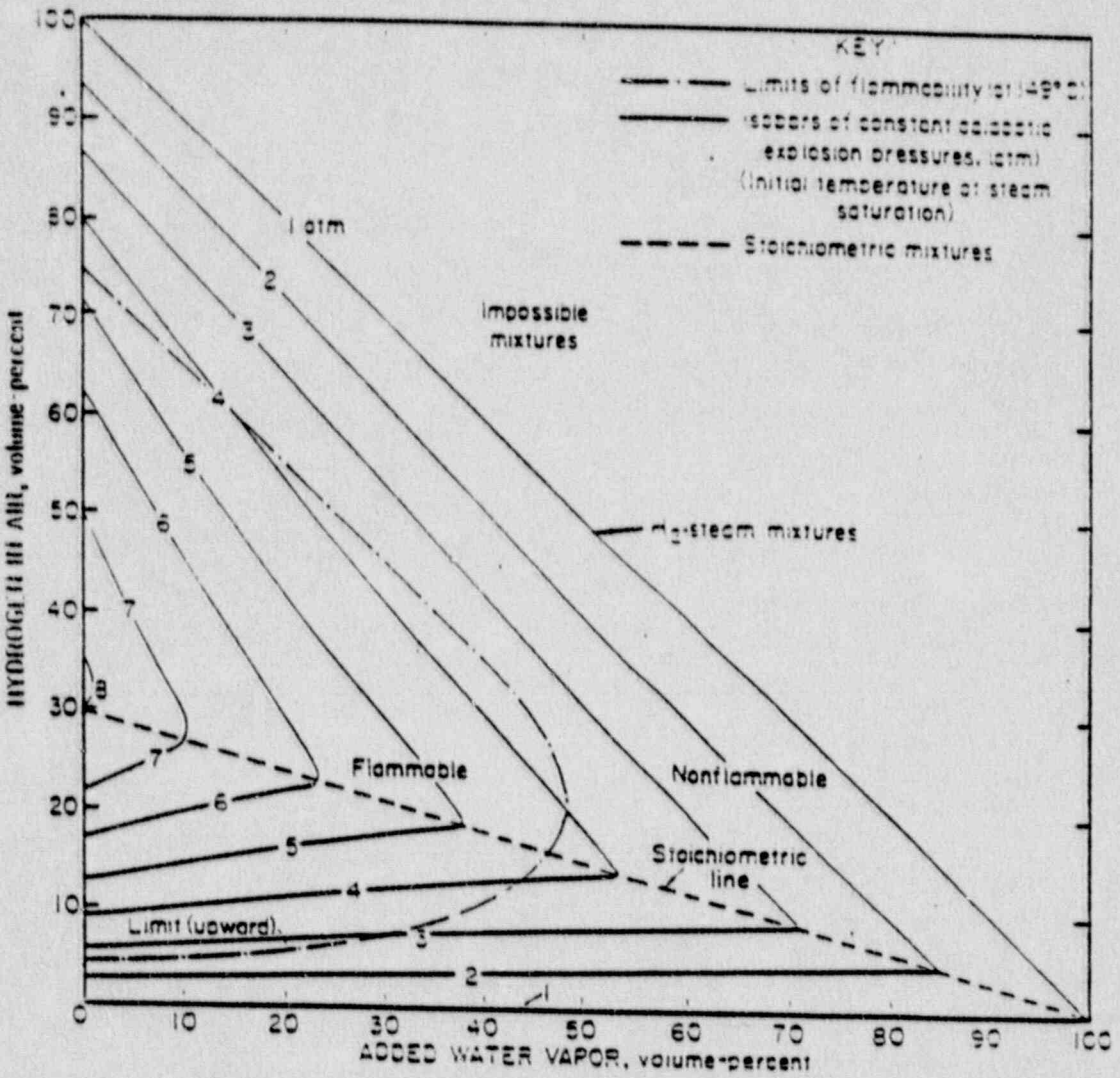

Figure 2-2 The flammability domain for upward flame propagation for H_2-Air-H_2O (vapor) mixtures. The flammability limit curve is superimposed on the isobaric contours of calculated. adiabatic explosion pressures (reproduced from Reference 27).

geometry, flow turbulence, and combustible mixture ignition sources. Composition and the initial thermodynamic state impose limits to both flammability and detonability, while geometry and turbulence can determine the potential for detonation. Classical limits for flammability and AICC maximum equilibrium final pressures are presented in Figure 2-2.[27] The region of concern for ALWR requirements lies below the line of stoichiometric mixtures, in which hydrogen is the limiting reactant. The ALWR requirement specifies a lean limit of 13% hydrogen in dry air, which lies along the vertical axis in the flammable region. Addition of steam to this mixture of hydrogen and dry air would reduce the hydrogen volumetric concentration and increase the required threshold concentration for combustion. The minimum amount of hydrogen necessary for combustion is slightly over 4% in dry air.

Figure 2-3 presents the AICC overpressure ratio resulting from combustion in air, and indicates classical deflagration and detonation limits.[28] As is evident from either figure, the ratio of final to initial pressure is about 5 at the ALWR requirement limit of 13% hydrogen. Figure 2-3 shows the lower limit corresponding to upward flame propagation (as indicated in Figure 2-2), and a higher limit corresponding to downward flame propagation (i.e., against the buoyancy forces acting on the flame.) Also, the hydrogen concentration required for detonation is shown as higher than the threshold for downward flame propagation. However, the detonation limits shown in this figure are too simplistic for reactor applications because detonation limits have been shown to be dependent on scale and temperature in a systematic fashion. The issue of how much and under what circumstances this limit can be lowered, and whether these conditions are applicable to ALWR containments is further discussed in Section 2.3.

2.2.3 Deflagration Experimental Basis

In the preceding section, a discussion of ideal adiabatic pressures resulting from hydrogen deflagrations was presented. In practice, at low hydrogen concentrations, this pressure limit is not achieved because combustion is incomplete. As illustrated in Figures 2-4 and 2-5, incomplete

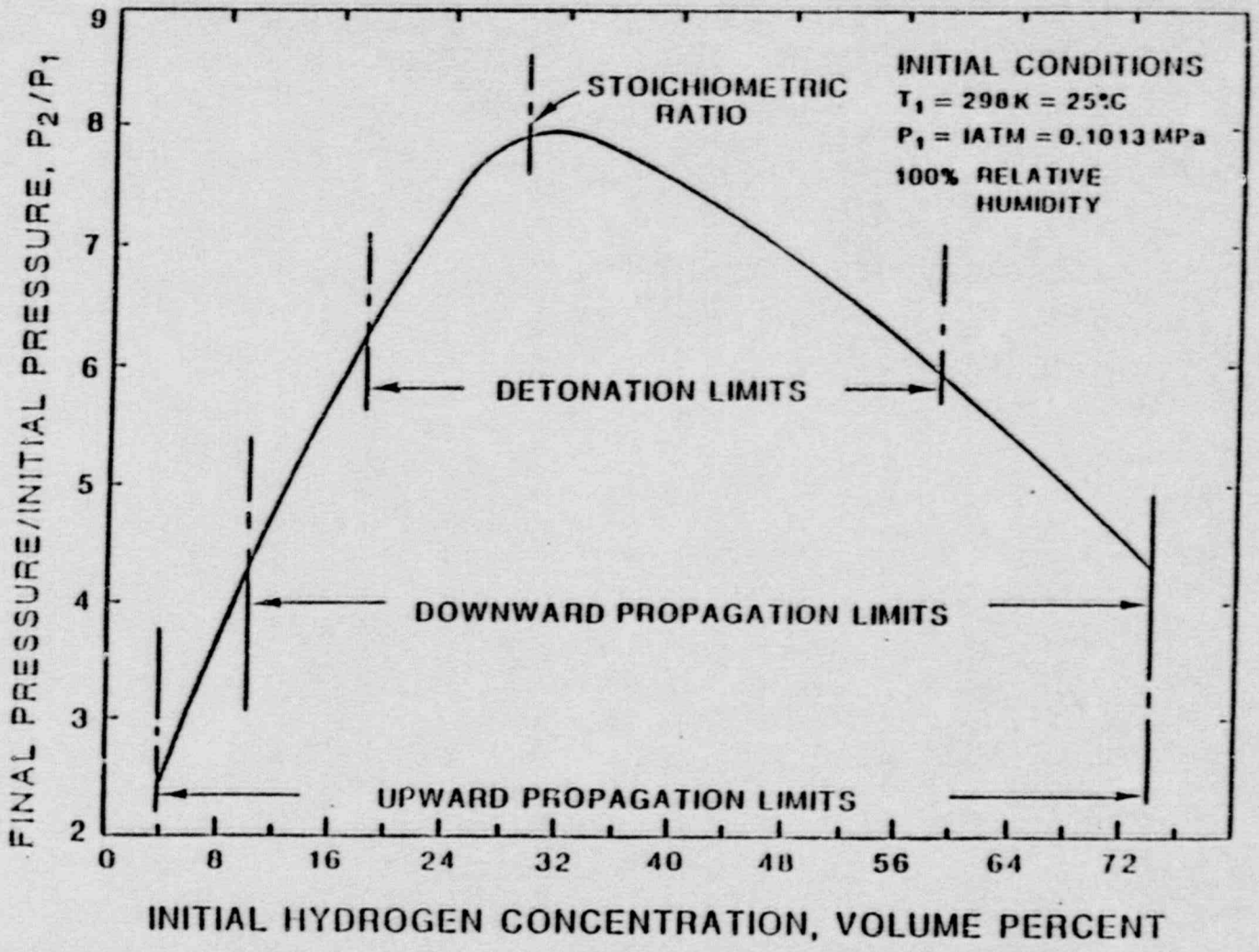

Figure 2-3 Theoretical adiabatic, constant-volume combustion temperatures of hydrogen-air mixtures (reproduced from Reference 28).

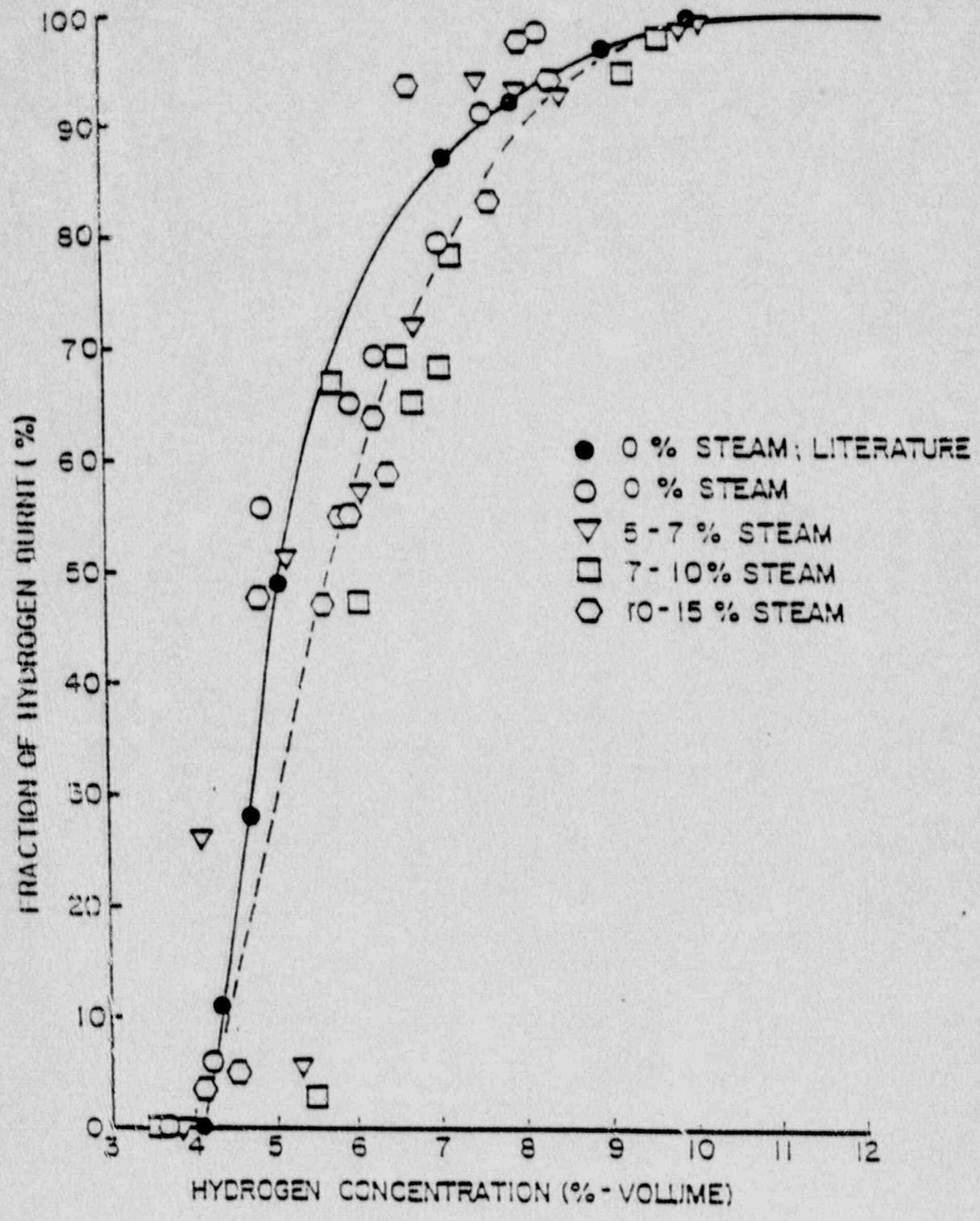

Figure 2-4 Degrees of combustion in hydrogen-air-steam mixtures (reproduced from Reference 29).

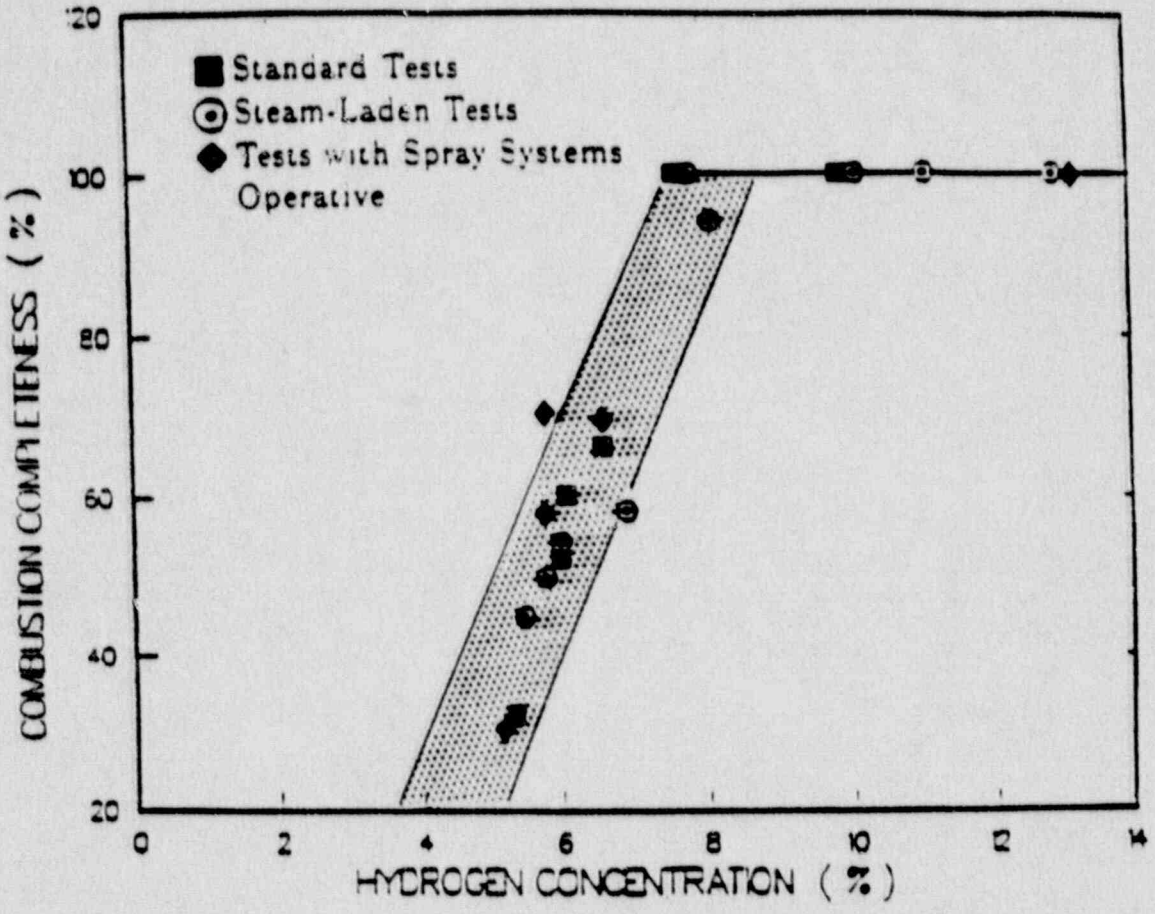

Figure 2-5 Combustion completeness for Nevada Test Site premixed combustion tests (reproduced from reference 30).

burning occurs for hydrogen concentrations below the downward flammability limit, but above that limit combustion is fairly complete. The effect of steam addition is also shown in these figures. There is close agreement between these sets of deflagration data despite a significant disparity in geometric scale of the vessels used in each experiment (i.e., .002 m^3 and 2048 m^3, respectively).[29,30] In both cases, it is evident that addition of steam has an effect on the completeness of combustion, shifting the required hydrogen concentration to a higher value as more steam is added.

Steam also affects the combustion completeness, flame velocity, inert heat capacity, and emissivity of the combustible gas mixture which, in turn, reduces the resultant system pressure rise. Figures 2-6 and 2-7 illustrate this reduction in combustion pressure as a result of increasing the relative concentration of steam for two different size systems (6.3 m^3 and 2048 m^3 spheres (see References 30 and 331 respectively). Both sets of data were taken with initial hydrogen concentrations of 8%. The pressure rise ratio is reduced by about 50% in the large apparatus, and by even a greater factor in the smaller apparatus. In each case, combustion was only about 38% complete for the highest steam addition test.

The effect of steam on system pressure is quantified for various initial saturation conditions as a function of hydrogen concentration in Figure 2-8.[32] In this figure, the initial pressure is calculated by adding the appropriate partial pressures of hydrogen and steam to a humid air mixture at 1.0 atmosphere pressure and 300°K. For example, at 400°K the steam partial pressure is about 2.5 atmospheres, and the partial pressure of the air plus hydrogen is about 1.15 atm because of both hydrogen addition and heating from 300°K to 400°K. A hydrogen mole fraction of 13% in dry air is reduced by steam addition to 4.9%. Therefore, the final pressure corresponding to 13% H_2 in dry air with steam addition to saturation at 400°K is that for an abscissa value on Figure 2-8 of about 5% H_2 in wet air, or 8.5 atm. The initial pressure is 2.5 + 1.15 = 3.65 atm, so the pressure rise ratio is 8.5/3.65 = 2.33. Note that the steam mole fraction is approximately 2.5/3.65 = 0.68 for this mixture, which is well outside the flammability limits (see Figure 2-2).

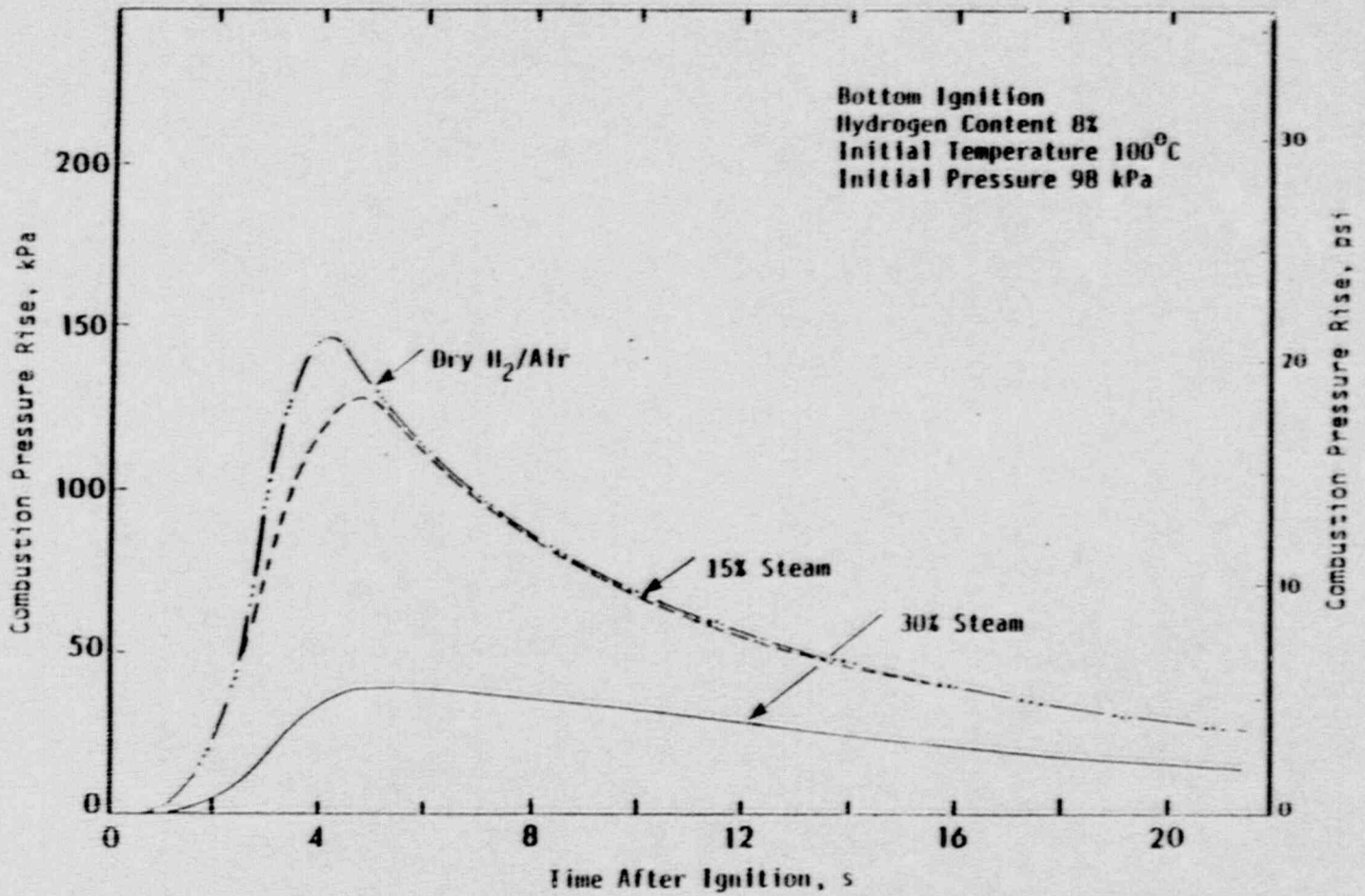

Figure 2-6 The effect of steam addition at intermediate hydrogen concentration (reproduced from Reference 31).

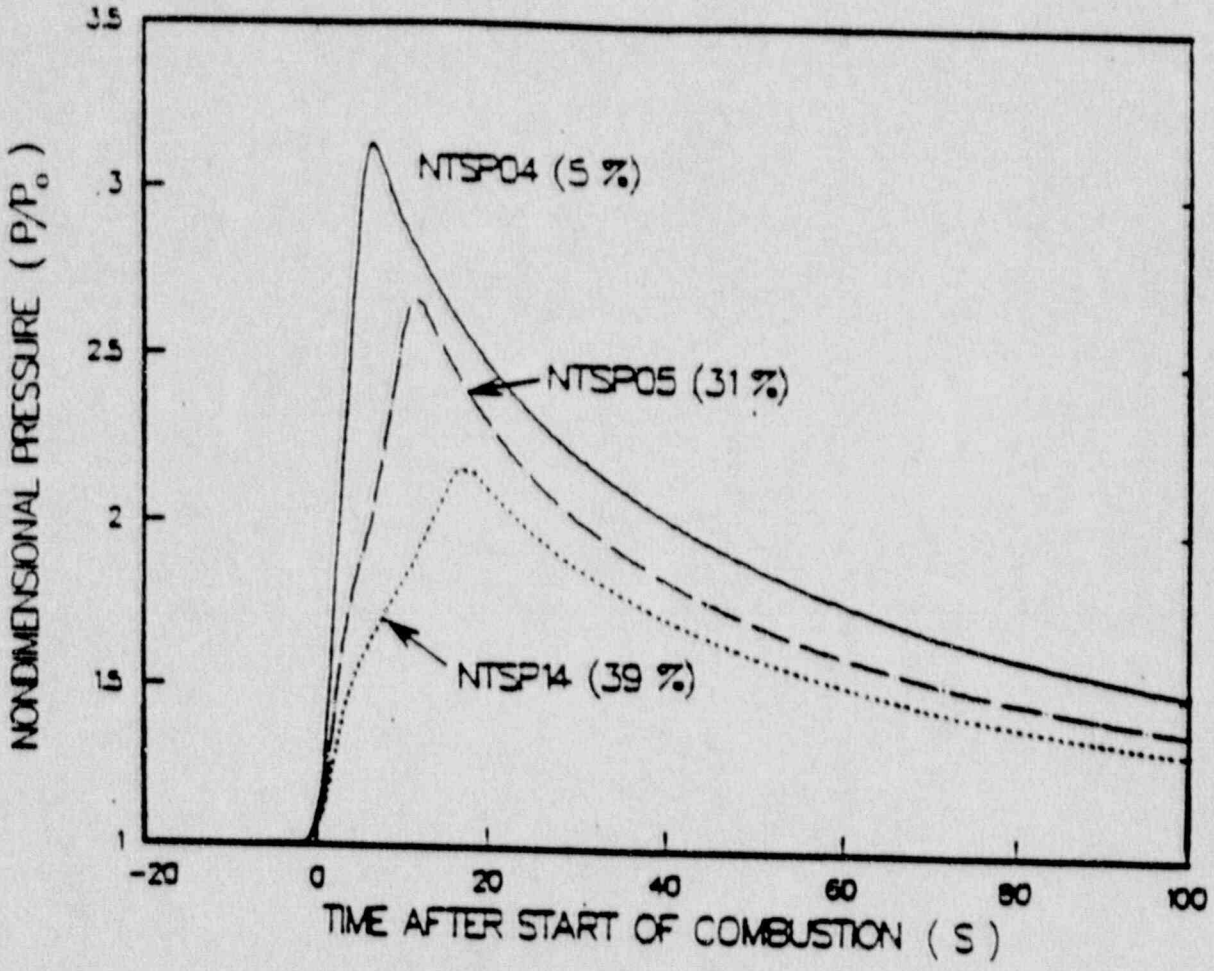

Figure 2-7 Comparative pressure profiles for three 8% (nominal) hydrogen combustion tests having different precombustion steam concentrations. Numbers in parentheses are the steam concentrations (reproduced from Reference 30).

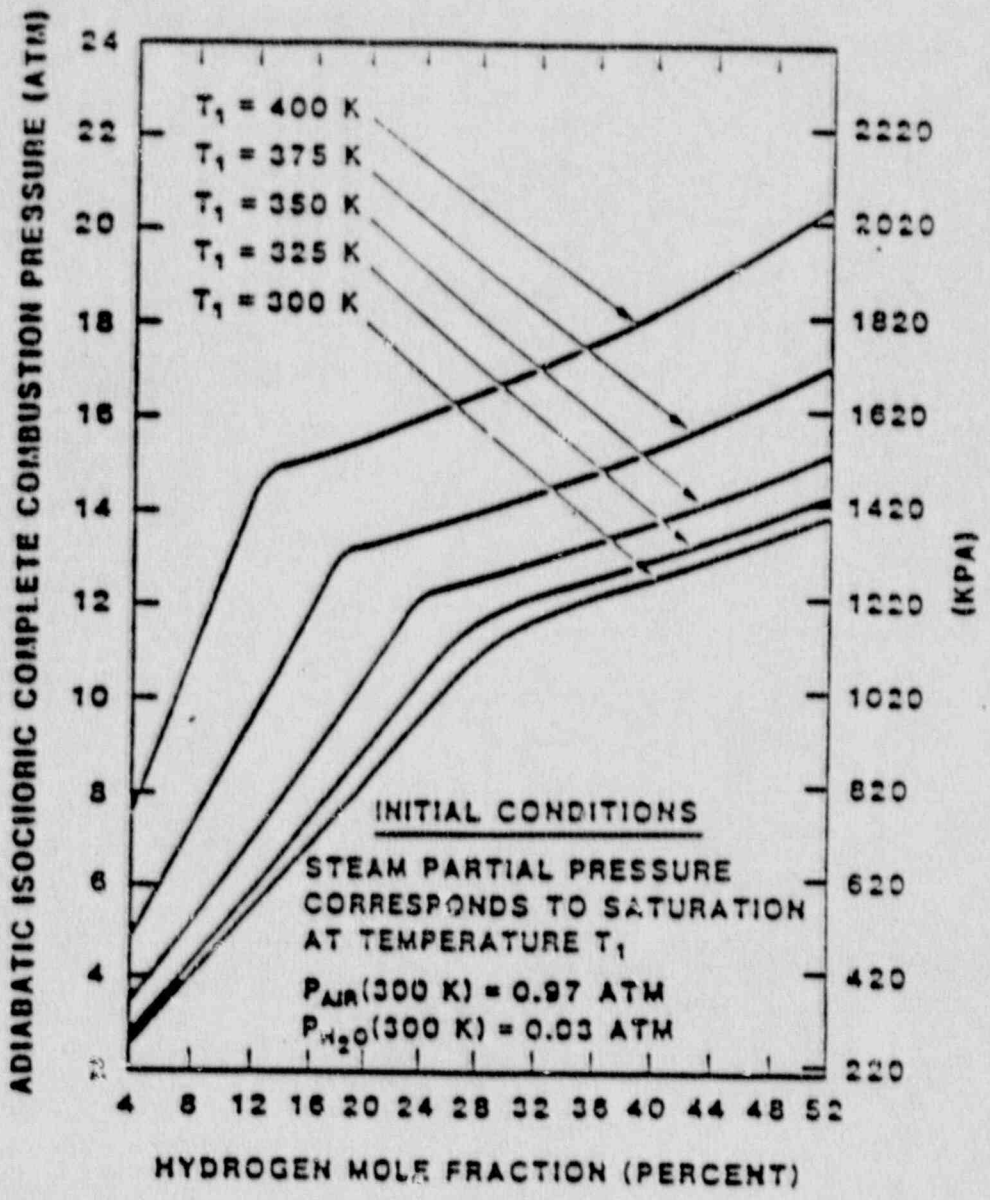

Figure 2-8 AICC pressures for various containment initial conditions (reproduced from Reference 32).

2.2.4 Deflagration Analytical Basis

The above example can be generalized to find the maximum post-combustion pressure for an ALWR containment. As steam is added to an atmosphere of air and hydrogen, the initial pressure and final post-combustion pressure both increase. However, eventually, the mixture becomes inert due to steam addition when the flammability limit is reached. An approximate method is derived in Appendix A, which can be used to determine final pressures resulting from complete combustion of 13% H_2 on a dry basis at various system steam pressures. A calculation using steam table values is presented here. The flammability limit of diagram of Figure 2-2 can be used to determine whether these mixtures are flammable. The maximum final pressure for a 13% dry basis H_2 plus steam mixture which is possible in a containment under initially saturated conditions is defined for the flammability limit. Containment conditions will not be superheated because such a condition is only possible when dry core debris exists in the containment, a situation precluded by the EPRI ALWR debris coolability requirement (see Section 3.1).

The results of this thermodynamic equilibrium calculation for possible containment atmospheres are shown in Table 2-5 and Figure 2-9. The final pressure increases as the initial temperature increases because the initial pressure must increase due to steam addition, but the pressure ratio decreases and is seen to be highest for the dry case (300°K). The maximum theoretical pressure in a containment following a burn is 6.6 atm based on the flammability limits. However, also shown in Figure 2-9 is the anticipated boundary between the complete and incomplete combustion regimes. The maximum probable pressure is thus about 6.4 atm. When more steam is present, incomplete combustion would be expected and the final pressure would be less than this value.

Table 2-5

PRESSURE RISE AND FLAMMABILITY RESULTS FOR
13% H_2 IN DRY AIR WITH SATURATED STEAM ADDITION

T(°K)	X_{HW}[a]	X_S[b]	P_W[c]	P_f[d]	P_f/P_w	Flam[e]
300	0.127	0.026	1.2	5.8	4.8	Y
325	0.117	0.097	1.4	5.9	4.2	Y
350	0.099	0.240	1.8	6.0	3.3	Y
375	0.074	0.430	2.5	6.6*	2.6*	Y
380	0.069	0.470	2.8	-	-	N

[a] wet H_2 mole fraction

[b] H_2O mole fraction

[c] initial pressure (atmosphere)

[d] final (postburn) pressure (atmosphere)

[e] Y = flammable, N = not flammable

*overestimate due to incomplete combustion

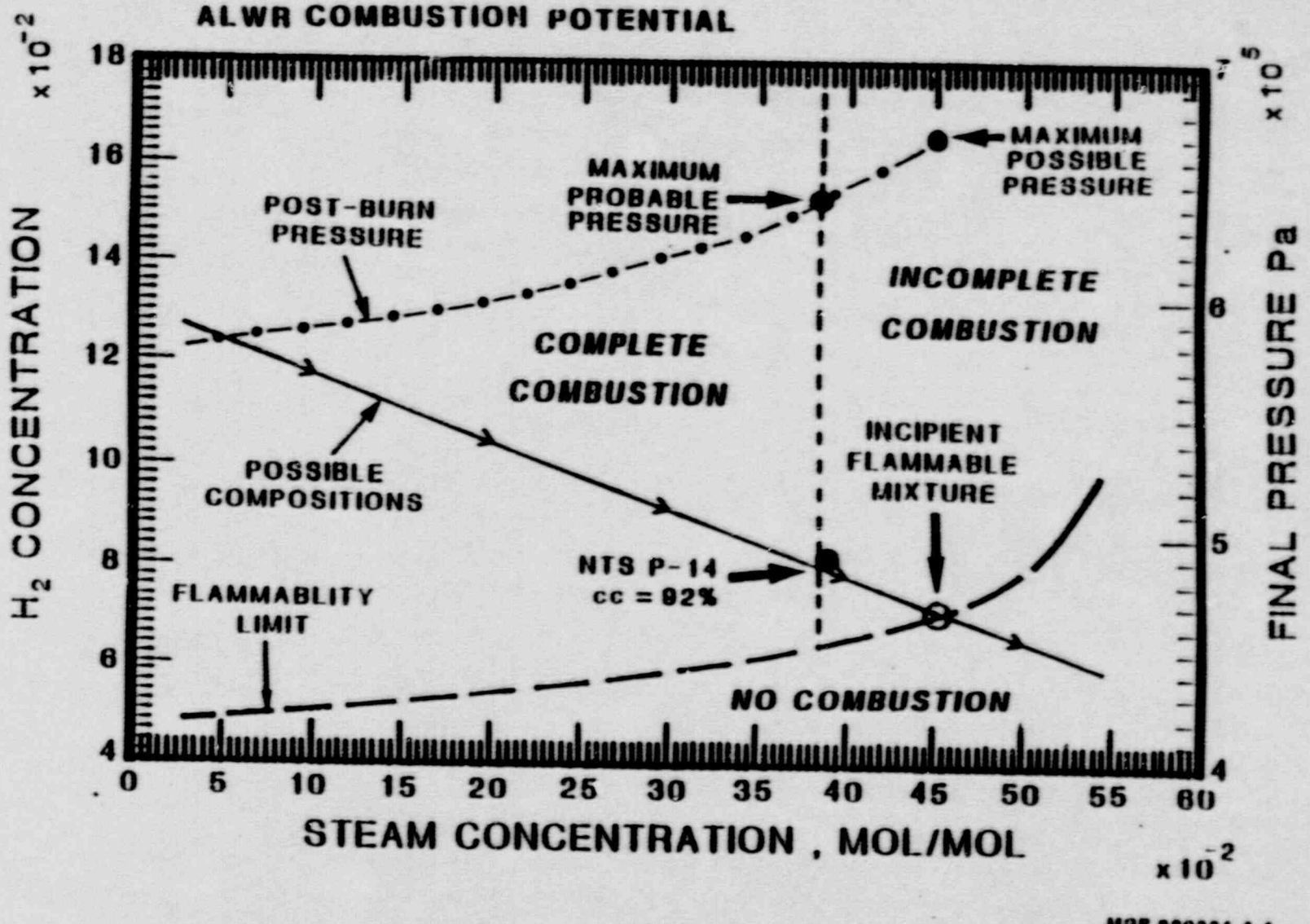

Figure 2-9. ALWR Combustion Potential.

The post-combustion pressure can be compared with the containment pressure capability. A typical design pressure for a current large, dry containment is 4 atm. The containment is required to survive service level C requirements which are 1.75 times design pressure[5], or 7 atm in this case. Since the maximum post combustion pressure is less than the service level C pressure, a current large, dry containment design can survive this deflagration. It should be noted that the containment ultimate strength is approximately 2.5 times design pressure, or 10 atm, so considerable margin exists.

2.2.5 LDB Hydrogen Deflagration Summary

The EPRI ALWR requirement for hydrogen in containment is therefore supported by the following logic: Given the maximum credible initial steam concentration for which a burn can occur, the maximum initial and final pressures can be determined. The maximum estimated final pressure is 6.4 atm. This final postburn pressure is within the design capability of an ALWR containment. Hence, the ALWR design requirement can clearly meet the goal of ensuring containment integrity after a hydrogen deflagration event.

2.3 Hydrogen Detonation Evaluation

2.3.1 Introduction

In this section the potential for hydrogen detonation is considered given a hydrogen concentration of 13% in a dry containment atmosphere. In the experimental basis, Section 2.3.2, two physical initiation mechanisms for detonation are considered for a containment, direct initiation by energy deposition and indirect initiation by flame ignition and acceleration. In both cases, an intrinsically detonable mixture (i.e., a mixture in which a detonation, once initiated, can be sustained) is required. and the initiation is dependent thereafter upon existence of an ignition source, appropriate

geometry, and environmental conditions. Since detonability is composition and environment dependent, the potential for detonation in containments must be assessed with respect to both aspects of the phenomenon. For each initiation mechanism the lowest possible hydrogen concentration for detonation must be established. In the analytical basis, Section 2.3.3, detonation limits are estimated from the leanest experimentally measured values for a variety of conditions, and if necessary extrapolated to the bounding containment environmental conditions. An ALWR containment analysis is presented.

2.3.2 Detonation Experimental Basis

2.3.2.1 Intrinsic Detonability The lowest value of hydrogen concentration for intrinsic detonability is now understood to be dependent upon geometric scale. Increasing scale allows the possibility of detonations at lower hydrogen concentrations. For example, the detonability limits shown in Figure 2-3 were based on observations in a small apparatus. Recently, detonability has been observed for mixtures of 13% hydrogen in dry air at 100°C[33] and 9.5% hydrogen in dry air at 100°C[34] in a much larger apparatus (43 cm diameter tube). In both cases, these detonations were initiated by large explosive charges. The National Research Council reached the conclusion that mixtures of 9 to 11% hydrogen might be detonable based upon these experiments with hot, dry mixtures driven by explosive charges[35]. Of course, explosive charges cannot exist in an ALWR containment.

The ability for a detonation to be sustained or to propagate has been empirically found to be closely related to an intrinsic property of the mixture known as the detonation cell width, λ (see References 33, 35, 36). The value of λ is lower for mixtures which are more easily detonable (hereafter termed more sensitive mixtures). Detonations have a three-dimensional cellular structure formed by multiple interactions of transverse waves and the main shock front. The cell width can be determined

by the diamond or "fish-scale" pattern left on a smoked foil by shock wave intersections. The lowest stable detonation wave mode, called the single-head spin mode, can be related to a tube diameter D through the relation $\lambda = \pi D$ (see Reference 33). For less sensitive mixtures, where λ is larger and $\lambda/\pi > D$, detonation is still possible given a sufficiently strong initiator. For an open, unconfined cloud, the detonation criterion is more strict than for tube geometry. The minimum cloud diameter d_s is related to the detonation cell width by $\lambda = d_s/6.5$ (see Reference 35).

Measured cell widths for mixtures of hydrogen in dry air at 25°C are shown in Figure 2-10. A minimum value of λ occurs near stoichiometry (29.7% hydrogen). For leaner mixtures λ increases rapidly, indicating a decrease in sensitivity. Similar data are shown in Figure 2-11 for higher temperatures. Detonation cell widths are uniformly lower at higher temperatures, indicating greater mixture sensitivity, that is, increased intrinsic detonability. These are plotted in terms of the equivalence ratio, denoted by ϕ or ε, which is the ratio of the number of moles of hydrogen divided by the number of moles of air to that quotient at stoichiometry. The equivalence ratio has a value of 1.0 at stoichiometry, and lower values for leaner mixtures. Useful relations between equivalence ratio ϕ, the hydrogen mole fraction X_{H_2}, and the steam mole fraction (or other diluent) X_d are

$$\phi = S\, X_{H_2}/(1 - X_{H_2} - X_d)$$

$$X_{H_2} = \phi(1 - X_d)/(\phi + S)$$

where $S = 2.387$. The equivalence ratio for 13% hydrogen in dry air is 0.357. This figure is unchanged by addition of steam to the dry mixture because the overall H_2 and O_2 mole fractions decrease in the same proportion.

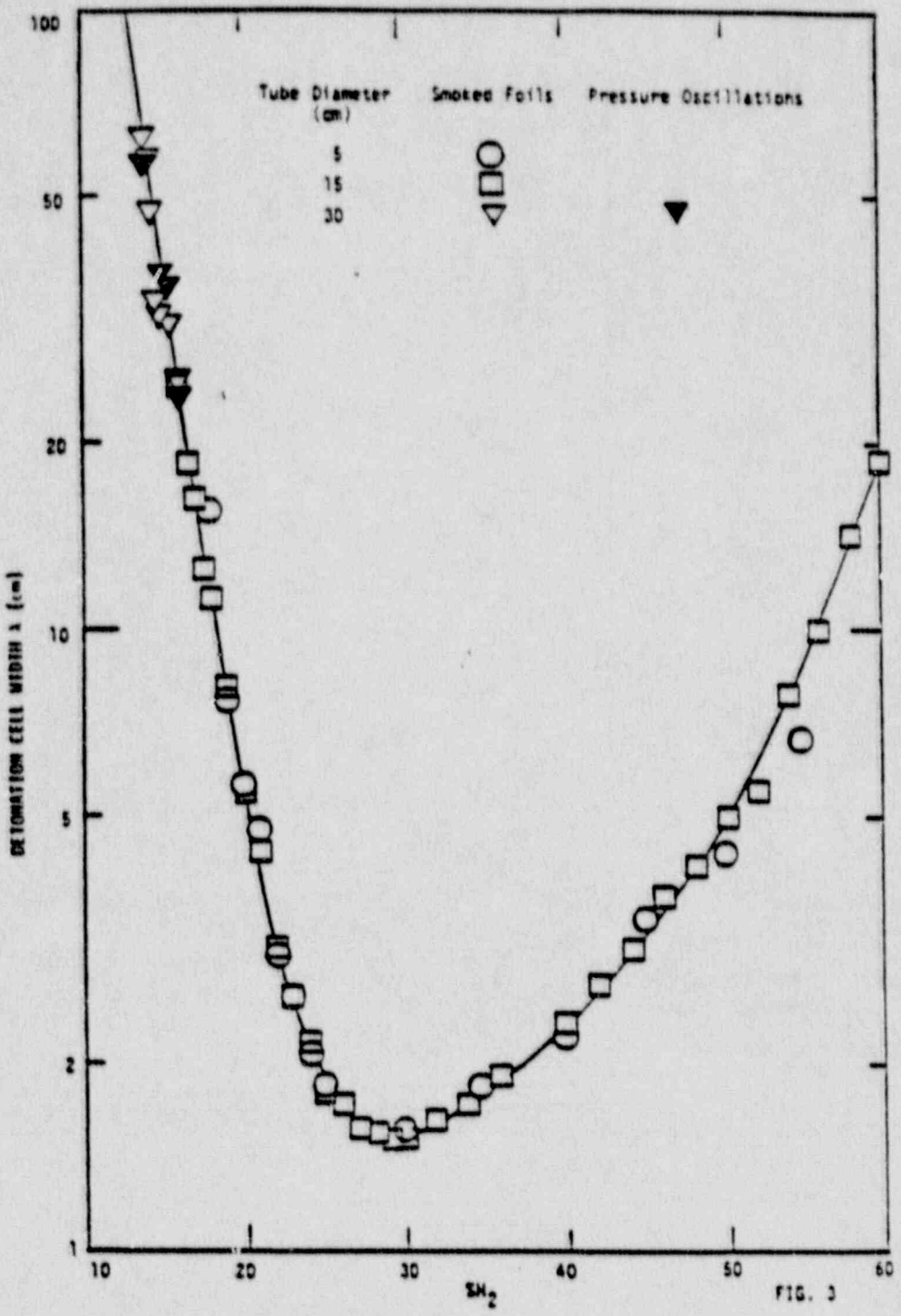

Figure 2-10 Measured values (McGill, Sandia) of the detonation cell width (λ) as a function of hydrogen concentration (reproduced from Reference 38).

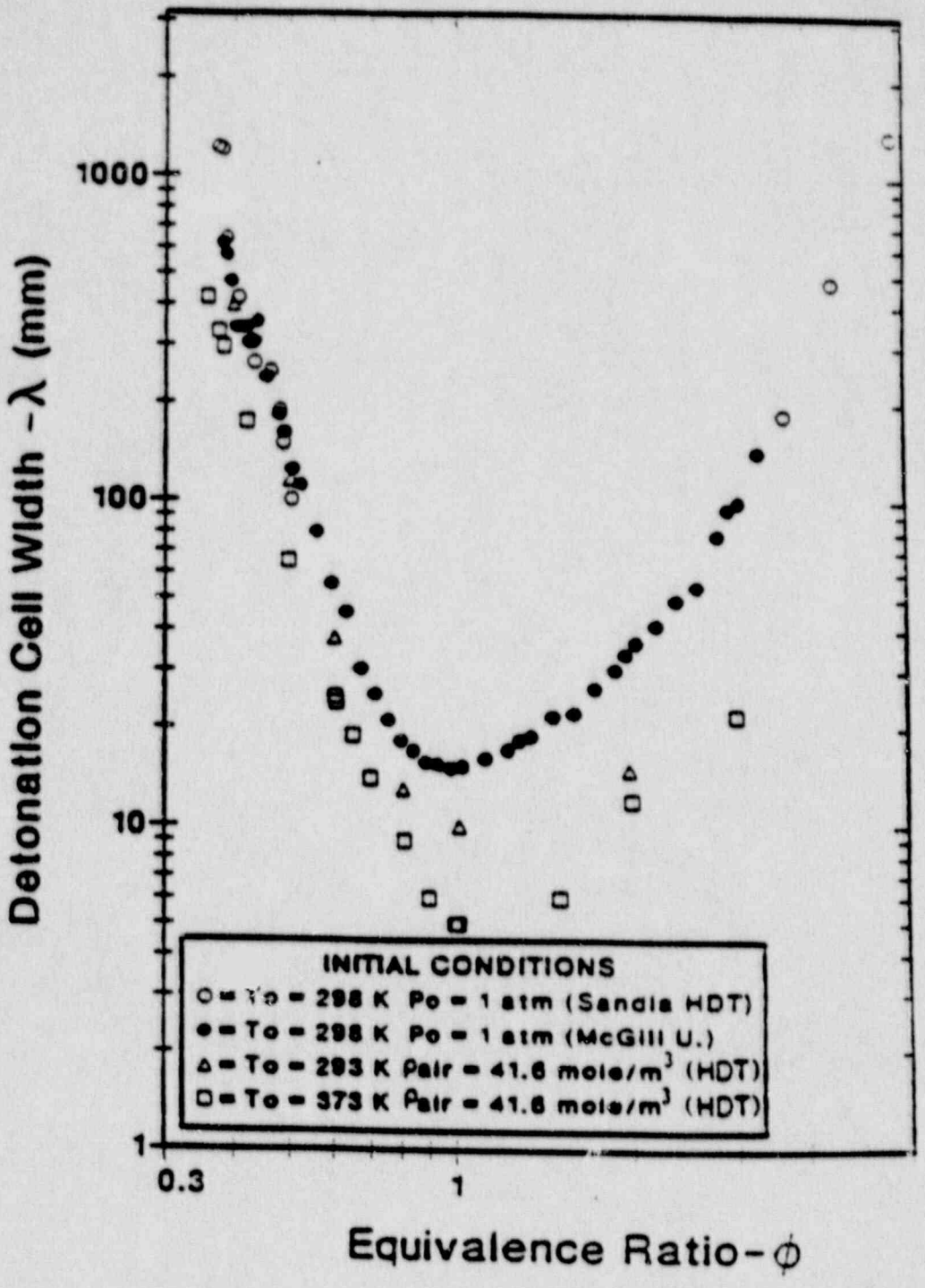

Figure 2-11 Detonation cell width, λ, as a function of the equivalence ratio for various temperatures and densities (reproduced from Reference 33).

For the 43-cm-diameter heated detonation tube (HDT) apparatus described in Reference 33, the critical cell width is 3.14 * 0.43 = 1.35 meter, which corresponds to roughly 13% hydrogen from extrapolation of the curves on Figures 2-10 or 2-11. Thus, the observation of a detonation at 9.5% hydrogen[34] demonstrates that sufficiently strong triggers can induce a detonation in less sensitive mixtures. In that experiment 106 grams of high explosive, or about 0.5 MJ, was the trigger size.

2.3.2.2 Influence of Steam and Temperature The detonation cell width increases dramatically with the addition of steam as shown in Figure 2-12 (see Reference 33) for mixtures at 100°C. Thus, steam as a dilutent makes detonation more difficult to achieve. As temperature increases, detonation becomes easier as seen by the decrease in cell width in Figure 2-13 (see Reference 33). Comparing the two figures, one can clearly see that in this temperature range the steam inerting effect is far more pronounced than the heating effect on detonation cell size. Additional effects of higher temperature will be discussed in Section 3.3, under the risk evaluation basis topic. For ALWRs, the impact of steam is quite significant. According to Figure 2-12, the detonation cell width increases by a factor of 5 with 10% steam, by 25 with 20% steam, and by 125 for 30% steam. ALWR atmospheres are anticipated to have significant steam content and no superheat. Sample cases for steam content are discussed further in Section 3.3.

2.3.2.3 Initiation by Energy Deposition Regarding detonations directly initiated by energy deposition, the amount of energy required is a minimum for mixtures near stoichiometry but increases rapidly for leaner and richer hydrogen-air mixtures. Extensive experimental and theoretical work has been done in this area (see References 33, 37, 38). Extrapolating work on energy deposition to 13% hydrogen, a trigger between 2.5 MJ and 14 MJ energy is required (see Reference 39). The trend is presented graphically in Figure 2-14.[39] The required energy is stated in terms of grams of high explosive; a good value for conversion to energy is between 4.5 and 5 kJ/gram. It can be seen that these curves for spherical propagation overpredict the charge needed to initiate the planar detonation in a confined space such as the HDT

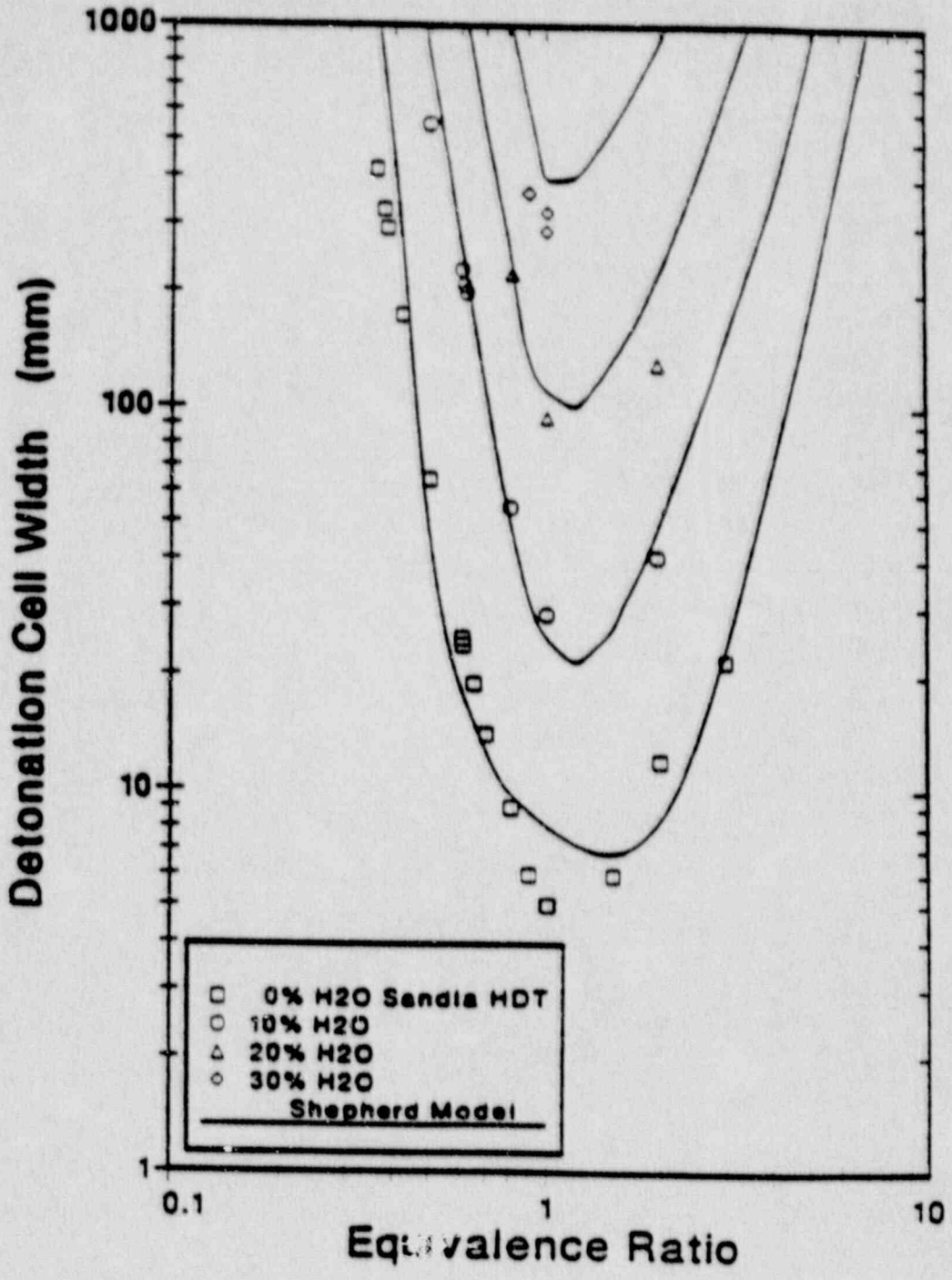

Figure 2-12 Detonation cell width as a function of the equivalence ratio for various steam concentrations (reproduced from Reference 33).

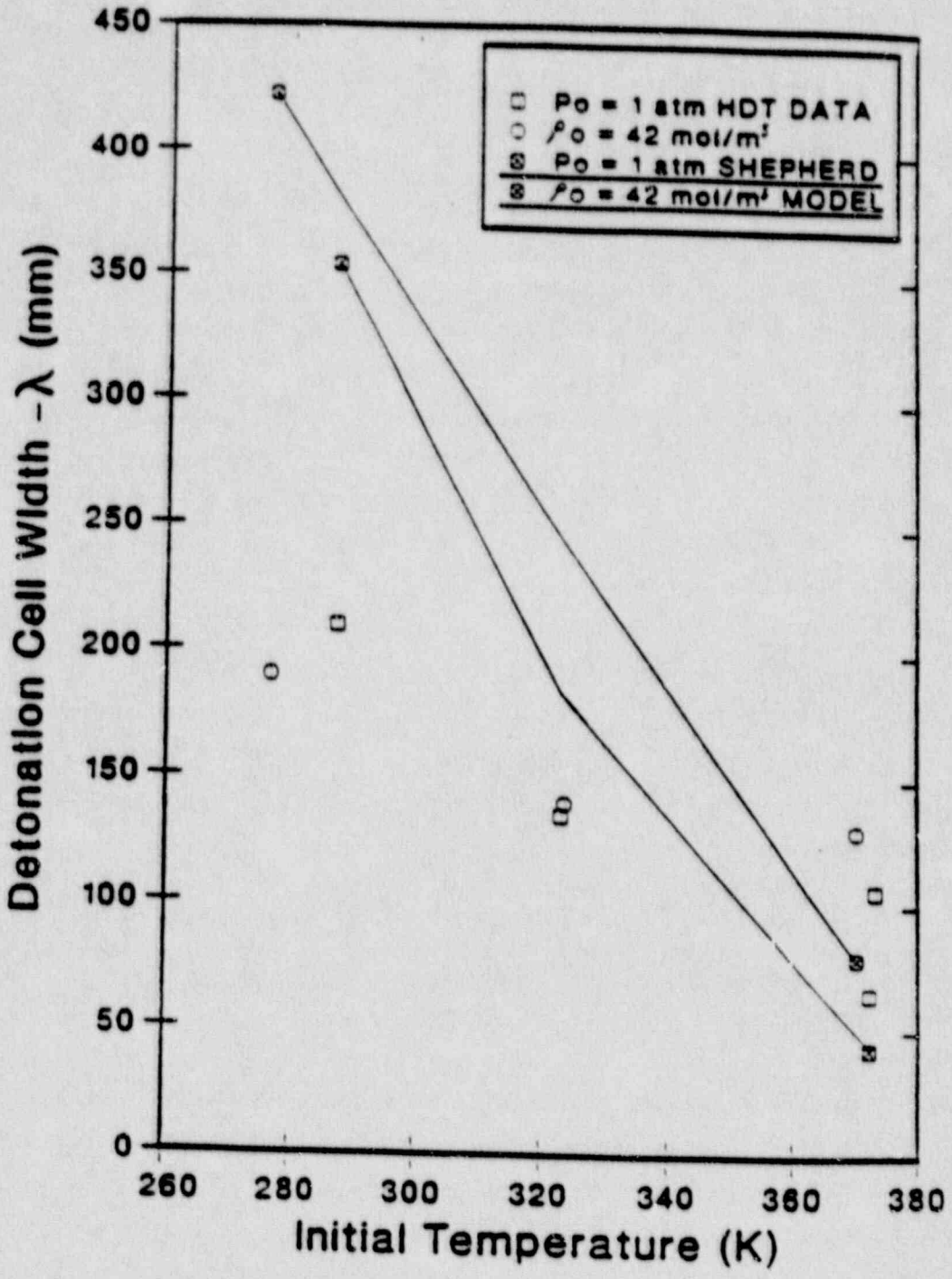

Figure 2-13 Detonation cell width as a function of temperature (reproduced from Reference 33).

apparatus, about 100 g. Values near 10 MJ are more appropriate for the open regions of a containment, indeed Figure 2-14 implies over 2000 g high explosive, which is equivalent to 10 MJ. In contrast, the energy required to initiate a deflagration, shown in Figure 2-15,[40] is more than 10 orders of magnitude lower than that for a detonation.

The energy required for a detonation can also be compared with energies of various ignition sources as shown in Figure 2-15. The largest possible ignition source in a containment, a 12 kv arc, results in a maximum arc energy of 40 MJ over four cycles, i.e., a peak rate of energy deposition of 600 MJ per second.[41] This rate of energy deposition is about two orders of magnitude lower than the value for initiation of a planar detonation of 13% hydrogen in a confined tube (80 grams of high explosive per reference 34) and over three orders of magnitude lower than the value for that of a spherical unconfined detonation per Figure 2-14. All the ignition sources indicated in Figure 2-16 are sufficient to cause a deflagration.

Considering this evidence, it is clear that hydrogen deflagration is far more likely to occur than a detonation as a result of initiation from sparks or other forms of energy deposition. Consequently, it is unreasonable to consider detonation initiation by direct energy deposition for ALWR containments.

2.3.2.4 Initiation by Deflagration to Detonation Transition Flame acceleration occurs due to turbulence induced by fans, structural roughness, obstacles, or changes in geometry; by interactions with pressure waves; or by precompression. Flame acceleration is important only for mixtures which can be characterized as highly flammable.[42] For lean mixtures, concentrations above 10% or 12% hydrogen in dry air are strongly flammable. Flame acceleration which results in sonic propagation of a detonation front is called deflagration to detonation transition (DDT), and requires a greater hydrogen concentration. The addition of steam inhibits DDT and shifts the required equivalence ratios to higher values, as discussed in Section 3.3.

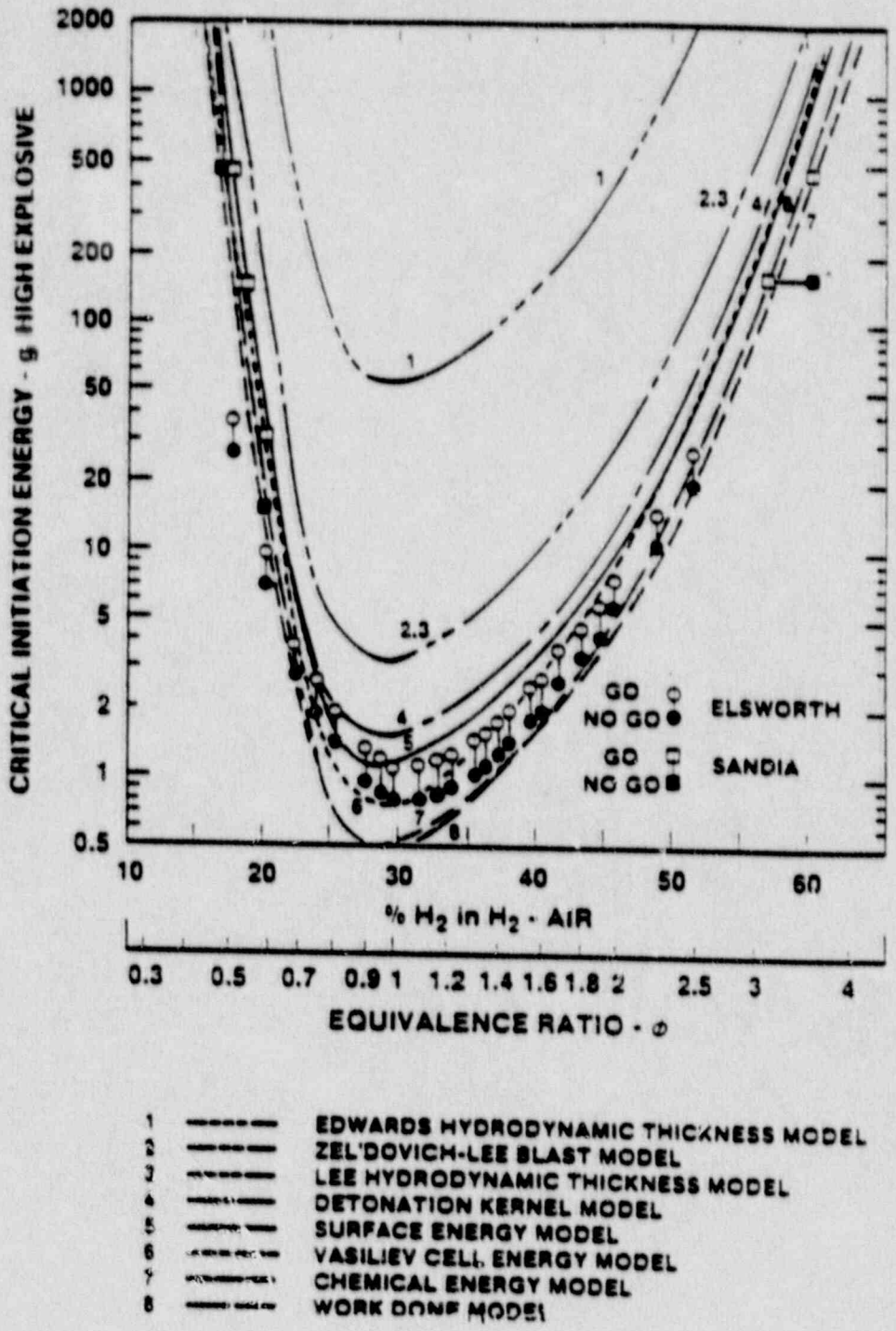

Figure 2-24 Critical detonation initiation charge as a function of composition (reproduced from Reference 39).

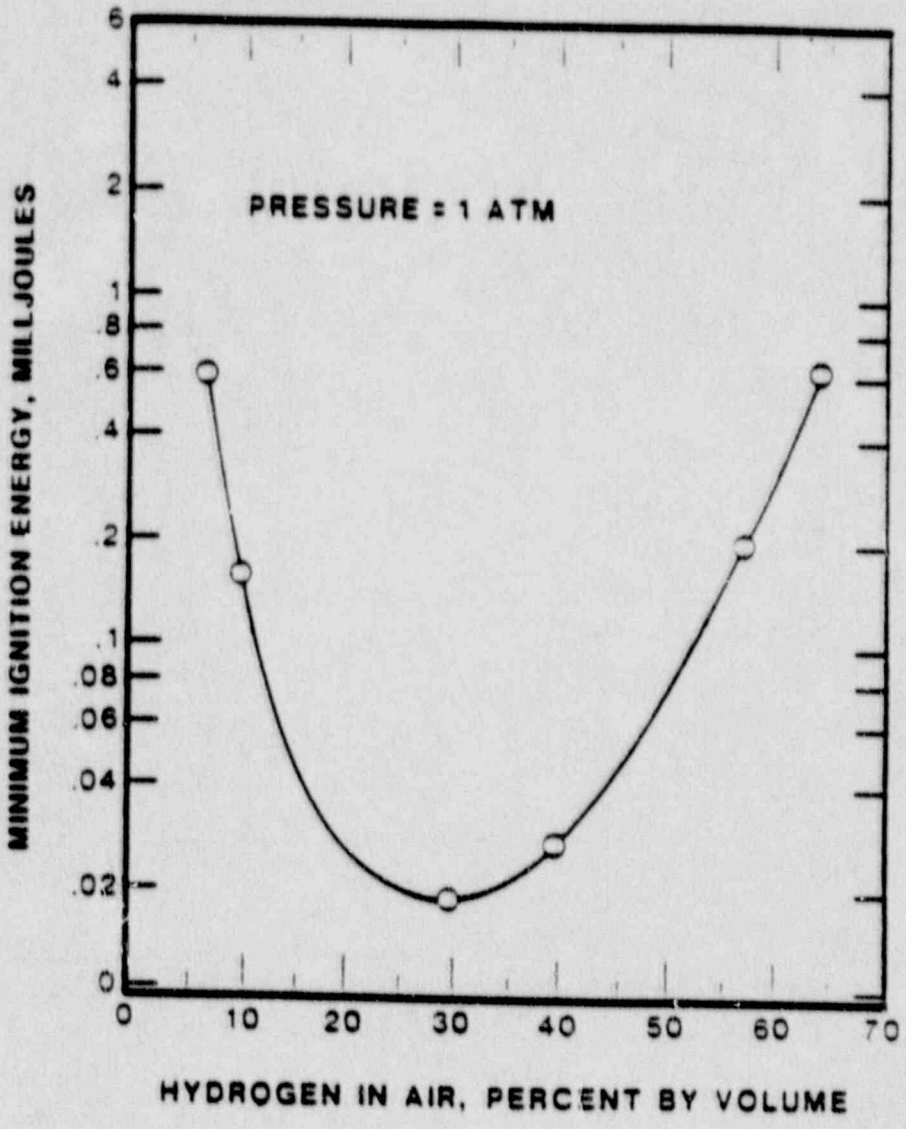

Figure 2-15 Minimum ignition energy for hydrogen deflagrations (reproduced from Reference 40).

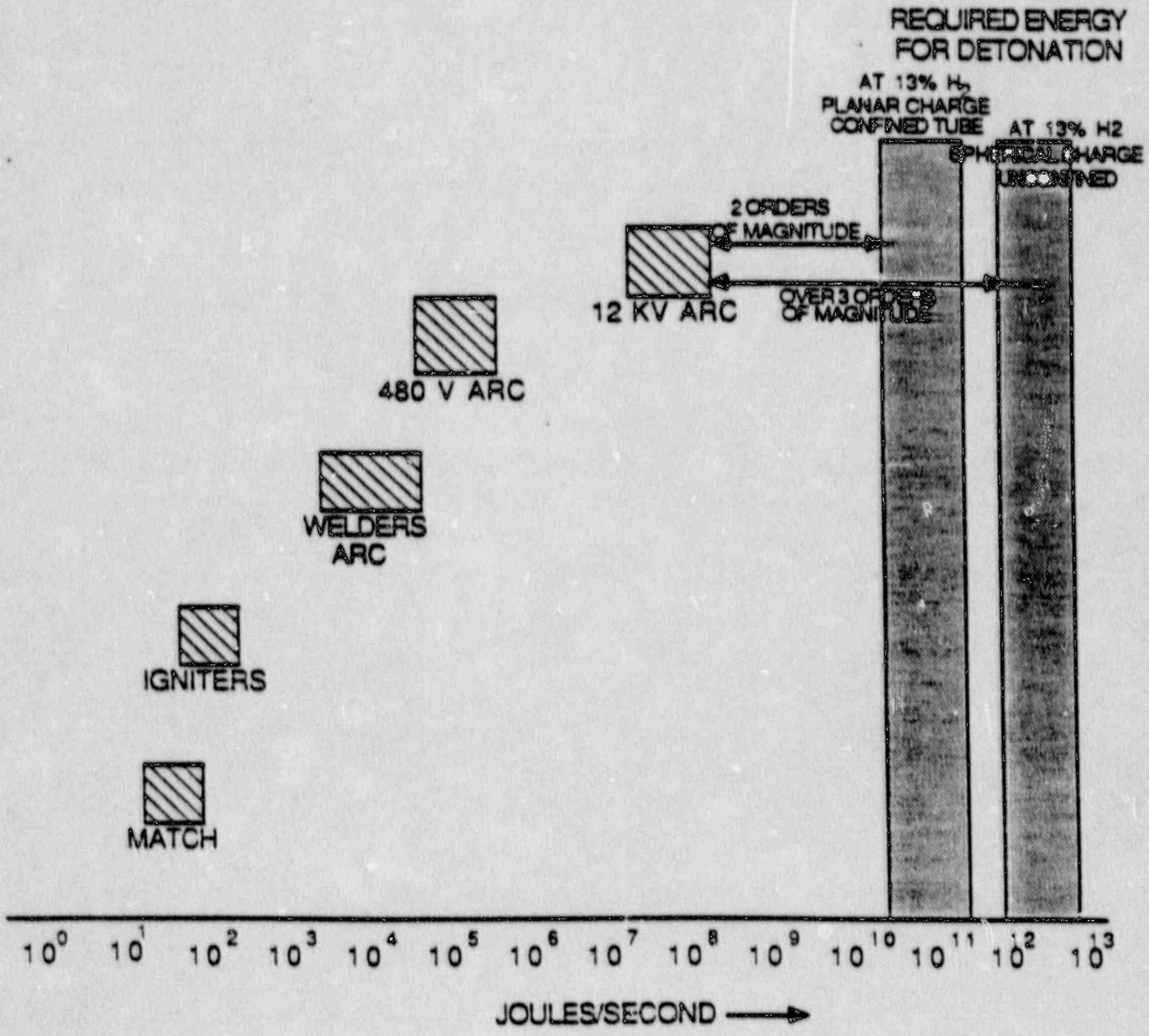

Figure 2-16 Comparison of ignition source energies with sources required for detonation.

In reactor containments, turbulence-induced acceleration is more important than the other means identified above, because containment size limits the effectiveness of pressure pulse propagation through dissipation and interference, and because precompression requires substantial confinement of gases in front of a propagating deflagration front. At low hydrogen concentrations, accelerations are most likely to occur in somewhat confined regions of a containment and then propagate into more open regions. This is supported by the fact that the leanest observed detonations occur in confined geometries such as tubes, while richer mixtures are required in open geometries.

The lowest hydrogen concentration for which DDT has been observed is 15%.[43] The apparatus used was the FLAME facility at Sandia, which is a half-scale model of an ice condenser upper plenum, 2.44 m high, 1.83 m wide, and 30.5 m in length. To promote turbulence, this long rectangular channel can be partially vented on top, and obstacles can be placed along the interior. The 15% low limit corresponds to a case with no venting and periodic obstacles every 1.83 m. In a case with no obstacles, 25% hydrogen was required, as shown by Figure 2-17, and for a case with obstacles but 50% venting, 20% hydrogen was required. This latter case corresponds more closely to an ALWR situation although there are still significant differences between FLAME geometry and expected ALWR containment arrangements based on Chapter 6 of the Requirements Document which will make the ALWR less prone to DDT. These differences include:

(1) FLAME is more confined. This confinement significantly lowers the hydrogen concentration necessary for DDT.

(2) The FLAME channel length to diameter ratio is long relative to large, channel-like enclosures expected in the ALWR.

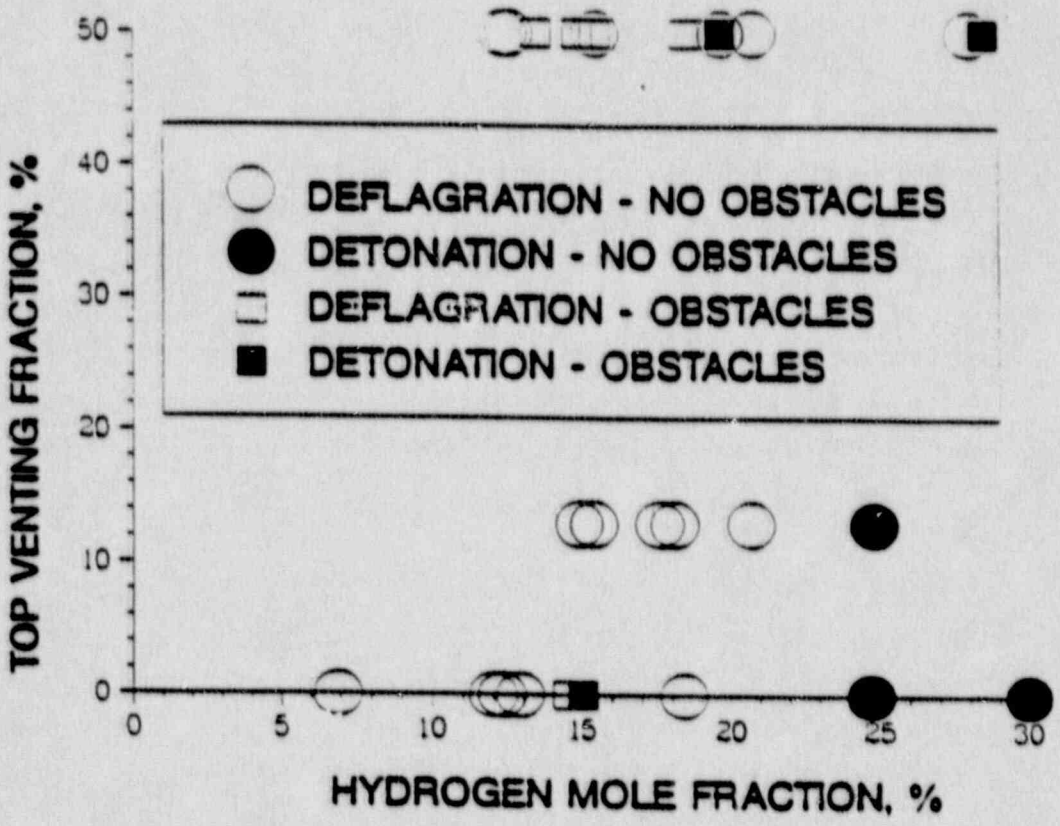

Figure 2-17 FLAME apparatus DDT results (reproduced from Reference 43).

(3) The periodically spaced obstacles necessary to promote turbulence and produce DDT at lower hydrogen concentrations in FLAME are unlike what would be expected in channel-like enclosures in an ALWR.

It is very difficult to relate the detonation cell width to a necessary or sufficient criterion for DDT because other characteristic lengths of the geometric configuration are influential. A case of attempted scaling of DDT by λ is reported by Berman who compares two sets of experiments (see Reference 36), one in a 1 m by 1 m channel and another in a 3 m by 3 m channel. The smaller experiments were performed at stoichiometry, and the larger experiments were performed at lower concentrations in the belief that scaling with λ could occur. At a concentration of 21% hydrogen (ϕ = 0.63), for which λ (ϕ = .63)/λ (ϕ = 1) = 3, DDT occurred. This supports the hypothesis that in similar geometries DDT may occur for mixtures with similarly scaled cell widths. In both cases the apparatus included obstacles and was unvented.

It is important to note that even for these ideal geometries, hydrogen concentrations much above those of the 13% ALWR requirement were required for DDT. Consider a scaling of the unvented FLAME result to a reactor containment: At X = 15% H_2, the equation in Section 2.3.2.1 yields ϕ = 0.42, and from Figure 2-11 λ = 200 mm. For X = 13% H_2, ϕ = .357, and λ = 1 m, so a scale factor of 1000/200 = 5 applies. Using this scale factor on the FLAME channel dimensions, an unvented channel between 5 * 1.83 = 9 m and 5 * 2.44 = 12 m on a side would be necessary for a DDT. Considering a vented channel, at X = 20% H_2, ϕ = 0.6, λ = 25 mm, a scale factor of 40 applies, leading to a channel at least 73 m on a side. This implies that DDT is quite unlikely in an ALWR containment, since this channel width exceeds the containment diameter.

2.3.2.5 Propagation Into Unconfined Regions Given that a detonation can be initiated in a local region, the possibility of its continued propagation throughout the containment was investigated. Propagation of

detonations from confined to open regions also depends upon the detonation cell width λ, and is related to a critical tube diameter d_c. The critical tube diameter is the minimum diameter for which a detonation in the tube will propagate into an open volume. It is related to the cell width by a simple proportionality factor which depends upon tube shape and the exit conditions as shown in Figure 2-18 (see Reference 34). The value of d_c has been observed to vary between 3λ and 13λ, and hypothesized to be as low as 1.5λ.

Consider propagation of a detonation in a dry containment atmosphere with a hydrogen concentration of 13% and, from Figures 2-10 and 2-11, a corresponding detonation cell width of roughly 1 m. From Figure 2-18 this implies a critical slit height of 3 m or a square tube width of 11 m to transmit a detonation from one region to another. That is, assuming a DDT occurs in some confined region, that region must have a dimension greater than 3 m if it is a long, narrow slit (meaning its long dimension is 15 m or more) or a dimension greater than 11 m on a side in order for the detonation to propagate into a larger, confined region. These dimensions are large relative to confined spaces expected in an ALWR.

Thus, even if it were possible to generate an initial detonation in a containment building with a dry atmosphere and a hydrogen concentration near 13%, it would not be possible to propagate this detonation because the critical passage size (tube diameter) is much larger than available connecting pathways. This conclusion is further strengthened when the realistic case of steam addition is considered, for which the critical tube diameter is even larger. For example, just 10% steam increases the required critical dimensions by a factor of about 10.

2.3.2.6 Effect of Sprays and Fan-Induced Turbulence Evidence has been presented which shows that detonations are suppressed by sprays. In his review for IDCOR, Zalosh describes two pertinent experiments.[37] In one set of experiments, propagation of detonations from a driver tube to a test section was suppressed by sprays as indicated by pressure histories with and

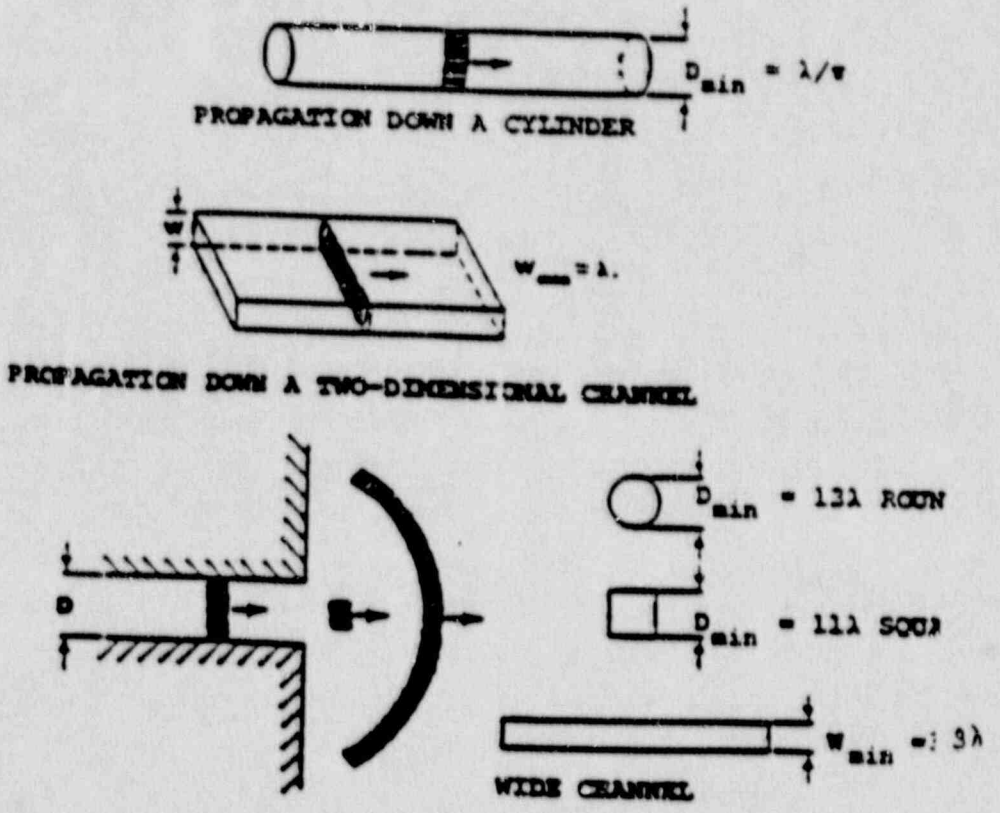

Figure 2-18 Effect of geometry on propagation of detonation waves (reproduced from Reference 33).

without sprays. In another series of experiments, the initiation energy to detonate hydrogen-air mixtures was significantly increased in the presence of water sprays.

There is also evidence that DDT is enhanced by fan-induced turbulence. Berman (see Reference 36) cites experiments in which DDT was caused by fan-induced turbulence, though these are for rich mixtures beyond stoichiometry, with equivalence ratios near 1.6. If detonation cell width can be used to relate these results to lean mixtures below stoichiometry, then similar results might be anticipated for equivalence ratios between 0.7 and 0.8 (i.e., about 25% hydrogen). There is however, no evidence that fan-induced turbulence causes DDT at concentrations near the 13% ALWR requirement.

2.3.3 Detonation Analytical Basis

2.3.3.1 Detonation Cell Width Model Prediction of detonability currently relies upon the Shepherd Model for prediction of detonation cell widths.[44] This model assumes the Zeldovich-Von Neumann-Doring (ZND) one-dimensional detonation shock configuration, and calculates the chemical reaction zone length, E. This length is then related to the detonation cell width λ by a proportionality constant A, $\lambda = AE$, typically chosen so that agreement is achieved at stoichiometry. As shown in Figure 2-19 (see Reference 39), A is not truly constant as a function of hydrogen concentration. This parameter probably also depends upon temperature and pressure. Nonetheless, use of this model yields excellent agreement for the range of currently available experimental data (see Figure 2-12).

Using the Shepherd model detonation cell sizes can be predicted for mixtures with hydrogen concentrations lower than 13% in dry air, or steam concentrations greater than zero for hydrogen concentrations near 13%. Existing facilities are not large enough to measure cell sizes greater than about 1 m, a condition implied by these concentrations. Extrapolation of

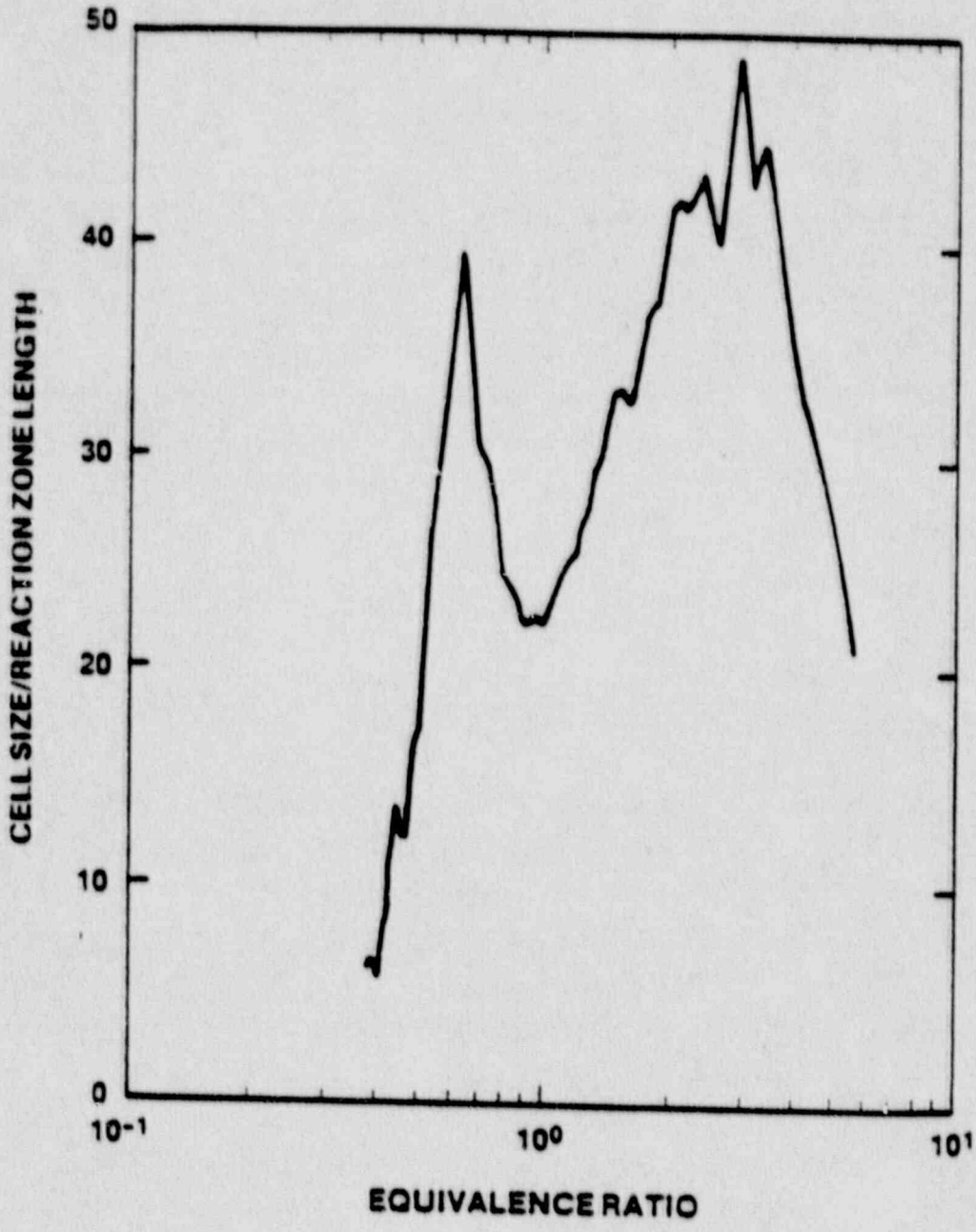

Figure 2-19 Ratio A of cell size λ to reaction zone length Δ for dry H_2-air detonations near 25°C (reproduced from Reference 35).

data with this model aided in the conclusion of Section 2.3.2.5 that detonations, if initiated, cannot propagate to adjacent compartments in ALWR configurations.

No comprehensive model yet exists for prediction of DDT which simultaneously accounts for effects of geometry, turbulence, and inertants expected in an ALWR containment. However, empirical scaling arguments can be applied for these features independently. The ALWR case against the possibility of DDT rests on experimental data which indicate the difficulty to induce DDT at lean hydrogen concentrations. Empirical scaling arguments together with results of the Shepherd model for detonation cell widths of lean or saturated mixtures lead to the conclusion of Section 2.3.2.4 that DDT is highly unlikely in an ALWR containment.

2.3.3.2 Empirical Evaluation of DDT Potential The potential for DDT in an ALWR containment has been evaluated using a procedure for engineering judgement developed by Sherman[45]. The procedure assumes that the potential for DDT can be evaluated based on the mixture intrinsic flammability (detonation cell width) and type of geometry. Five classes of mixture sensitivity are defined ranging from class 1, most detonable and near stoichiometry, to class 5, least detonable, hydrogen mole fraction less than 13.5% in dry air. Five classes of geometry were defined ranging from class 1, most conducive to DDT featuring large geometries with obstacles and partial confinement, to class 5, unfavorable to DDT featuring large scale and complete unconfinement or small scale spherical geometry with central ignition and no obstacles.

Mixture class 5 in this method corresponds to mixtures considered in the ALWR requirement. Geometry classes 1 and 2 of the method are worst case geometries to consider for DDT potential. An example of class 1 geometry is a large tube with numerous obstacles and ignition going from a closed end to an open end. This type of geometry is specifically identified in the ALWR requirements document as a geometry to avoid by design. Class 2 geometry is

defined as similar to class 1 but with some feature which hinders flame acceleration. An example of class 2 geometry is a tube open at both ends or with large amounts of transverse venting. Such a geometry is recommended in the ALWR requirements document in order to promote hydrogen mixing and minimize the potential for DDT.

Results of this engineering judgement procedure for a combination of mixture class 5 and geometry class 2 are appropriate for an ALWR containment. In reference 46, there are five categories of probability of DDT, ranging from category 1, DDT highly likely, to category 5, DDT highly unlikely to DDT impossible (see reference 46). The expert judgement for the combination of mixture class 5 and geometry class 2 is result category 5, DDT highly unlikely to impossible. This is a best judgement for the potential for DDT in an ALWR containment. Even if a class 1 geometry were to exist in an ALWR containment, the result category is 4, defined as DDT possible but unlikely.

This evaluation supplements the scaling arguments put forward above and reinforces the conclusion that DDT will be unlikely to impossible in an ALWR containment designed according to the EPRI ALWR requirements document.

2.3.3.3 ALWR Containment Analysis Experimental data and the predictions of the Shepherd model can be applied to an evaluation of an ALWR containment for the potential for detonability.

Predictions of hydrogen mixing and combustion in an ALWR containment have been carried out[46] using the MAAP 3.0B auxiliary building model[47] and the ARSAP combustion model.[48] The MAAP 3.0B auxiliary building model uses state-of-the-art correlations for intercompartmental flow based on experiments by Epstein.[49] An arbitrary volume junction, and heat sink nodalization is allowed by the model. A schematic of the nodalization of the ALWR containment appears in Figure 2-20.

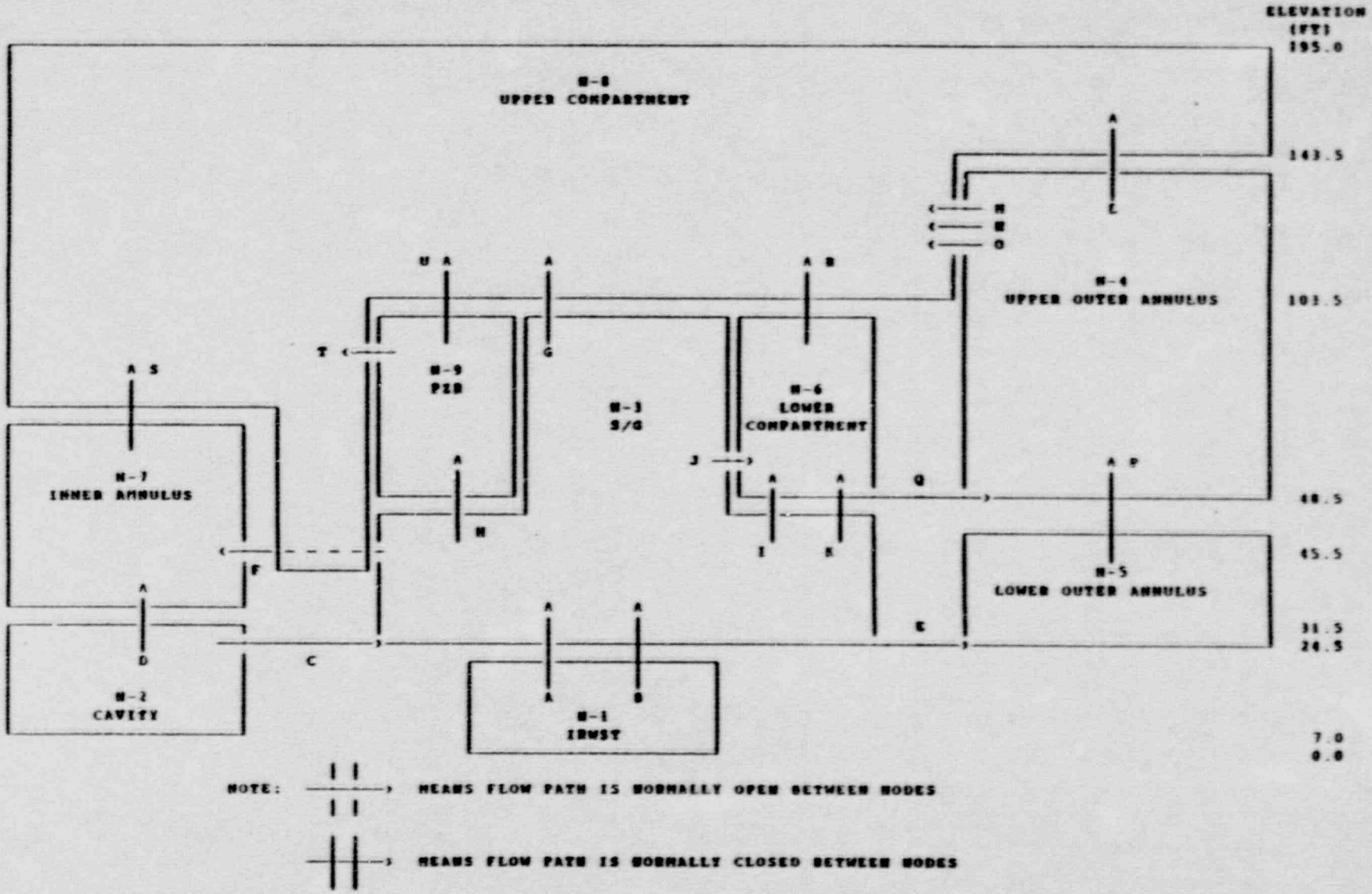

Figure 2-20 **Nodalization of System 80+ Spherical Containment used for Hydrogen Mixing Studies.**

The ARSAP combustion model contains a state-of-the-art flammability limit model and a model for combustion completeness. It was designed to resolve NRC concerns about differences between MAAP and HECTR[50], the NRC model. The ARSAP model uses a temperature-dependent H_2-CO-Air-H_2O-CO_2-N_2 flammability limit diagram. Burn time and combustion completeness agree well with large scale experiments and burn time is conservatively underpredicted for low hydrogen concentrations.[48]

In these simulations, the MAAP 3.0B code was used to provide a hydrogen source rate for a variety of accident sequences. An amount of hydrogen equivalent to 75% clad oxidation was forced for all runs by adding a "tail" onto the source. This was necessary because MAAP models predicted lower than 75% clad oxidation in all cases.

The ALWR containment mixing simulations showed that the only region with the potential for greater than 13% hydrogen was the IRWST (Internal Refueling Water Storage Tank) gas plenum. All other regions had peak hydrogen concentrations below this value for all cases. Design of the IRWST to include a large vent area and to allow faster heatup of the pool (to promote high containment steam fractions during an accident) is possible to promote mixing and prevent hydrogen accumulation. Figures 2-21 and 2-22 show hydrogen concentrations for a base case IRWST design and a modified IRWST design respectively during a high pressure station blackout sequence. This sequence was chosen because it is the limiting case of low flow rates to the IRWST and hence the least pool heatup, steam generation, and hydrogen mixing. The base case hydrogen concentration goes into the rich realm in the IRWST, while the modified IRWST case exhibits a steady buildup to the maximum value.

2.3.4 LDB Hydrogen Detonation Summary

The EPRI ALWR requirement for hydrogen in containment is supported by the following logic which demonstrates that the possibility of detonation in containment is remote. Detonations can be initiated through either direct

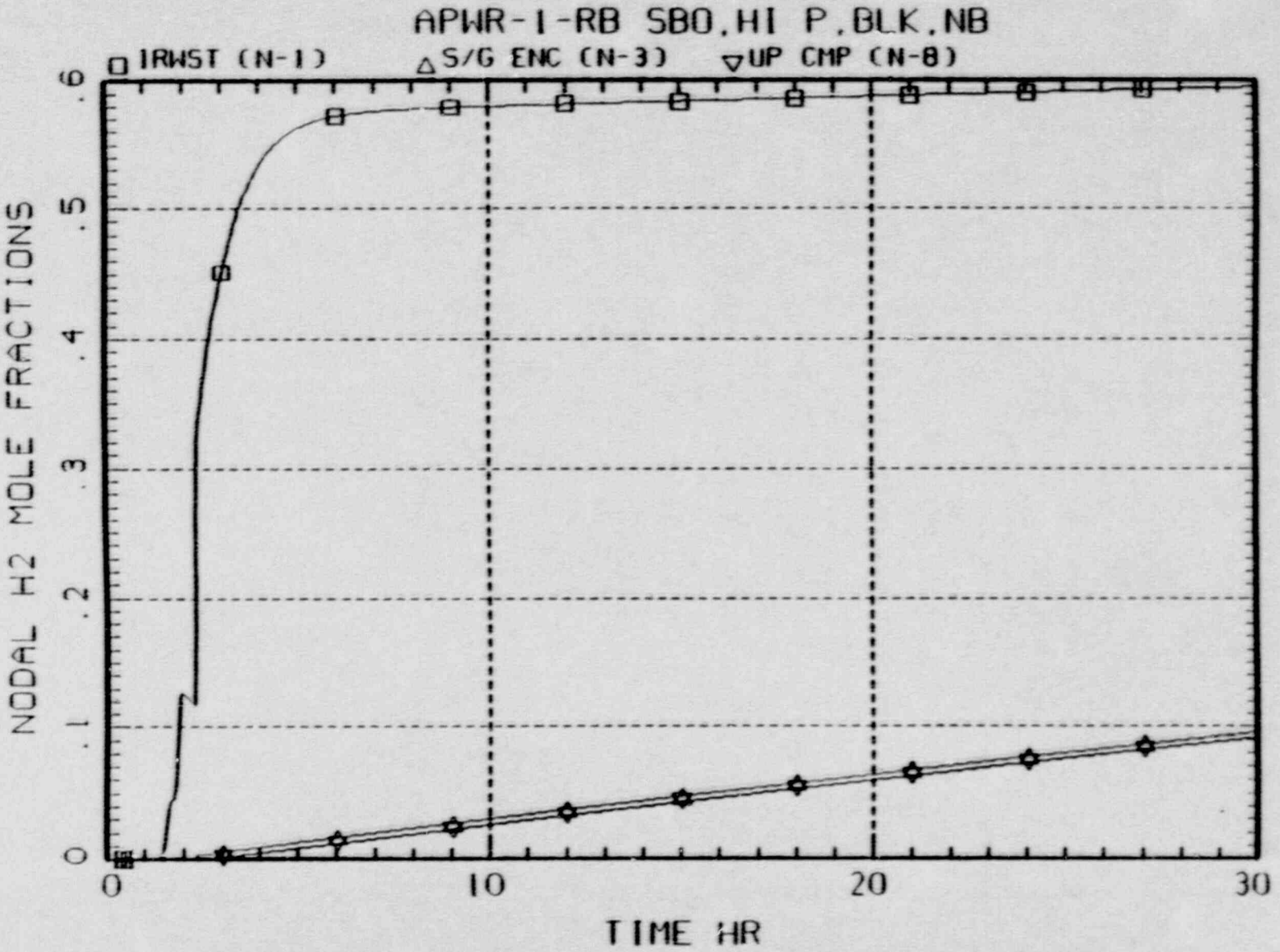

Figure 2-21 Hydrogen concentrations in the base case IRWST. (Steam generator enclosures and upper compartment during a high-pressure SBO with blockage and no burns.)

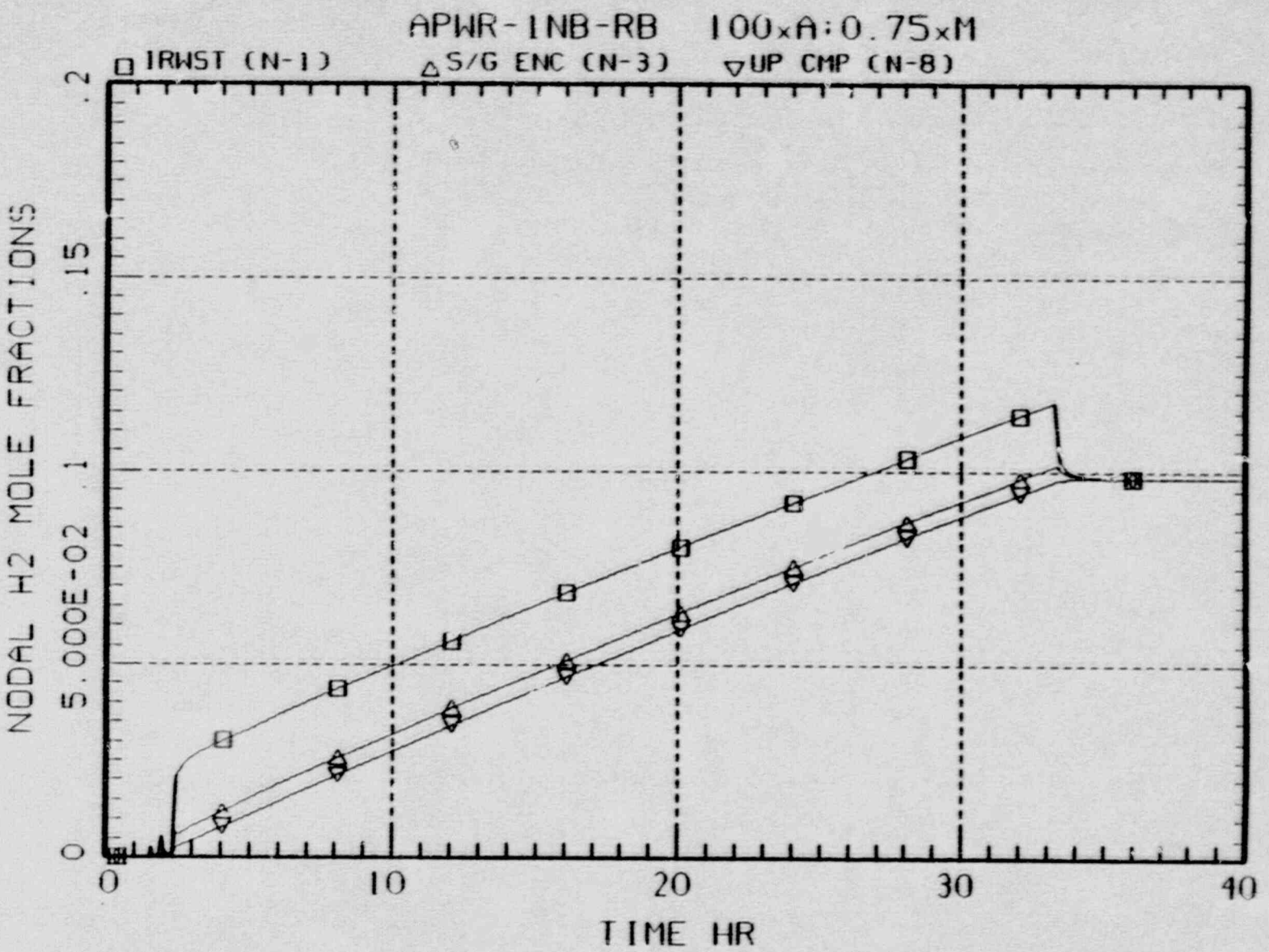

Figure 2-22 Hydrogen concentrations in the modified IRWST. (Steam generator enclosures and upper compartment during a high-pressure SBO with blockage and no burns.)

initiation by energy deposition or by DDT. Direct initiation of a detonation requires energy deposition in an amount about 10 orders of magnitude higher than necessary for initiation of a deflagration, and 2 to 3 orders of magnitude higher than conceivably available in a containment. Therefore, it is extremely improbable that a detonation would be initiated rather than a deflagration due to energy deposition, or in other words, it is virtually certain that energy deposition will initiate a deflagration and not a detonation in a containment. This leaves DDT as the only reasonable physical mechanism for initiation of a detonation.

DDT is influenced by mixture composition, temperature, pressure, and geometry. The former three parameters can be combined into a single parameter which represents the sensitivity of a mixture. This is the detonation cell width and it can be related to the intrinsic detonability of a mixture. The potential for DDT can be judged by examining the cell width of a mixture and geometry of a region. When experimental results are extrapolated to calculate cell widths for possible ALWR mixtures, and when experimental observations of DDT are used to relate the cell widths to geometry, a judgement of the potential for DDT can be made for ALWR mixtures in ALWR geometry. From this assessment, it is concluded that DDT is unlikely to impossible for ALWR geometry when the EPRI ALWR requirements document is followed.

3.0 RISK EVALUATION BASIS (REB) TECHNICAL EVALUATION

The Risk Evaluation Basis (REB) for the EPRI ALWR hydrogen requirement is presented here in separate sections for the hydrogen source, deflagrations, and detonations. Cases considered within the REB include those accidents which involve reactor vessel failure. Therefore, hydrogen sources due to debris quenching and core concrete interactions are considered. Since the hydrogen source can potentially exceed 75% MWR, the pressure rise due to deflagrations is reconsidered. The effect of additional hydrogen and steam on detonations is also examined. In accordance with the EPRI Requirements Document, REB evaluation uses probabilistic arguments and is based on best-estimate analysis of phenomenology.

3.1 Ex-Vessel Hydrogen Generation Evaluation

In Section 2.1.4, ALWR hydrogen generation predictions were introduced (see Table 2-3 and 2-4) and a discussion of the matrix of sequences studied was provided. Results for the REB cases are presented in Tables 3-1 and 3-2 (note that the case numbering is consistent with the numbering in Table 2-3). For these ex-vessel sequences the potential contributors to hydrogen generation are: in-vessel oxidation prior to vessel failure, oxidation during core melt ejection, core concrete interaction (CCI), in-vessel oxidation after vessel failure, and quenching during long-term relocation. The logic for evaluation of these contributors is illustrated in Figure 3-1.

In these analyses, no credit has been taken prior to one hour after RV failure for water from the IRWST being present in the reactor cavity. In the ALWR, water from the IRWST should flood the cavity before one hour after vessel failure and thereby quench the corium in the cavity such that the hydrogen produced by core-concrete interaction would be greatly reduced. (Note that for the cases in Table 3-1 the corium in the cavity at the time of RV failure was less than 40% of core inventory and did not exceed 60% by one hour after vessel failure. For these quantities of debris in a large ALWR cavity, corium is coolable whenever the cavity is flooded).

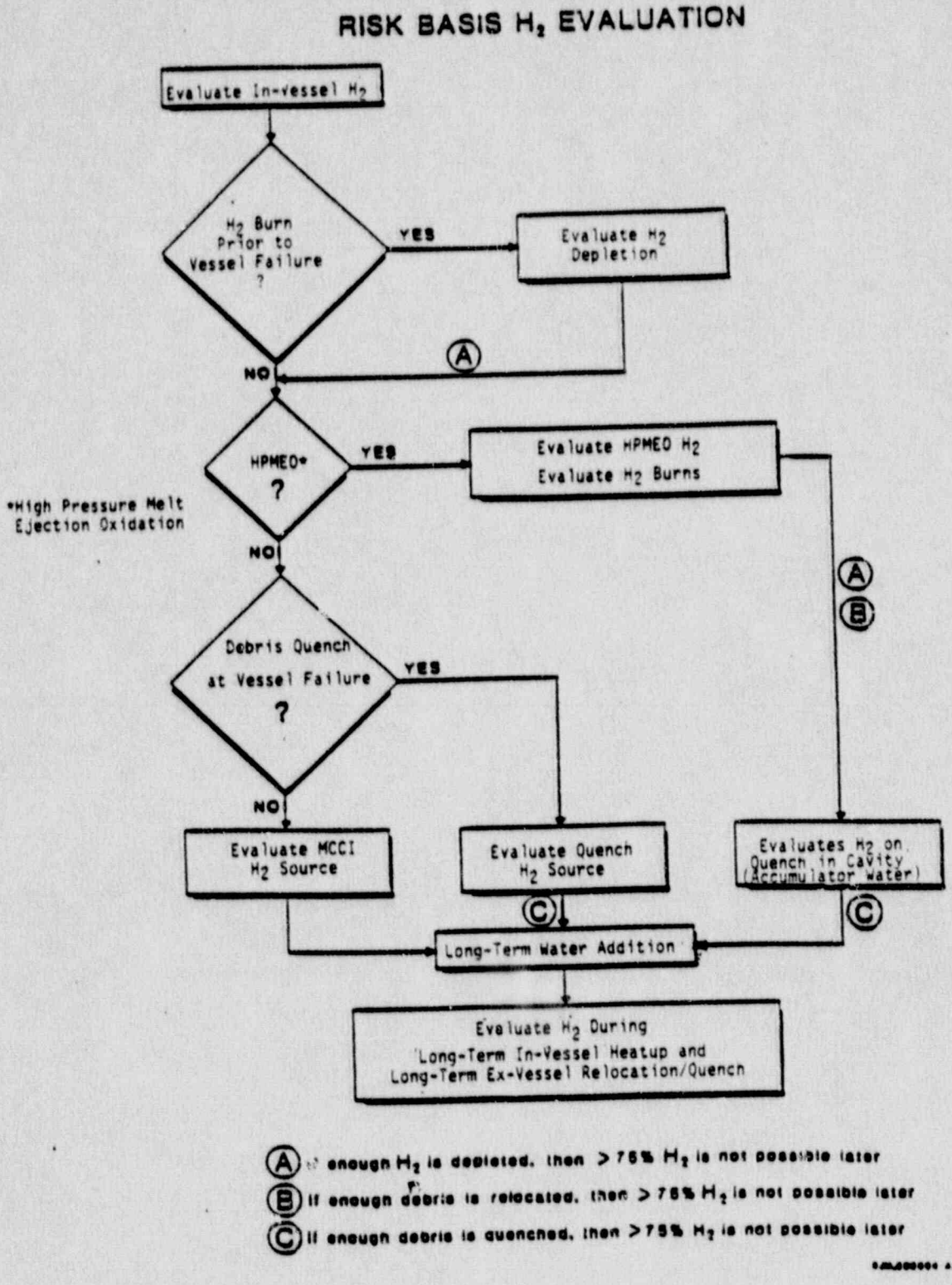

Figure 3-1 Logic diagram for risk evaluation basis hydrogen evaluation.

Table 3-1 Risk Evaluation Basis: MAAP-DOE Summary For Ex-Vessel (No Recovery) Cases

Sequence Number	Sequence Type[1]	Core Uncovery (Sec)	Vessel Failure (Sec)	Hydrogen Contributions[4]				
				In-Vessel Before VF	DCH	CCI[3]	In-Vessel After VF	Long Term Relocation[2]
1	Large LOCA	119	2840	27.3%	0%	4.3%	3.0%	13.7%
4	Medium LOCA	1068	7189	32.0%	0%	0%	8.7%	12.1%
5	Small LOCA	4768	7378	32.7%	0%	0%	6.1%	12.4%
7	Small LOCA	4243	11835	29.2%	0%	0%	5.2%	13.1%
12	SBO	6694	9974	28.5%	27.5%	0%	3.0%	9.4%
14	SBO	6688	9638	20.8%	11.7%	0%	2.9%	12.9%
15	SBO	5892	13810	32.2%	0%	0%	4.2%	12.8%

(1) All cases assumed a dry cavity at vessel failure, conservatively delaying the effects of cavity flooding from the IRWST for one hour to bound the best-estimate range.

(2) Long term relocation refers to the continued core heatup after vessel failure and relocation of debris from the vessel to the water pool in the cavity. The relocation is modeled as debris droplets which are quenched in the pool. Hydrogen is produced during the droplets falling through the steam-rich cavity and their quenching in the cavity's water pool.

(3) Concrete attack was calculated when dry debris conditions were predicted up to one hour after vessel failure pending effective cavity flooding by the IRWST.

(4) Hydrogen contributions are reported as percent of active fuel cladding oxidized.

Table 3-2 Risk Evaluation Basis: MAAP-DOE Results Summary for Ex-Vessel (No Recovery) Cases (1)

Sequence Number	Sequence Type	Hydrogen Burned Before VF	Hydrogen Burned After VF	Total[2] Ex-Vessel Hydrogen	Mass Zirconium Quenched in Cavity
1	Large LOCA	0%	0%	48.3%	74.4%
4	Medium LOCA	0%	0%	52.8%	69.9%
5	Small LOCA	3.5%	0%	47.7%	71.5%
7	Small LOCA	0%	0%	47.5%	75.2%
12	SBO	3.7%	34.6%	30.1%	54.3%
14	SBO	0%	0%	48.3%	74.4%
15	SBO	0%	0%	49.2%	73.5%

Note: (1) All percents are reported as percent of active cladding.

(2) Provided to demonstrate that total zirconium inventory is conserved. Does not necessarily represent the peak containment hydrogen level.

All the ex-vessel or REB cases (except case 14) reported in Table 3-1 and 3-2 did not allow the recovery of core cooling capability and thus, are low probability sequences. Case 14 considered recovery but it was too late in the sequence to effectively cool the damaged core, so vessel failure was still predicted. The majority of the hydrogen production for these sequences was predicted to be in-vessel before vessel failure. The most significant ex-vessel hydrogen sources were high pressure melt ejection oxidation (HPMEO) and long term relocation. HPMEO requires high pressure in the primary system which usually means that some water remains in the primary system and that accumulator water is not depleted at the time of vessel failure. Therefore, following the reactor vessel failure, water is available to quench the corium in the cavity and prevent a core-concrete interaction until the cavity becomes dry, even if no water is initially supplied from the IRWST. With the exception of the large LOCA, the sequences with low pressure at vessel failure also provide sufficient water to quench the corium in the cavity and prevent core-concrete interaction.

These best-estimate assessments indicate that hydrogen may burn prior to vessel failure and thereby limit the maximum containment hydrogen concentration to a value less than that corresponding to the integral total hydrogen production for the sequence. Appendix B provides time histories which demonstrate this point. Also, Table 3-2 summarizes the hydrogen burned both before and after vessel failure for each REB sequence.

A significant result of the REB cases is presented in Table 3-2. The four columns represent an accounting of the total zirconium inventory at approximately one hour after vessel failure. It should be noted that the best-estimate calculations provided in this report considered the total Zr inventory in the reactor vessel for a conceptual ALWR design. The total inventory exceeds the Zr inventory that resides in the cladding on the active fuel. The calculated amounts of Zr reacted for each sequence have all been presented as percent of the mass of Zr in the active fuel cladding. This basis was chosen to be consistent with the nomenclature in the Federal Regulations. This reporting basis leads to the possibility of

reporting up to 122.7% metal water reaction (MWR) for this conceptual ALWR design if the total Zr mass inside the reactor vessel should be oxidized. Thus, the sum of the four columns (Hydrogen Burned Before VF, Hydrogen Burned After VF, Total Ex-Vessel Hydrogen, Mass Zirconium Quenched in Cavity) for each sequence is 122.7%. Per the logic illustrated in Figure 3-1, all the REB sequences (1, 4, 5, 7, 12, 14, and 15) show that the quenched Zr inventory equals or exceeds 47.7% (122.7%-75%) and therefore, they can not produce more than 75% MWR as long as the quenched debris remains cooled. The ALWR Requirements Document provides for the capability of providing long term flooding of the reactor cavity and thereby long term debris cooling. These results are favorable for the REB as they do not exceed the LDB design value for Hydrogen generation. When a hydrogen burn prior to vessel failure is considered (which is possible for an SBO sequence and is calculated to occur by the improved MAAP-DOE combustion model), then a larger margin is provided to satisfy both the LDB and REB requirements.

The timing of the manual initiation of depressurization was also studied by looking at times before and after steam generator dryout at different depressurization capacities. The results suggest that the impact of timing of the manual initiation of depressurization is sequence specific. All cases at prototypical depressurization capacity involved in-vessel hydrogen generation well below the LDB limit, however, so this timing sensitivity does not impact the conclusions drawn for the LDB evaluation.

Perhaps the key insight from the REB sequences is the potential for significant hydrogen generation during manual depressurization sequences. Optimizing operation can involve the interface between emergency operation procedures and severe accident management actions. This interface must be provided on a plant-specific basis, supported by an appropriate PRA. Highest priority is expected to be assigned to vessel failure prevention (recovery) strategies with some latitude remaining to affect mitigation. ALWR depressurization system designs afford sufficient capacity to minimize any conflict. The sequences provided in this report demonstrate that such an optimization is within the capability of the conceptual ALWR design without exceeding the LDB hydrogen generation limit.

It can be concluded that analysis using the MAAP-DOE model confirms the expected range of peak hydrogen for more-severe accidents is bounded by the EPRI ALWR requirement for LDB hydrogen generation even when representative uncertainties are considered in the modelling of controlling phenomena.

3.2 Hydrogen Deflagration Evaluation

The maximum hydrogen production found during the REB sample cases was less than 75% MWR when cavity flooding was considered. Therefore, the thermodynamic calculations presented in Section 2.2.4 provide a bounding calculation of containment pressure following a burn. This emphasizes the importance of debris quenching and cavity flooding to prevent or terminate core concrete interactions.

3.3 Hydrogen Detonation Evaluation

3.3.1 Potential for Mixture Detonability

Conclusions reached in Section 2 regarding the potential for hydrogen detonation in a reactor containment were made primarily from consideration of experimental data with dry hydrogen-air mixtures at relatively low temperatures. Two important differences between these ideal cases and a prototypical reactor containment case are elevated temperature and the presence of steam as a dilutent gas. In a reactor containment, it is unrealistic to consider the temperature effect alone.

When steam is present, it was shown in Section 2.3.2.2 that the detonation cell width is strongly affected, and that the cell width increases with steam concentration (Figure 2-11). While the potential for detonations in mixtures varies by the same proportion, the change in the

cell width varies proportionally with equivalence ratio in a nonlinear manner, so extrapolation to leaner hydrogen concentrations is somewhat difficult. Near stoichiometry, 10% steam addition at 100°C raises the detonation cell size by a factor of 7, and at the leanest available mixture data pair from Figure 2-11, the ratio is about 10.

A scale factor of 10 can therefore be applied to the numbers derived in Section 2.3.2.2 as an exercise in determining the effect of steam addition. Cell width scaling is performed by taking the ratio of detonation cell widths and applying this ratio to physical scale, as suggested by the proportionality of cell width and physical scale at incipient detonation (see section 2.3.2.1). Considering the potential for DDT, the FLAME facility dimensions of 1.83 m x 2.44 m would require an increase to 18.3 m x 24.4 m in cross section in order to potentially lead to DDT at 15% H_2 for an unvented configuration. Even for this mixture which is more sensitive than the maximum predicted for an ALWR, since such an unvented duct would not exist in an ALWR, DDT is clearly unlikely, even at 15%. Considering the potential for propagation of a detonation, a critical slit height of 3 m (see Section 2.3.2.5) would require an increase to 30 m in order to potentially transmit a detonation to another region. Since no intercompartmental connection would be of this size in an ALWR containment, propagation of a detonation is clearly unlikely for an ALWR. Indeed, these extrapolations suggest that a facility larger than a containment would be required to observe detonations in mixtures corresponding to the ALWR requirement and containing realistic concentrations of steam (see Section 3.3.2).

It is also significant to observe that for realistic accident sequences the presence of steam in the containment and elevated temperatures are coupled. Elevated temperatures always occur with high steam mole fractions. The elevated containment temperature range is of the order 120-140°C with a corresponding steam mole fraction in excess of 30%. The absolute level of the containment temperature does not result in a small cell size. Additionally, the co-existence of steam significantly increases the detonation cell width such that for realistic containment conditions detonations would not be predicted.

The model for prediction of detonation cell widths (see Reference 44) has recently been used to extrapolate to higher temperatures, beyond available experimental data (see Reference 34). According to these predictions, the cell width for lean concentrations in dry air is reduced by over an order of magnitude as temperature is increased from 300°K to 500°K, as shown in Figure 3-2 (see Reference 35). The leanest mixture shown in Figure 3-2 is one with 15% hydrogen, and leaner concentrations (lower equivalence ratios) would lie to the right of that curve at low temperatures, and exhibit minima at correspondingly higher temperatures. The important results of this extrapolation are that for lean concentrations, cell width can be reduced to under 10 cm at temperatures between 500 and 600°K, and that all mixtures of hydrogen in dry air appear to be nearly equally sensitive to detonation above these temperatures.

When the model is applied to cases with steam, as shown in Figure 3-3, temperatures in excess of 600°K are required to bring the cell size under 1 m for 30% steam and 17% hydrogen. Again, for leaner mixtures, curves above and to the right of those shown would apply, and the minima would be shifted to higher temperatures. This extrapolation shows that the inerting effect of steam, which is remarkable at low temperatures, diminishes and appears to vanish at temperatures above 800°K. Also, all mixtures are equally sensitive at such high temperatures.

The potential for such high temperatures in an ALWR simply does not exist because of the presence of water in the containment as specified through the EPRI requirements document. For an ALWR, the atmosphere thermodynamic state is constrained to saturated (100%) humidity states with limiting hydrogen concentrations given by the line of possible compositions in Figure 2-8. As shown in Table 2-4, a maximum temperature of 375 K (102 °C) prior to a burn would be expected. Therefore, the inerting effect of steam will dominate the effect of temperature by several orders of magnitude on cell size.

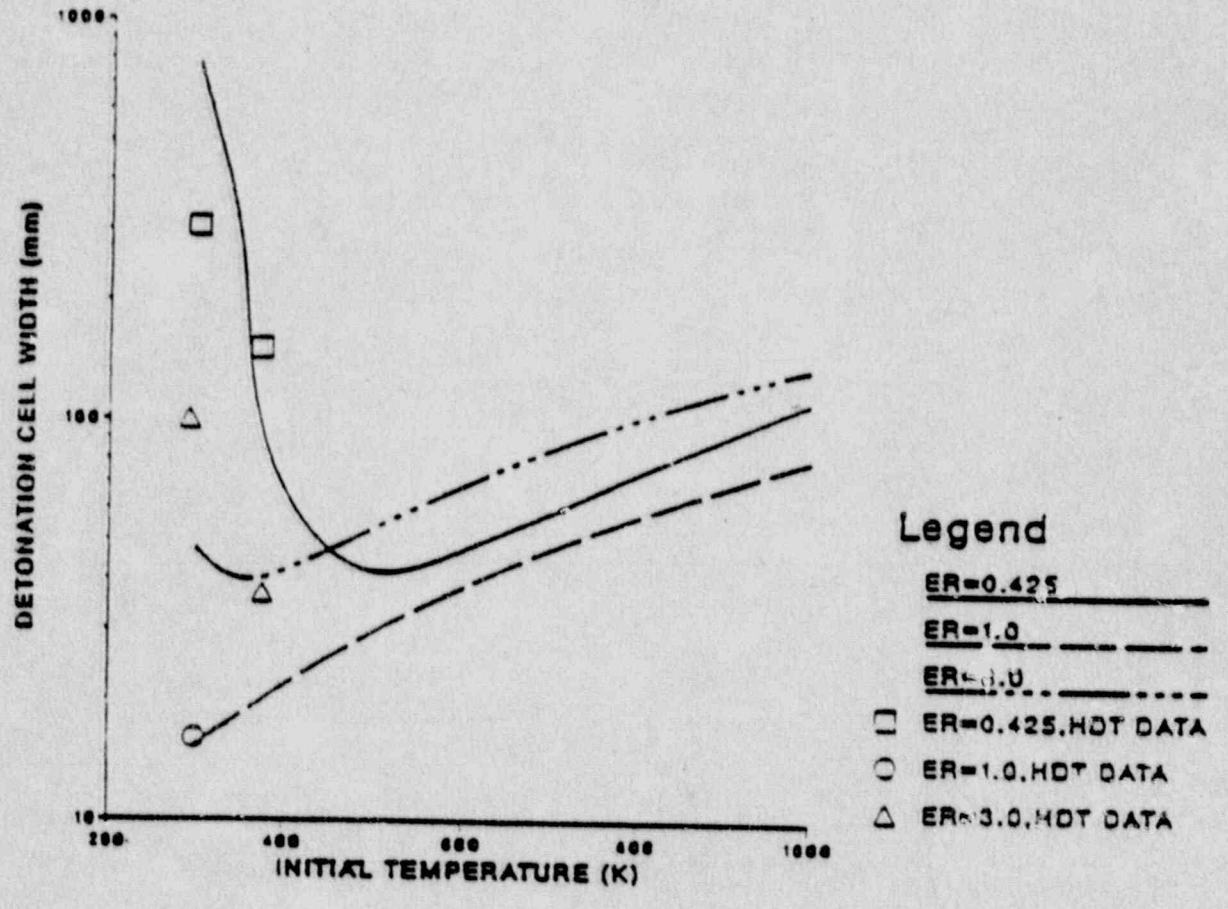

Figure 3-2 Calculated detonation cell width as a function of initial temperature for various equivalence ratios, ER (reproduced from Reference 34).

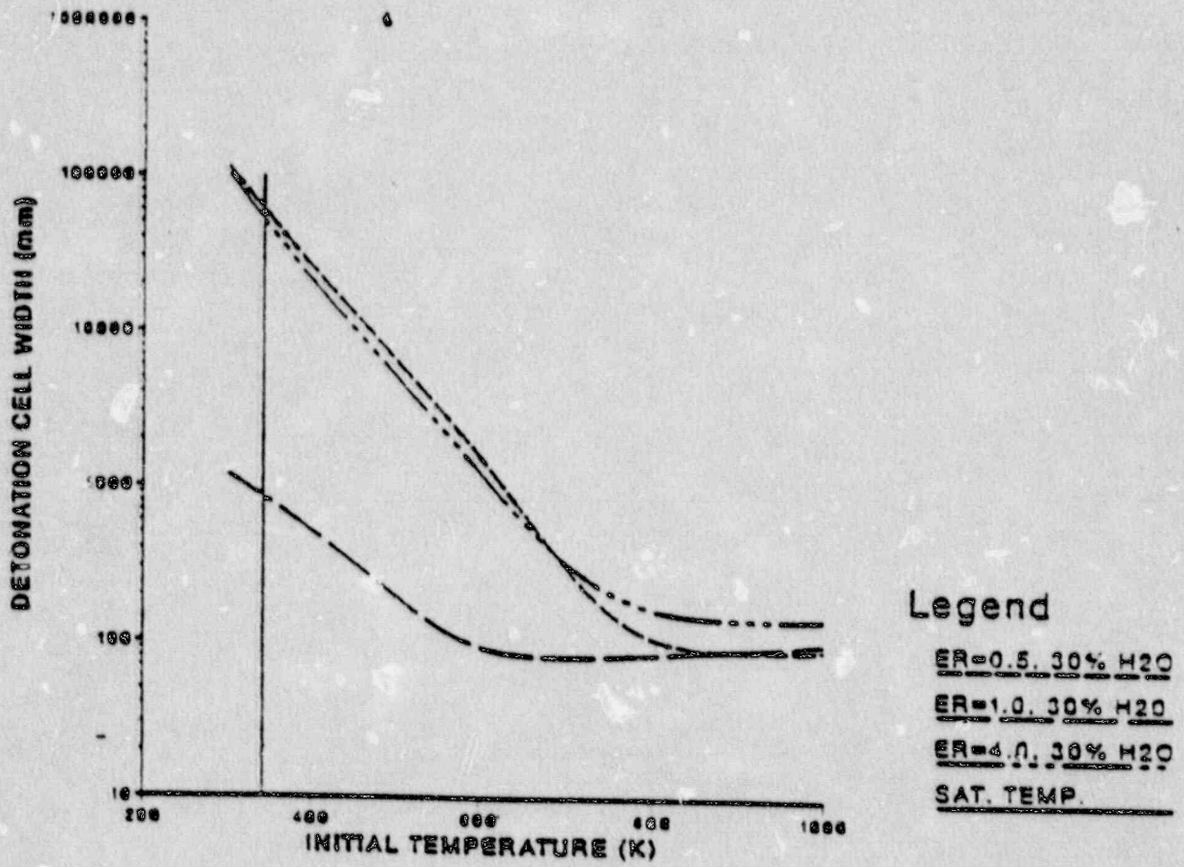

Figure 3-3 Calculated detonation cell width as a function of initial temperature for various equivalence ratios and 30% steam (reproduced from Reference 34).

Uncertainty in the model used to predict detonation cell widths exists because of uncertainty in the parameter A which relates the detonation cell width λ to the chemical reaction zone width Δ (see Figure 2-13). A factor of two is generally considered to be reasonable for uncertainty in this parameter, although it may be larger for conditions outside the realm of experimental data. When realistic containment conditions including high steam concentrations are considered, this uncertainty is not significant because of the increased cell width due to steam.

The detonation cell width has also been predicted to decrease slightly with increasing initial pressure for atmospheres of interest in ALWR cases [51]. However, the decrease is less than a factor of two for mixtures flammable in an ALWR, and it would be dwarfed by the increase due to steam addition.

3.3.2 ALWR Containment Analysis

Containment hydrogen concentrations were described in Section 2.3.3.2 for an ALWR design including an IRWST. Because the primary system is vented through the IRWST, the potential for low steam content and high hydrogen content is higher for certain sequences in this design compared to a design lacking the quenching that can be provided by an IRWST. The steam content in various containment regions for four sequences is presented here and is summarized from a larger set of sequences in reference 32. Cases with no hydrogen burns are selected to minimize steam content.

Table 3-3 compares the long-term steam mole fraction in three containment locations: the IRWST, the upper (main) compartment, and "lowest" meaning the lowest observed value throughout the containment. The time history of steam content is presented for these sequences in Figures 3-4 to 3-7. It can be seen that the case of lowest steam content is for a high pressure station blackout. This is because steam and hydrogen enter the

Table 3-3. Steam Content in an ALWR Containment with an IRWST for Selected Sequences

Sequence	Steam Content (%)		
	IRWST	Upper Compartment	Lowest Value
High Pressure Blackout	7	8	8
Low Pressure Blackout	25	17	17
Large LOCA	15	30	30
Small LOCA	13	26	25

RWST only when the pressurizer safety valve lifts; thus, there is substantial condensation. Because of the ALWR depressurization capability, high pressure station blackout is expected to be a very low probability sequence. In the case of a low pressure station blackout, depressurization leads to heating of the IRWST and significant steam in the atmosphere. Naturally the steam content is high in LOCA cases since the primary system relieves directly into the containment atmosphere.

3.3.3 Scaling Analysis of DDT Potential

Using the above information together with the information from Section 2.3.2, the margin to detonability for a realistic ALWR design may be estimated by scaling detonation cell width, λ. The potential for DDT considering the effects of hydrogen concentration, geometry, and steam concentration will be considered here by relating experimental data to an ALWR containment situation. Initiation by energy deposition is not considered due to the large trigger energy required.

As pointed out in Section 2.3.2.4, the ratio of detonation cell widths for χ = 15% H_2 (observed DDT for unvented FLAME experiments) and χ = 13% H_2 is about 5. Also, the ratio of cell widths for χ = 20% H_2 (observed DDT for vented FLAME experiments) and χ = 13% H_2 is about 40. Finally, a cell width ratio of about 10 applies for steam concentrations slightly above 10% at stoichiometry and for about 10% steam at lower hydrogen concentrations.

Temperatures under 120 °C are of interest because the steam concentration would be high enough to inert a mixture at any higher temperature in an ALWR (see Section 2.2.4).

For these conditions, close to the range of available data, the scaling factors for geometry and steam are roughly separable. A factor of two will nonetheless be applied for uncertainty. This implies that an unvented ALWR

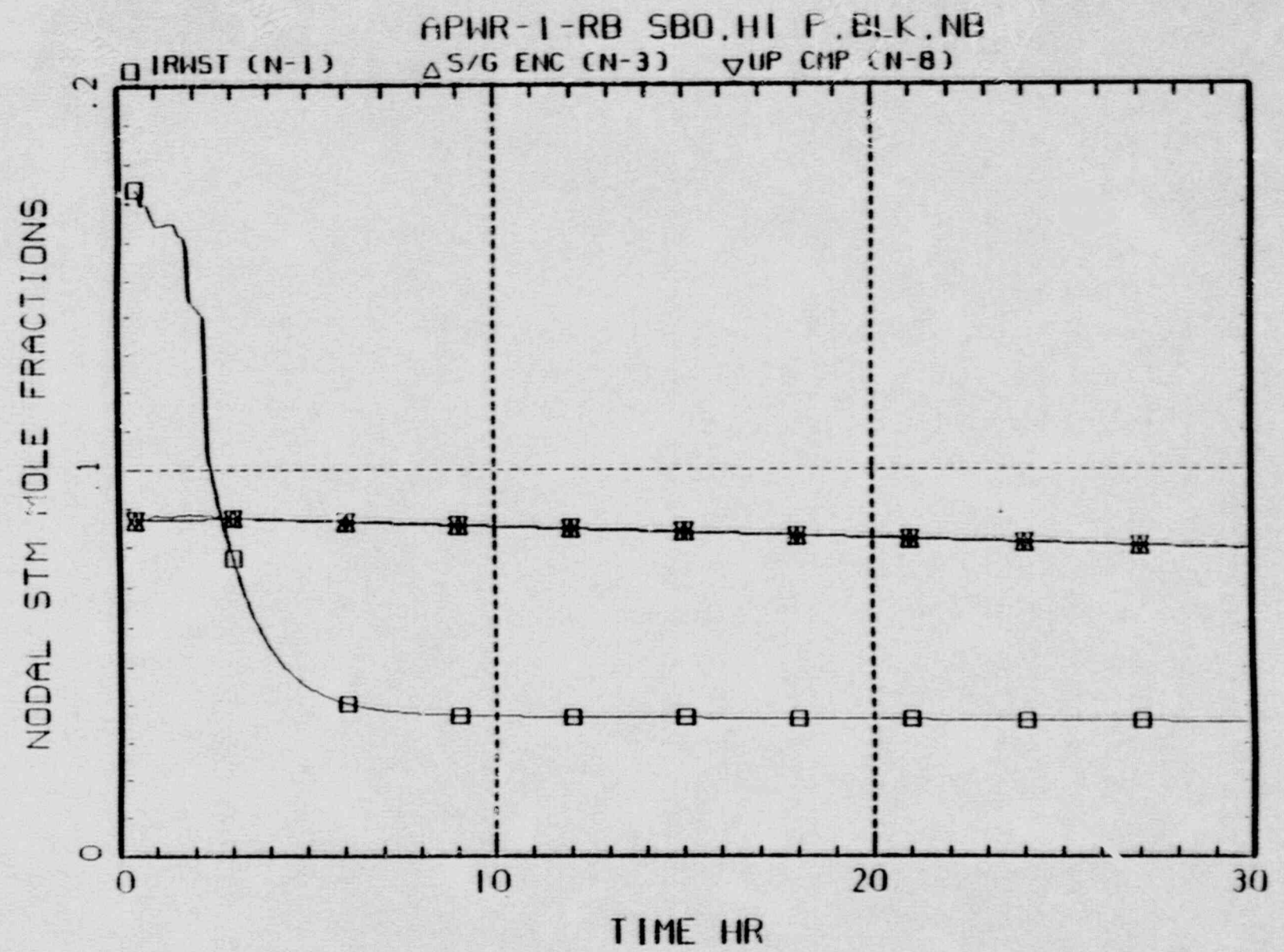

Figure 3-4 Steam Concentrations in the IRWST. Steam Generator Enclosures, and Upper Compartment during a High-Pressure SBO with Blockage and No Burns.

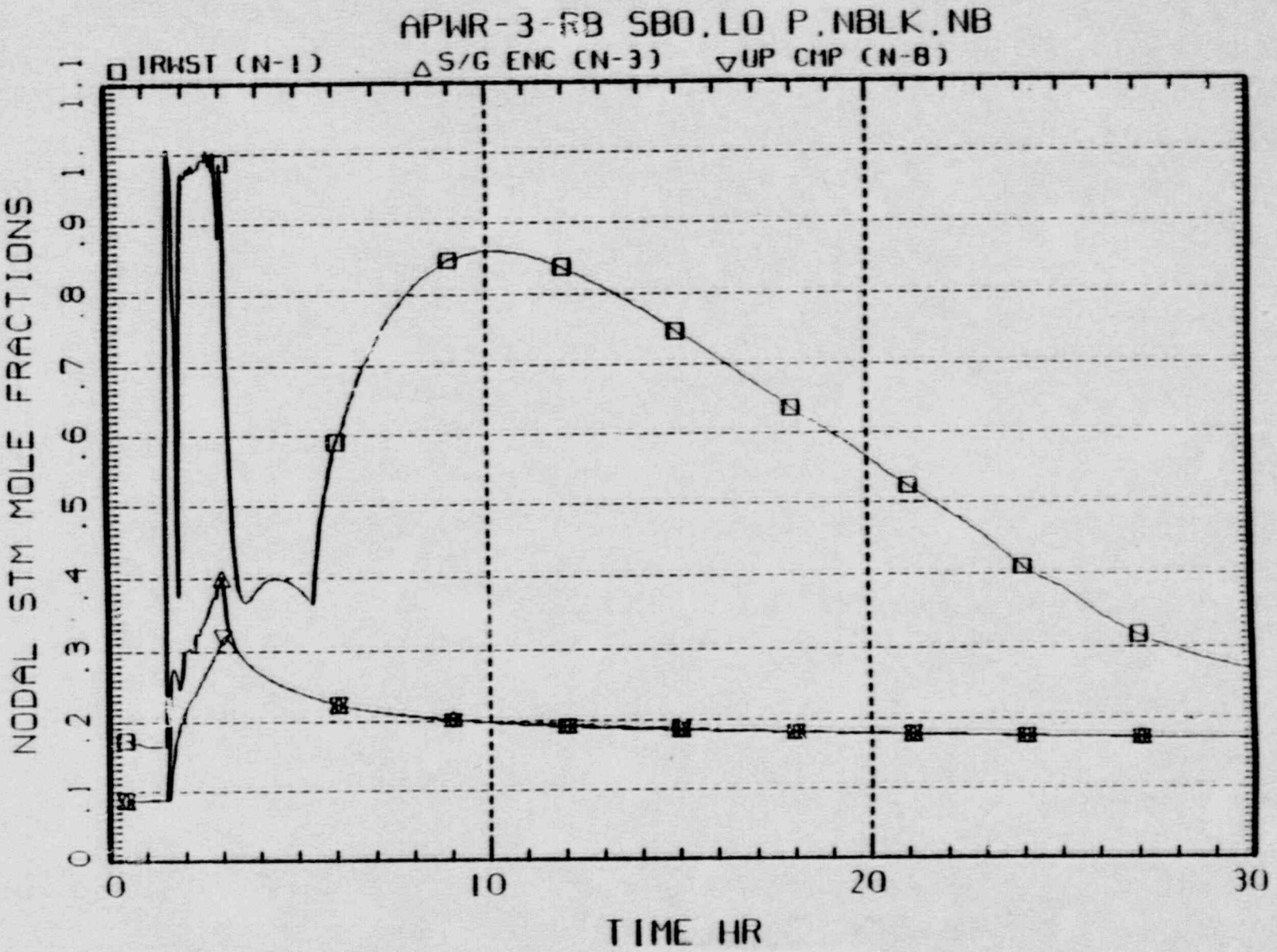

Figure 3-5 Steam Concentrations in the IRWST. Steam Generator Enclosures, and Upper Compartment during a Low-Pressure SBO without Burns (No Blockage).

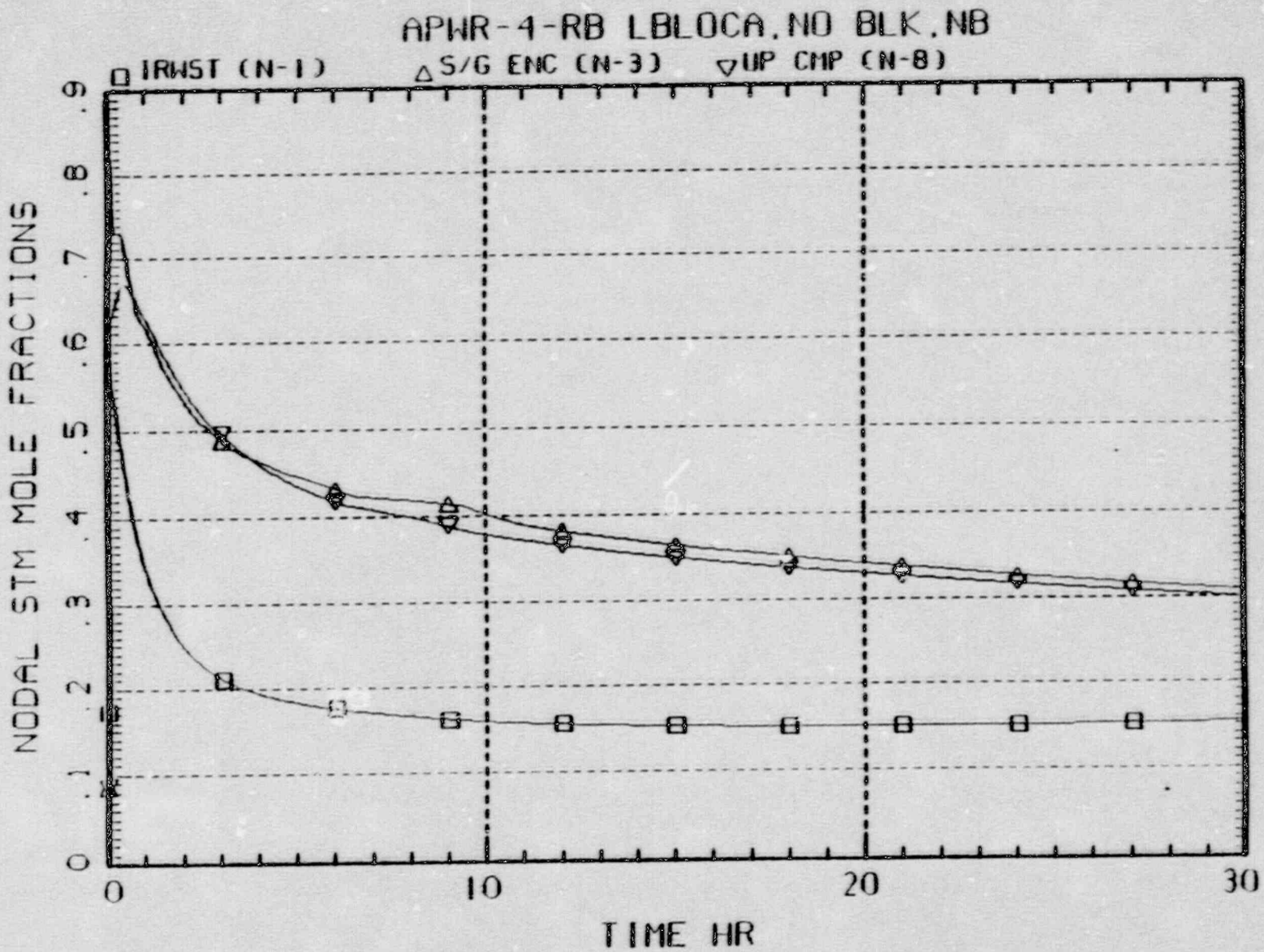

Figure 3-6 Steam Concentrations in the IRWST. Steam Generator Enclosures, and Upper Compartment during a Large Break LOCA without Burns (No Blockage).

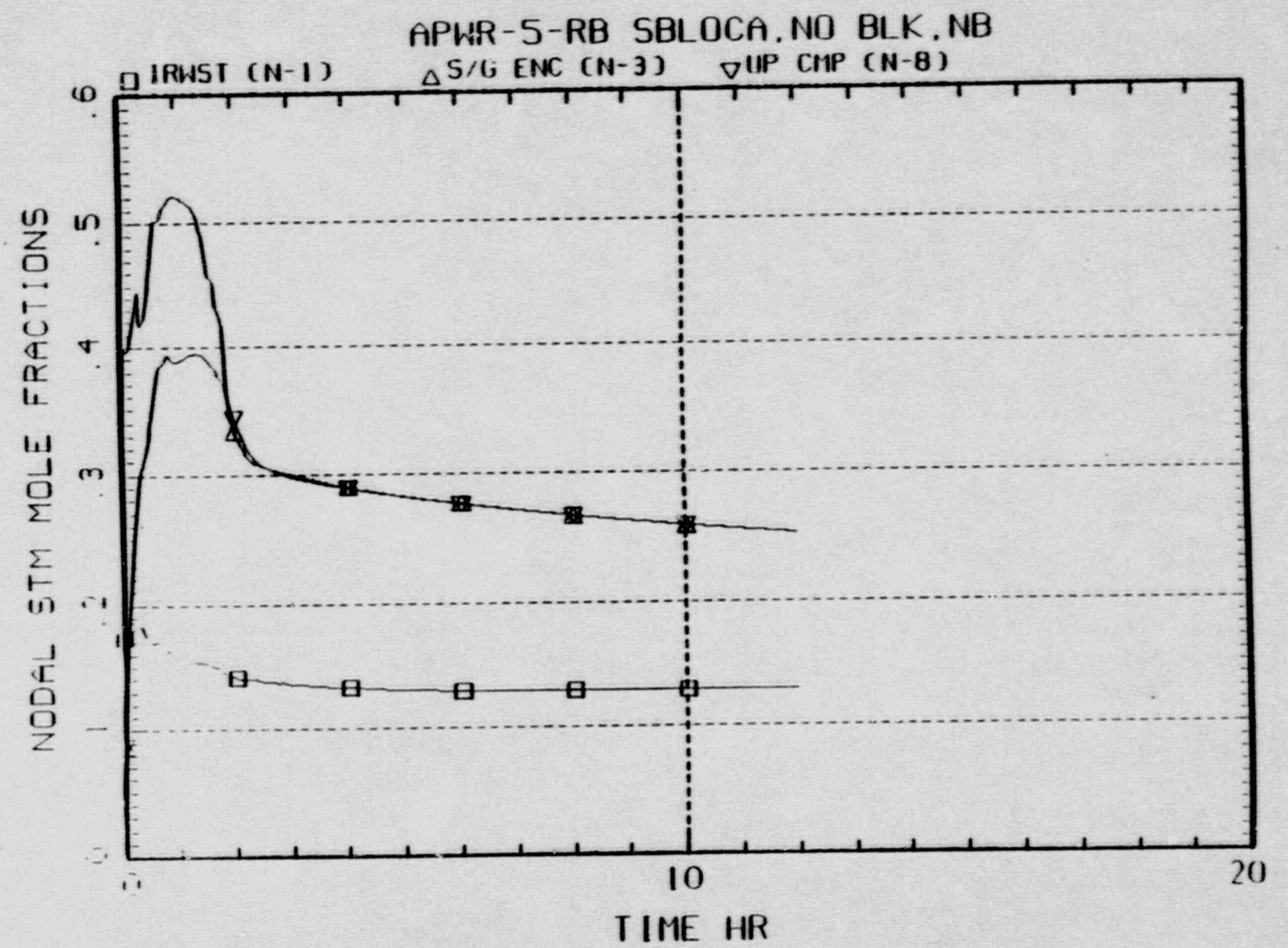

Figure 3-7 Steam Concentrations in the IRWST. Steam Generator Enclosures, and Upper Compartment during a Small Break LOCA without Burns (No Blockage).

compartment with dimensions scaled up from the FLAME dimensions to a minimum of 1.83 m x 5 x 20/2 = 45.75 m by 2.44 x 5 x 10/2 = 61 m would be necessary to observe DDT. This is beyond any conceivable unvented cross sectional area in an ALWR containment. When venting is considered, the required dimensions become a factor of 8 higher and are even more unlikely.

For DDT to be possible in an ALWR containment, these scaling factors must be reduced by changing the initial hydrogen concentration. Considering the available data, it would appear that at least 15% hydrogen in dry air would be required to allow DDT in an ALWR containment. The actual concentration necessary for DDT in an ALWR containment is expected to be higher due to the presence of steam and design to allow venting.

3.3.4 Conclusions on Uncertainty in Detonability

It can be concluded that extrapolations of detonation behavior have been carried out into temperature and composition ranges which are not representative of those anticipated in ALWRs. When realistic containment conditions are considered, detonations are extremely unlikely because of both the low temperatures and steam inerting. It is further concluded that when reasonable uncertainty is considered, the ALWR requirement for maximum hydrogen concentration has significant margin to detonability.

4.0 CONCLUSIONS

It is concluded that the EPRI requirement for hydrogen control in ALWRs is confirmed as a suitable ALWR design basis considering both in-vessel and ex-vessel hydrogen generation and the potential for containment challenge by either combustion or detonation.

Hydrogen generation has been evaluated based on relevant in-pile experiments with real reactor materials, and on the use of phenomenological models to both simulate these experiments and extrapolate to prototypical reactor cases. In the licensing basis evaluation, it has been demonstrated that for in-vessel recoverable accidents the hydrogen source will be limited to less than 75% MWR by ALWR design features as they are utilized for severe accident recovery and mitigation. In the risk basis evaluation, additional in-vessel and ex-vessel contributors to the hydrogen source have been analyzed, the impact of ALWR design features on this source has been quantified, and it has been shown that the 75% MWR limit is unlikely to be exceeded. Design margins were found to accommodate appropriately any hydrogen generation above 75%.

An evaluation of hydrogen deflagrations has been made by calculation of the maximum theoretical pressure rise for a range of initial steam concentrations and pressures appropriate for realistic ALWR cases. Based on the design parameters of the ALWR requirement, an idealized maximum possible post-combustion pressure is calculated as about 6.6 atmospheres, a value within the service level C capability of current large, dry containment designs. Therefore, the EPRI ALWR requirement for hydrogen control assures a containment design that will survive hydrogen deflagration events, survival is also demonstrated for the REB containments either because the hydrogen source is limited to 75% MWR or because design margins accommodate potential excess.

Hydrogen detonations have been evaluated, and the conditions required for detonation are far more stringent than those for deflagration. In an ALWR containment, flame acceleration and a DDT, rather than by direct initiation by energy deposition is the most likely detonation mechanism. Experimental data on detonability limits and DDT prediction of detonability have been applied to evaluations of the potential for initiation and propagation of detonations. For LDB cases, it has been shown that DDT is highly unlikely to impossible for an ALWR containment following the EPRI ALWR requirement of 13% hydrogen and using, as required, comparatively open containment designs. Additional margin provided by ALWR geometry and steam content is predicted for ALWR containment simulations, and is used in the risk evaluation basis. In the REB, intrinsic detonability of the gas mixtures and thus the potential for propagation of a detonation are highly unlikely according to both theory and experiment. Hence, the possibility of detonations is extremely remote for ALWR containments which meet the EPRI requirement of a maximum 13% hydrogen by volume in dry air.

Based on these evaluations, a large dry containment design can provide the principal means of hydrogen control for an ALWR and meet the high standards for severe accident mitigation that are appropriate for an advanced reactor design.

5.0 REFERENCES

1. Electric Power Research Institute, Advanced Light Water Reactor Requirements Document, Chapter 5 - Engineered Safety Systems, Palo Alto, California, December 1987.

2. "Policy and Top Tier Design Requirements," Vol. I, EPRI ALWR Requirements Document, draft to be issued.

3. Electric Power Research Institute, Advanced Light Water Reactor Requirements Document, Chapter 1 - Engineered Safety Systems, Palo Alto, California, December 1987.

4. "Licensing Requirements for Pending Construction Permit and Manufacturing License Applications," Code of Federal Regulations parts 2 and 50, statements of consideration 47FR2286, January 15, 1982.

5. D. G. Strawson, MPR Associates, letter to D. E. Leaver, TENERA, May 22, 1989.

6. J. V. Cathcart, et al., "Zirconium Metal-Water Oxidation Kinetics IV. Reaction Rate Studies," ORNL/NUREG-17 (August 1977).

7. V. F. Urbanik and T. R. Heidrick, "High Temperature Oxidation of Zircaloy-2 and Zircaloy-4 in Steam," J. Nucl. Matls 75, 251 (1978).

8. A. D. Knipe, et al., PBF Severe Fuel Damage Scoping Test - Test Results Report, NUREG/CR-4683, EGG-2413, Idaho National Engineering Laboratory, Idaho Falls, Idaho, August 1986.

9. Z. R. Martinson, et al., Volume 1: PBF Severe Fuel Damage Test 1-1 Test Results Report, NUREG/CR 4684, EGG-2463 Volume 1, Idaho National Engineering Laboratory, Idaho Falls, Idaho, October 1986.

10. Z. R. Martinson, et al., PBF Severe Fuel Damage Test 1-3 Test Results Report, NUREG/CR-5354, EGG-2565, EG&G Idaho, Inc., Idaho Falls, Idaho, May 1989 (DRAFT).

11. D. A. Petti, et al., PBF Severe Fuel Damage Test 1-4 Test Results Report, NUREG/CR-5163, EGG-2542, Idaho National Engineering Laboratory, Idaho Falls, Idaho, February 1989.

12. Electric Power Research Institute, Analysis of Three Mile Island - Unit 2 Accident, NSAC-1, Palo Alto, California, March 1980.

13. Electric Power Research Institute, TMI-2 Accident Core Heat-Up Analysis, NSAC-24, Palo Alto, California, January 1981.

14. Electric Power Research Institute, TMI-2 Accident Core Heat-up Analysis, Supplement, NSAC-25, Palo Alto, California, June 1981.

15. R. G. Zalosh, Analysis of the Hydrogen Burn in the TMI-2 Containment, EPRI NP-3975, Electric Power Research Institute, Palo Alto, California, April 1985.

16. A. Sharon, et al., MAAP 3.0B Simulation of the First 174 Minutes of the TMI-2 Accident, EPRI NP-6206, Electric Power Research Institute, Palo Alto, California, May 1989.

17. Final LOFT Facility Tests to Provide Significant Data on Plant Accident Behavior, Atomic Industrial Forum Washington, D. C., August 1985.

18. Frank Panisko, PNL, Richland, WA, presentation to FAI staff, February 17, 1988.

19. Modular Accident Analysis Program Manual, IDCOR Technical Report Task 16, Atomic Industrial Forum.

20. "Core Melt Progression Modeling and Benchmarking," Advanced Reactor Severe Accident Program Task WBS 3.4.8, Prepared by Fauske and Associates, Inc., January, 1989.

21. A. Sharon, et al., Modifications for the Development of the MAAP-DOE Code, Volume V: A Model for Recovery of a Badly Degraded Core, WBS 3.4.7, DOE/ID-10216, Vol. V, Department of Energy, December 1988.

22. A. Sharon, et al., "Simulation of the Severe Fuel Damage Tests (SFD) Using the Modular Accident Analysis Program (MAAP)," Proc. International ANS/ENS Topical Meeting on Thermal Reactor Safety, San Diego, California, February 2-6, 1986, American Nuclear Society, LaGrange Park, Illinois.

23. Presentations made to the CSNI PWG-2 Task Group on TMI-2 Meeting, Karlsruhe, F.R. Germany, 29 May - 1 June, 1989.

24. P. D. Bayless, "Analysis of Natural Circulations During a Surry Station Blackout Using SCDAP/RELAPS," NUREG/CR-5214, EGG-2547, October, 1988.

25. R. Chambers, et al., "Depressurization to Mitigate Direct Containment Heating," Presented at Sixteenth Water Reactor Safety Information Meeting, Gaithersburg, Maryland, October 1988.

26. S. Hagen and P. Hofmann, "Physical and Chemical Behavior of LWR Fuel Elements Up to Very High Temperatures," KfK4104, June 1987.

27. Martin Hertzberg, "Flammability Limits and Pressure Development in Hydrogen-Air Mixtures," Proc. Workshop on the Impact of Hydrogen on Water Reactor Safety, Volume III, NUREG/CR-2017, SAND81-0661, Sandia National Laboratories, September 1981.

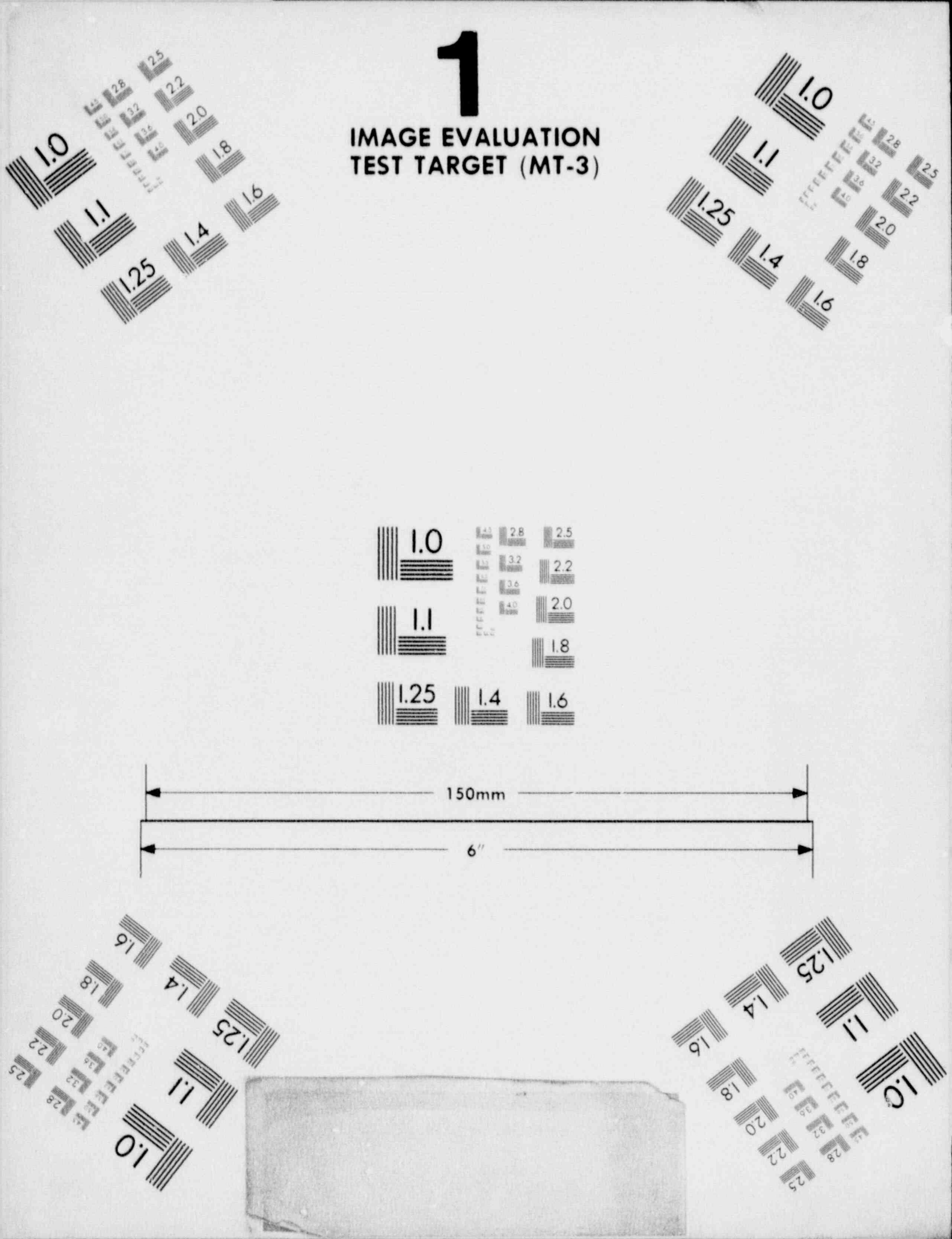
1
IMAGE EVALUATION
TEST TARGET (MT-3)
1.0
1.1
1.25
1.4
1.6
1.8
2.0
2.2
2.5
2.8
3.2
3.6
4.0
150mm
6"

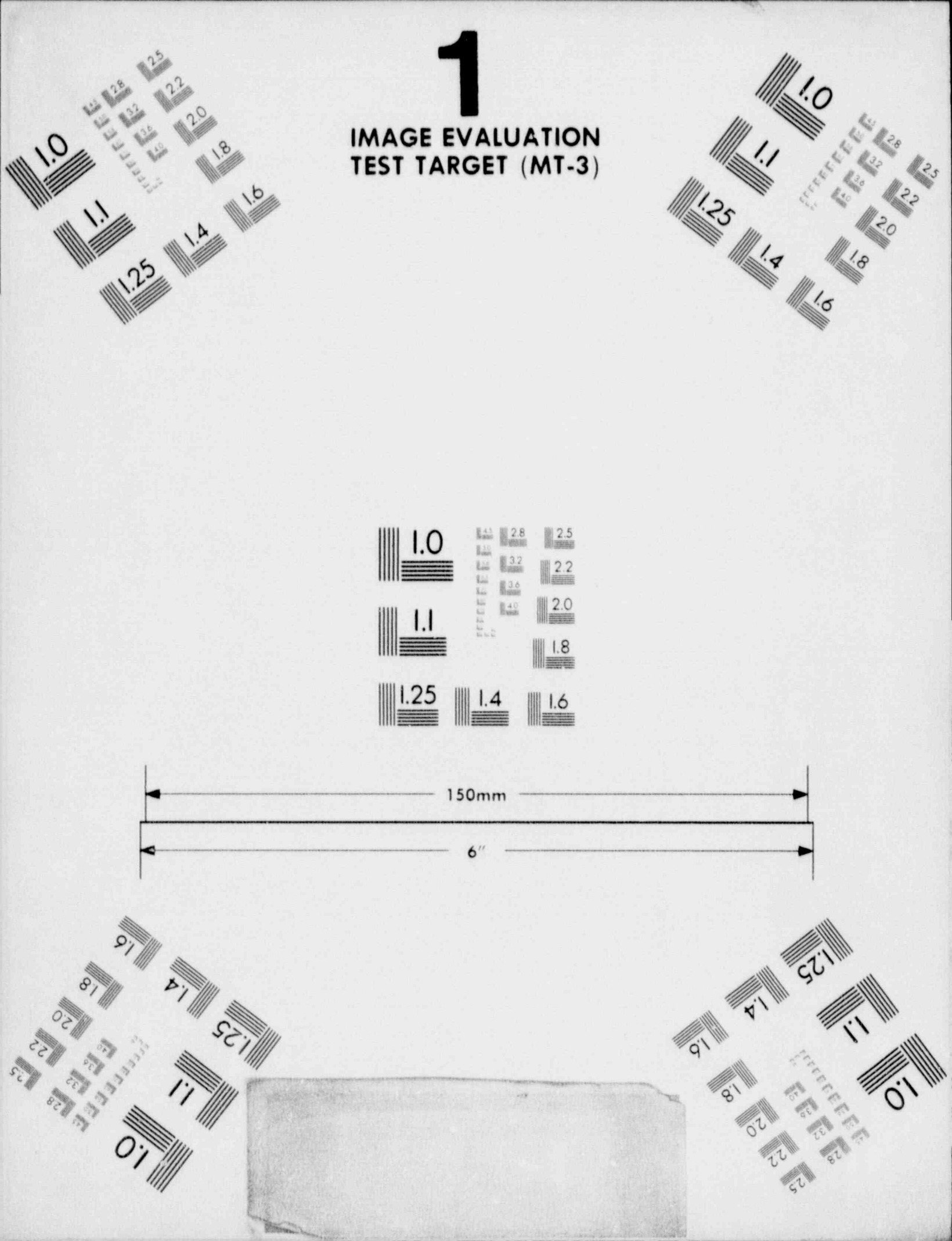
1
IMAGE EVALUATION
TEST TARGET (MT-3)
1.0
1.1
1.25
1.4
1.6
1.8
2.0
2.2
2.5
2.8
3.2
3.6
4.0
150mm
6"

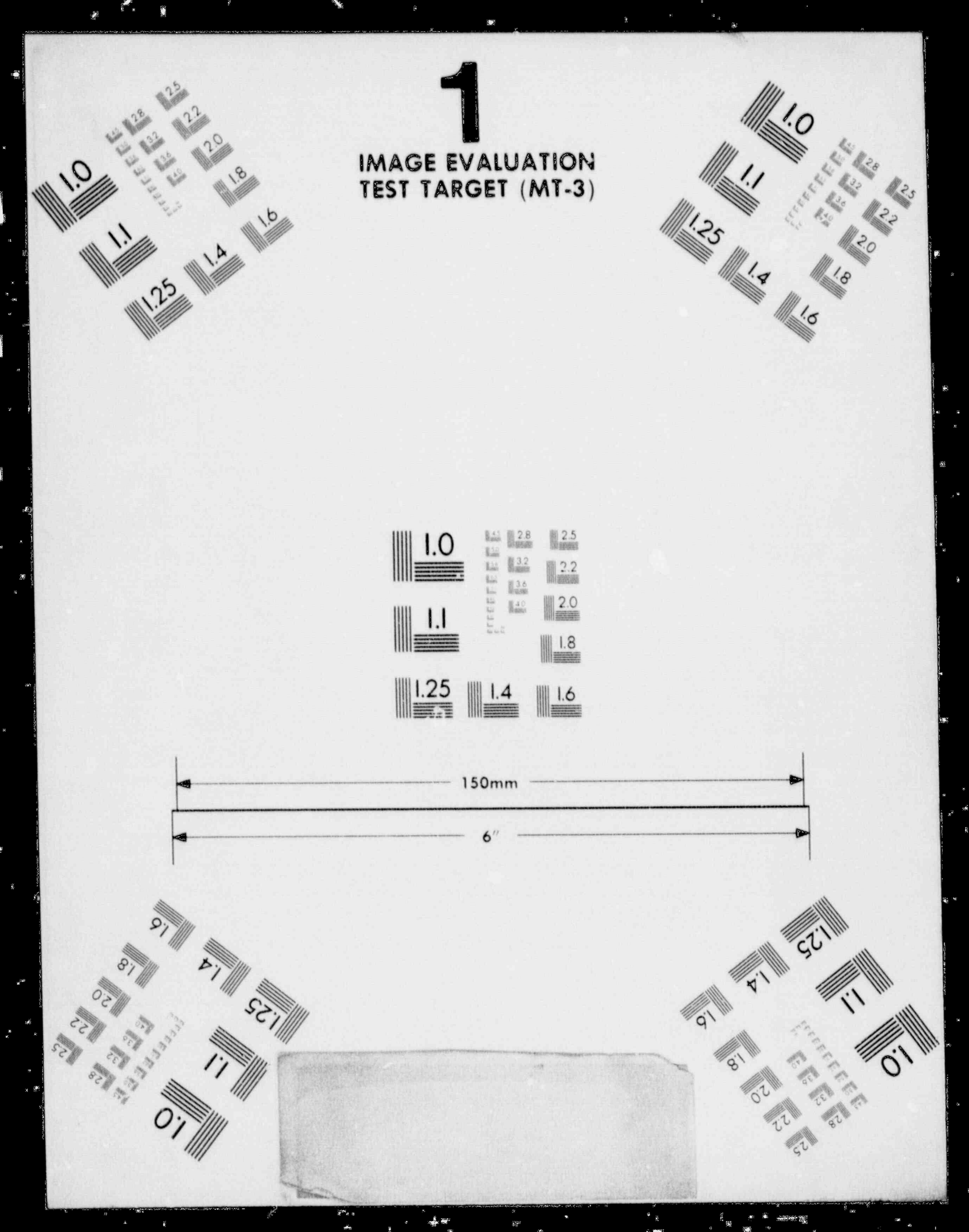
1
IMAGE EVALUATION
TEST TARGET (MT-3)
1.0
1.1
1.25
1.4
1.6
1.8
2.0
2.2
2.5
2.8
3.2
3.6
4.0
150mm
6"

28. M. P. Sherman et al., "Deliberate Ignition and Water Fogs as H_2 Control Measures for Sequoyah," Proc. Workshop on the Impact of Hydrogen on Water Reactor Safety, Volume IV, NUREG/CR-2017, SAND81-0661, Sandia National Laboratories, September 1981.

29. D. D. Liu et al., "Some Results of WNRE Experiments on Hydrogen Combustion," Proc. Workshop on the Impact of Hydrogen on Water Reactor Safety, Volume III, NUREG/CR-2017, SAND81-0661, Sandia National Laboratories, September 1981.

30. A. C. Ratzel, Data Analysis for Nevada Test Site (NTS) Premixed Combustion Tests, NUREG/CR-4138, SAND85-0135, Sandia National Laboratories, May 1985.

31. R. K. Kumar et al., Intermediate-Scale Combustion Studies of Hydrogen-Air-Steam Mixtures, EPRI NP-2955, Electric Power Research Institute, Palo Alto, California, June 1984.

32. M. P. Sherman, "Hydrogen Combustion in Nuclear Plant Accidents and Associated Containment Loads," Nuclear Engineering and Design, 82, 1984, p. 13-24.

33. S. R. Tieszen et al., Detonability of H_2-Air-Diluent Mixtures, NUREG/CR-4905, SAND85-1263, Sandia National Laboratories, Albuquerque, New Mexico, July 1987.

34. D. Stamps, Sandia National Laboratories, Handout at the Hydrogen Combustion Peer Review Committee Meeting, November 11, 1987, Washington, D.C., Called by M. Silberberg, Division of Reactor Accident Analysis, U.S. NRC.

35. Technical Aspects of Hydrogen Control and Combustion in Severe Light-Water Reactor Accidents, National Research Council Report, National Academy Press, Washington, D. C., 1987.

36. M. Berman, "A Critical Review of Recent Large-Scale Experiments on Hydrogen-Air Detonation," Nuclear Science and Engineering, 93, 1986, pp. 321-347.

37. Hydrogen Combustion in Reactor Containment Buildings, IDCOR Technical Report 12.3, Atomic Industrial Forum, September 1983.

38. J. H. S. Lee et al., "Hydrogen-Air-Detonations," Proc. of the Second International Workshop on the Impact of Hydrogen Water Reactor Safety, Albuquerque, New Mexico, October 1982.

39. Reactor Safety Research Semiannual Report, January-June, 2986, Volume 33, NUREG/CR-4340, SAND85-1606 (1 of 2), Sandia National Laboratories, Albuquerque, NM, October 1985.

40. A. Camp et al., Light Water Reactor Hydrogen Manual, NUREG/CR-2726, SAND82-1137, Sandia National Laboratories, Albuquerque, NM, June 1983.

41. Letter R. B. Bradbury (Stone and Webster) to W. R. Sugnet (EPRI), Hydrogen Ignition in Light Water Reactor Containments, June 20, 1989.

42. M. P. Sherman and S. E. Slezak, "Hydrogen-Air-Steam Combustion Regimes in Large Volumes," Proc. 25th Space Congress, April 26-29, 1988, Coco Beach, Florida, Canaveral Council of Technical Societies.

43. M. P. Sherman, S. R. Tieszen, and W. B. Benedick, "FLAME Facility," NUREG/CR-5275, SAND85-1264, Sandia National Laboratories, April, 1989.

44. J. E. Shepherd, "Chemical Kinetics and Hydrogen-Air-Diluent Detonations," Tenth International Colloquium on Dynamics of Explosions and Reactive Systems, Berkeley, CA, August 4-9, 1985.

45. M. P. Sherman and M. Borman, "The Possibility of Local Detonation During Degraded Core Accidents in the Bellefonte Nuclear Power Plant," NUREG/CR-4803, SAND86-1180, Sandia National Laboratories, January, 1987.

46. "Study of Hydrogen Mixing within the Combustion Engineering APWR Containment," Advanced Reactor Severe Accident Program Task 10.7, Prepared by Fauske and Associates, Inc., March, 1989.

47. MAAP 3.0B User's Manual, Fauske and Associates, Inc., 1989 (to be published).

48. M. G. Plys, R. D. Astleford, and M. Epstein, "A Flammability and Combustion Model for Integrated Accident Analysis," Proc. International ANS/ENS Conference on Thermal Reactor Safety, Avignon, France, October, 1988, paper 105, pp. 1262-1271.

49. M. Epstein, "Buoyancy-Driven Exchange Flow through Small Openings in Horizontal Partitions," Journal of Heat Transfer, November, 1988, Vol. 110, pp. 885-893.

50. Reactor Safety Research Semiannual Report January - June 1986, Sandia National Laboratories, NUREG/CR-4805, SAND86-2752, May 1987.

51. D. V. Stamps, SNL, Personal Communication to Mr. D. Leaver, TENERA, June 22, 1989.

APPENDIX A

Approximate Evaluation of H_2-Air-Steam Compositions for Pressure Rise Calculations

This appendix discusses the approximate method for evaluating the pressure rise from combustion of hydrogen-air-steam mixtures. An initially dry containment atmosphere at 300 K, 1 atm is assumed. Hydrogen is added to achieve a desired concentration, then the mixture is heated to a given temperature and steam is added at the saturation pressure at that temperature. The H_2 and H_2O mole fractions and initial preburn pressure are determined. This H_2 mole fraction is used in Figure 2-8 to determine the final postburn pressure, and then the burn pressure ratio can be found. Also, given the preburn H_2 and H_2O mole fractions, the flammability characteristics (yes or no) of the mixture can be estimated using Figure 2-2.

Define

n_o = initial dry air moles
P_o = initial dry air pressure (1 atm)
T_o = initial dry air temperature (300°K)
n_H = moles H_2 added
n_d = dry moles = $n_o + n_H$
P_d = dry pressure after H_2 added
X = mole fraction H_2 = 13% in the dry mixture
T_{wet} = final pre-burn temperature
P_s = steam partial pressure at T_{wet}
P_w = total pressure at T_{wet}
P_d = dry mix pressure at T_{wet}
n_w = total wet mix moles
n_s = moles of H_2O
X_w = wet H_2 mole fraction
X_s = wet H_2O mole fraction

In the dry mixture,

$$X = \frac{n_H}{n_d} = \frac{P_d - P_o}{P_d} \qquad [1]$$

so that the dry pressure is

$$P_d = P_o\,(1 - X)^{-1} \qquad [2]$$

The mixture is then heated, resulting in a new dry pressure.

$$P_d = P_o\,(1 - X)^{-1}\,(T_w/T_o) \qquad [3]$$

Steam is added at saturation pressure.

$$X_w = n_H/n_w = n_H/(n_d + n_s) = X\,(1 + n_s/n_d)^{-1}. \qquad [4]$$

The wet pressure is defined as

$$P_w = P_d + P_s \qquad [5]$$

Combining the following equation

$$1 + \frac{P_s}{P_d} = 1 + \frac{n_s}{n_d} \qquad [6]$$

with equation [4] yields

$$X_w = X\,(1 + P_s/P_d) \qquad [7]$$

and combining this with [3] the wet H_2 mole fraction is:

$$X_w = \frac{X}{1 + \frac{T_o}{T_w}\frac{P_s}{P_o}\,(1 - X)}. \qquad [8]$$

An approximate expression for the steam mole fraction is:

$$X_s = P_s/P_w. \qquad [9]$$

First, equation [8] is used to find the wet H_2 mole fraction, given P_s from steam tables. Then Figure 2-8 is used for the final pressure. The pressure rise ratio can be found by first getting the pre-burn wet pressure with [5]. Flammability can be judged by using [9] for the steam mole fraction and noting whether the X_s, X_w coordinate in Figure 2-2 lies within or outside the flammability envelope.

APPENDIX B

Results from MAAP DOE for H_2 Generation Analyses

This appendix provides the time histories for the reactor vessel water level, hottest core nodal temperature, total hydrogen production, and net hydrogen in the system (if hydrogen is burned) for all the cases reported in the Risk Evaluation Basis analyses. The hydrogen histories labelled "H_2 IN SYSTEM" are the net hydrogen within the primary system and containment and reflect the removal of hydrogen by burning. After vessel failure, it is appropriate to view these histories as the hydrogen within the containment. The results provided in these figures were calculated without including any cavity flooding during these sequences.

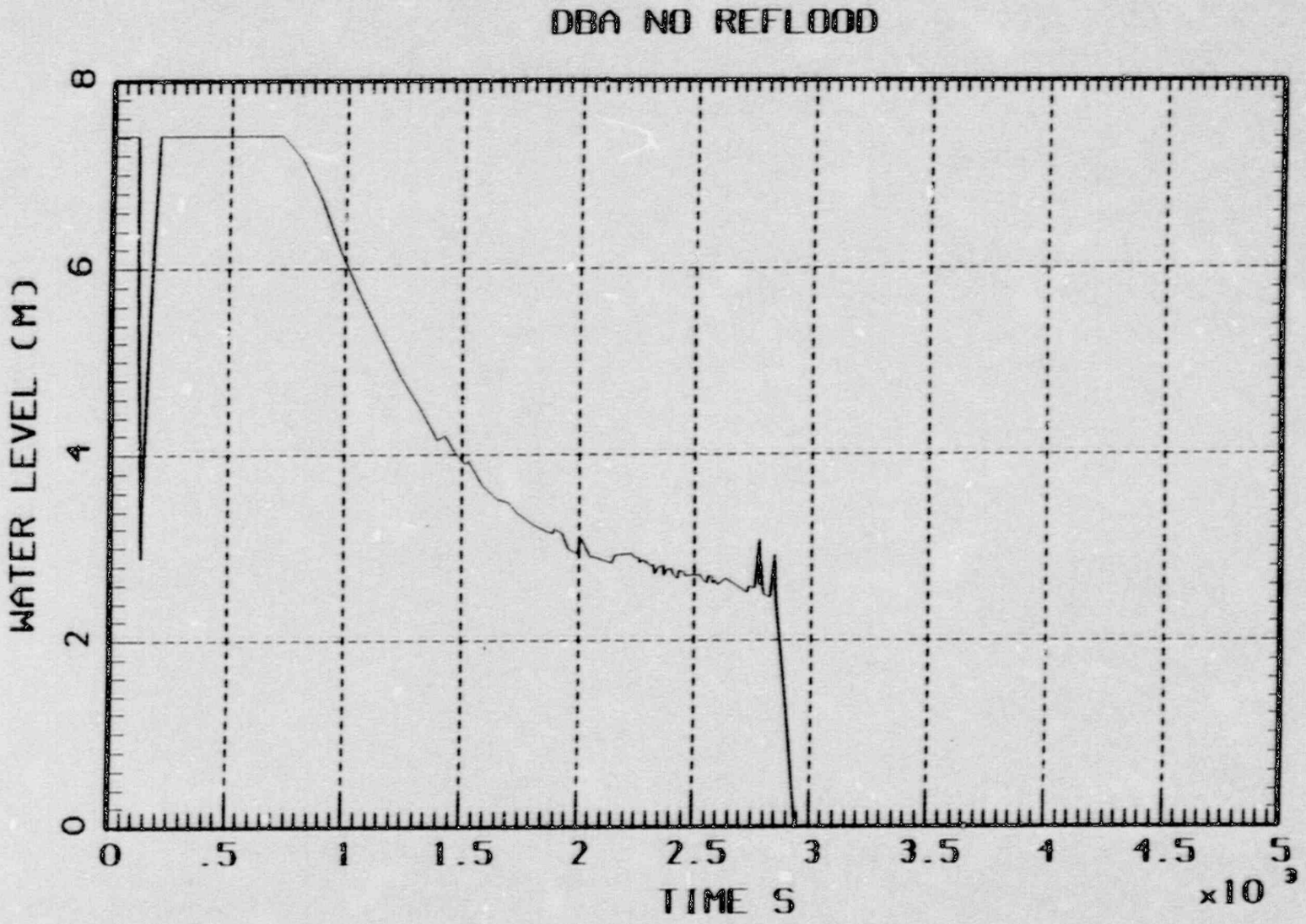

Figure B-1 Water level in reactor vessel for case 1.

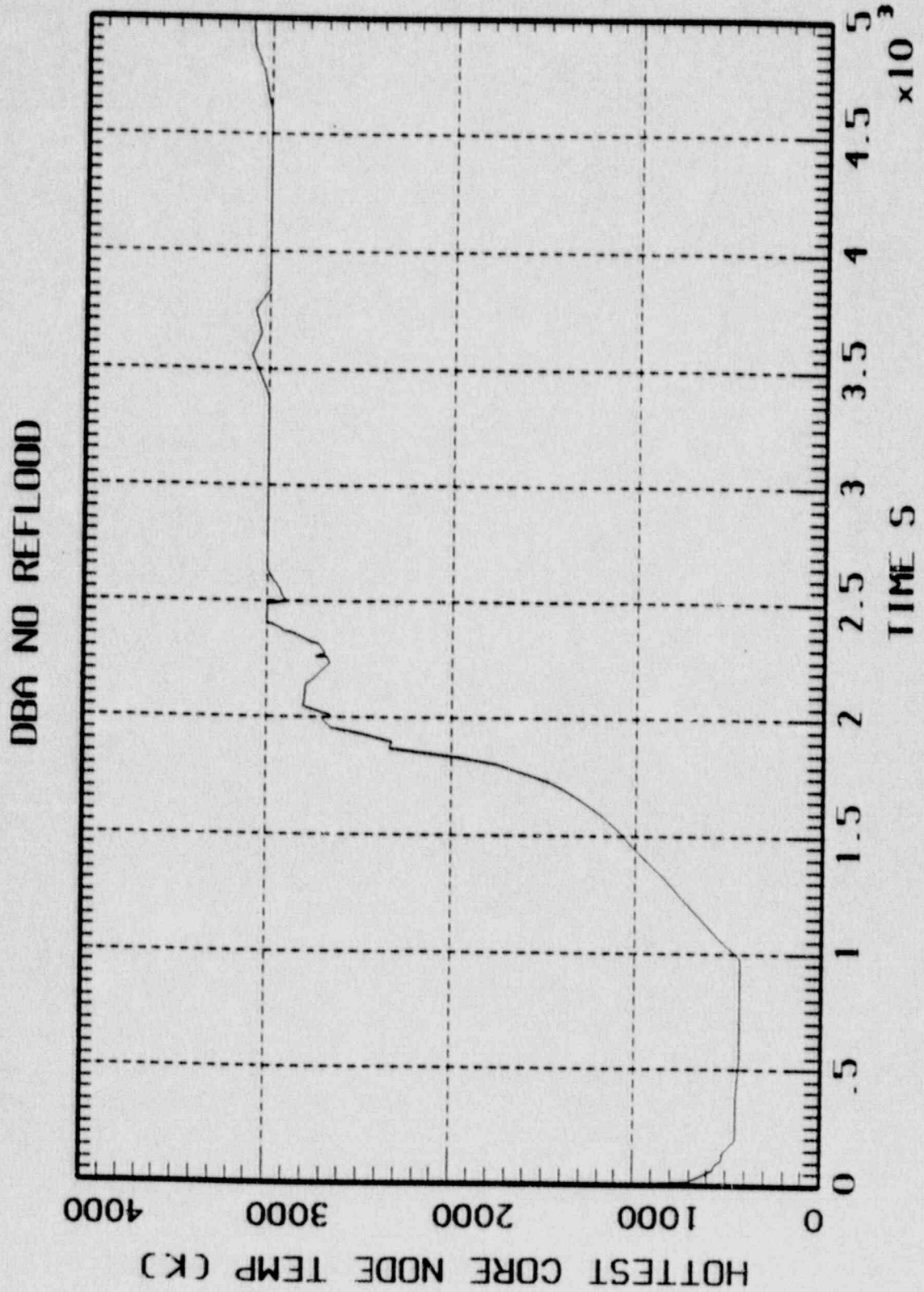

Figure B-2 Hottest core node temperature for case 1.

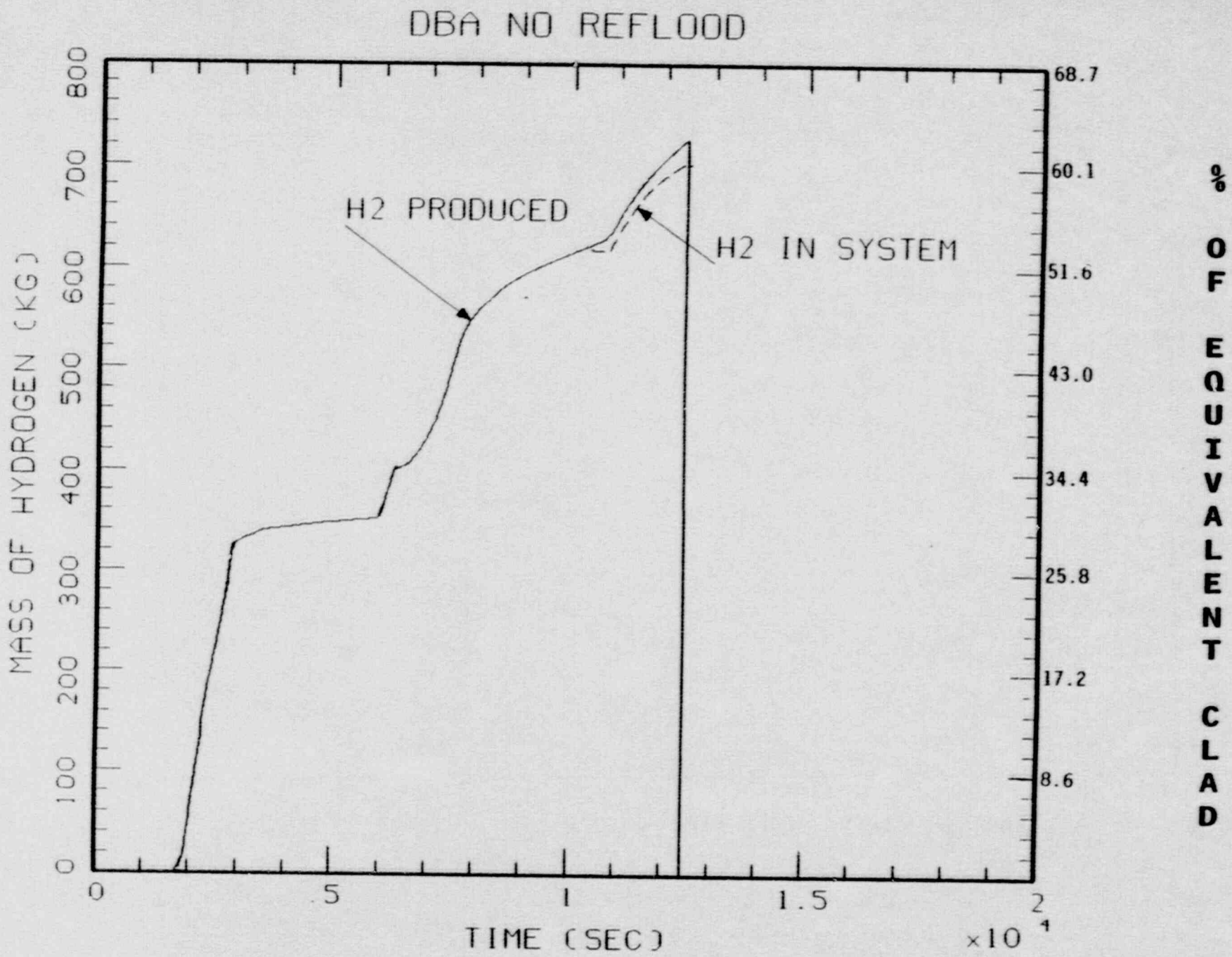

Figure B-3 Hydrogen history for case 1.

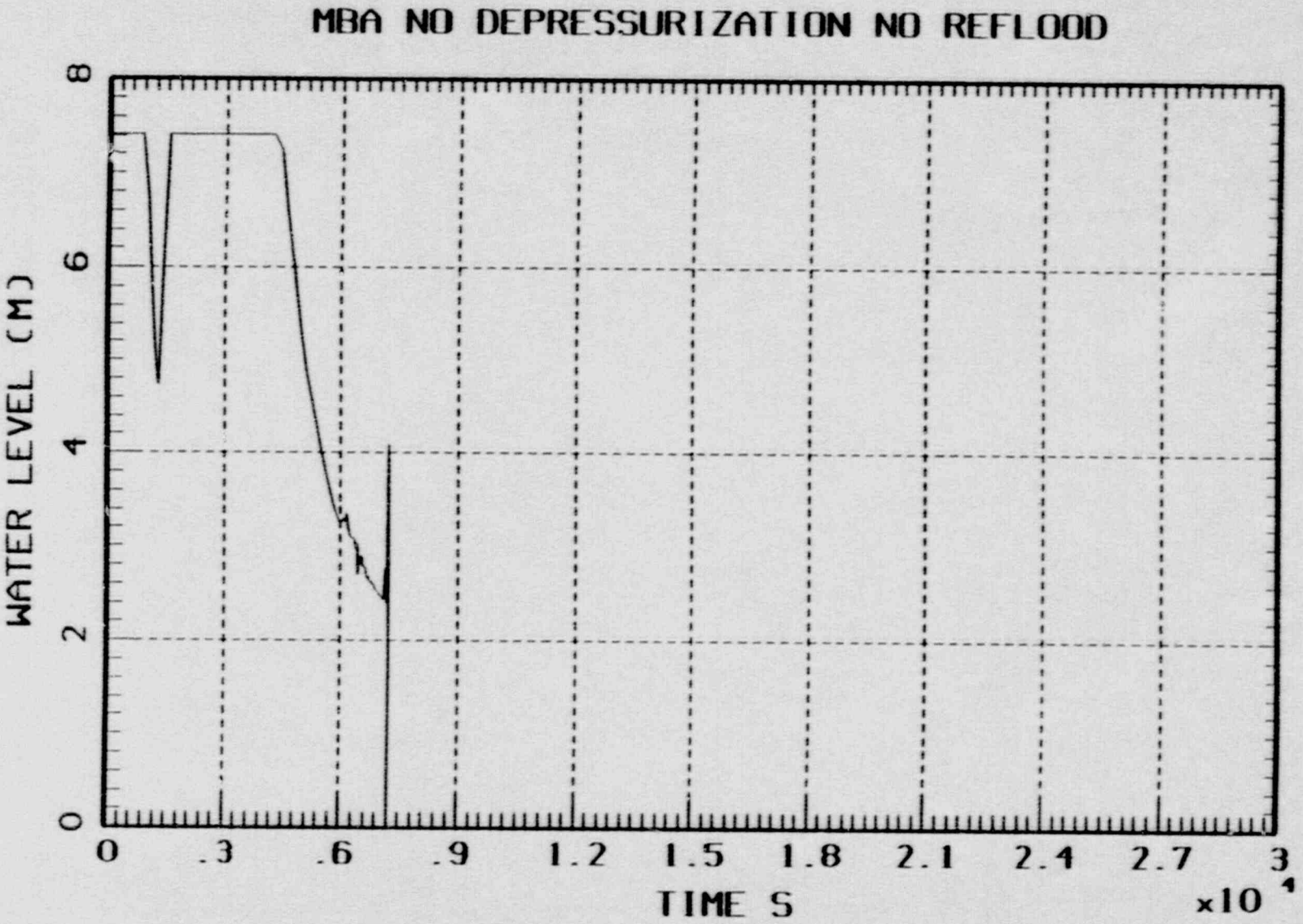

Figure B-4 Water level in reactor vessel for case 4.

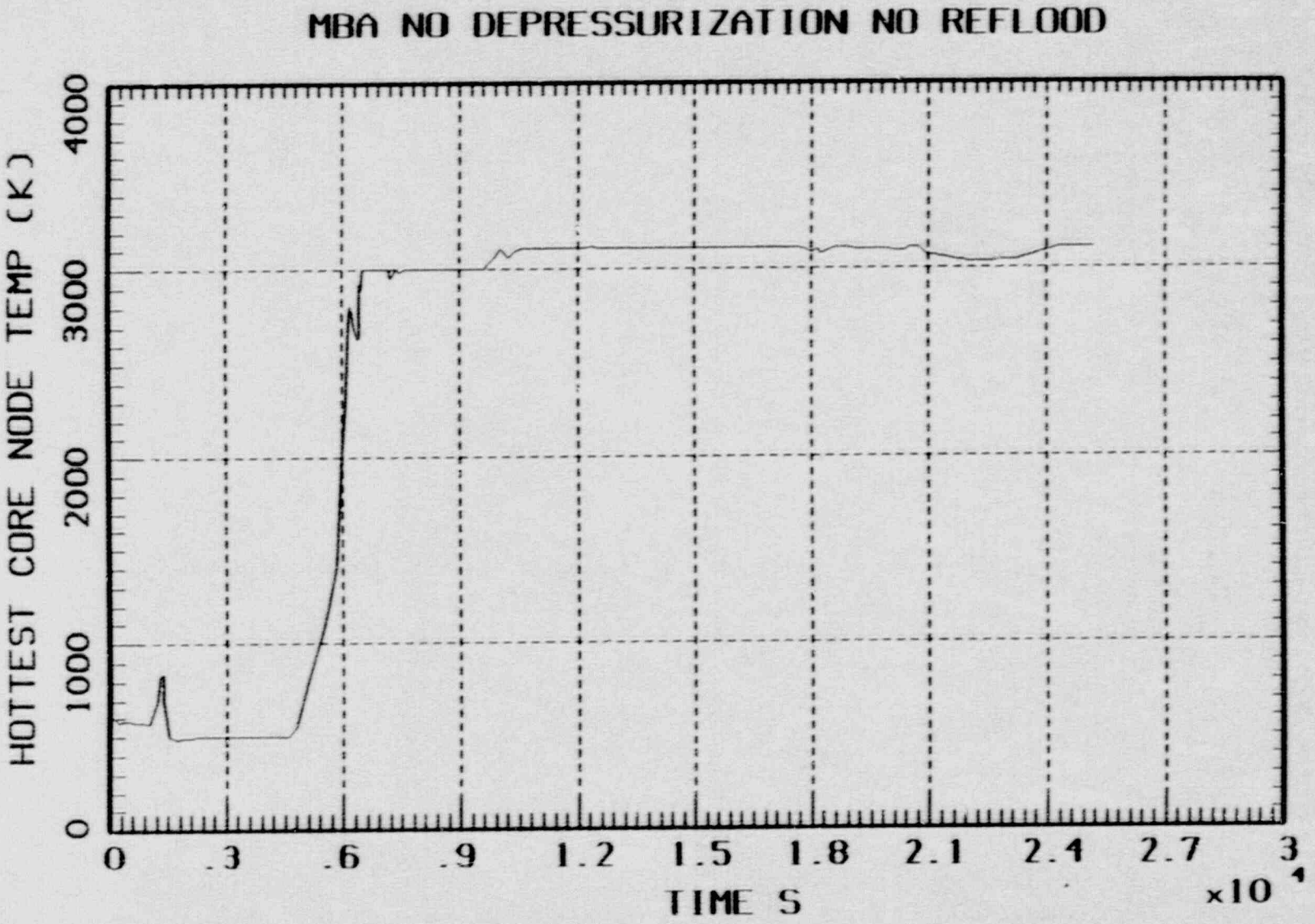

Figure B-5 Hottest core node temperature for case 4.

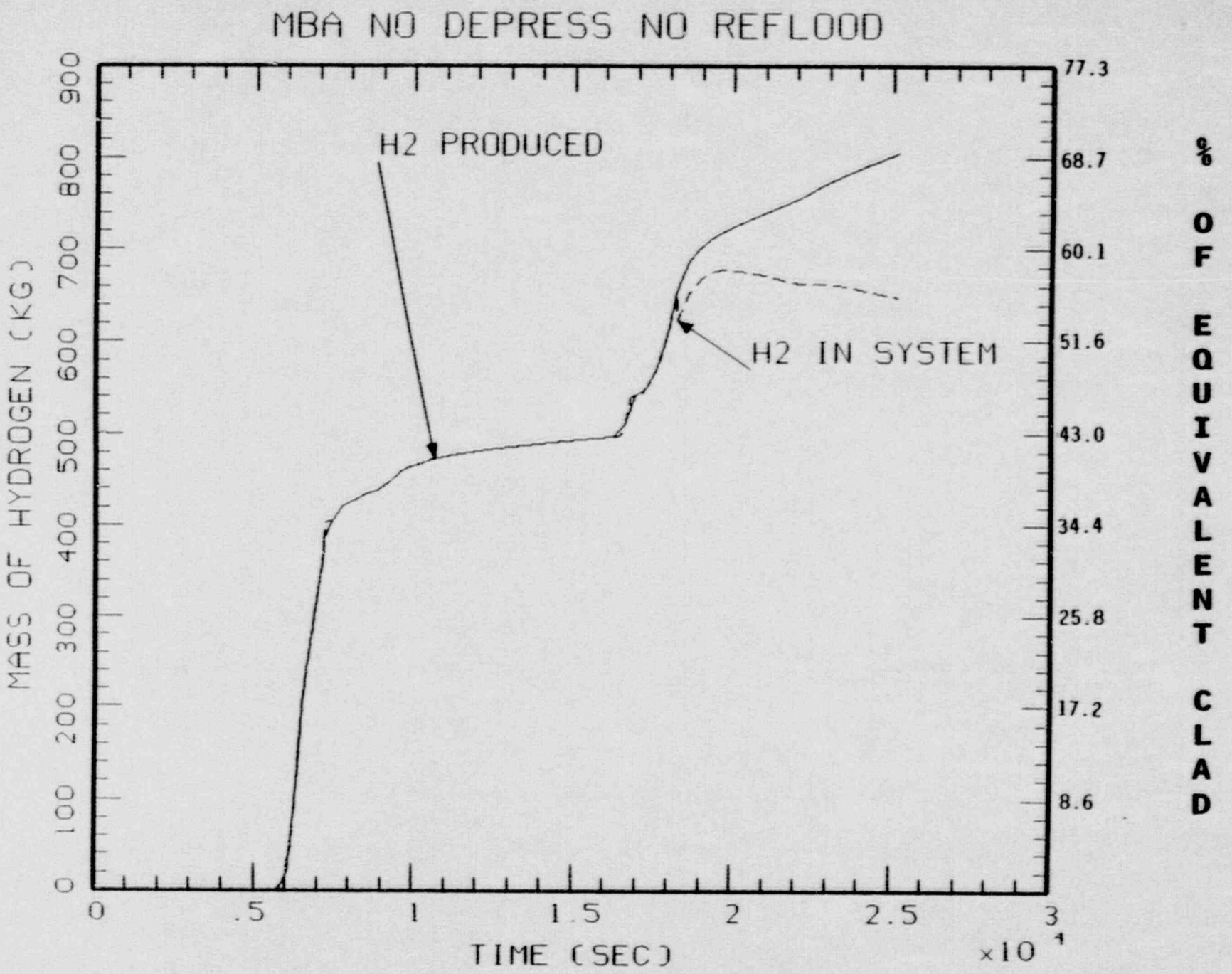

Figure B-6 Hydrogen history for case 4.

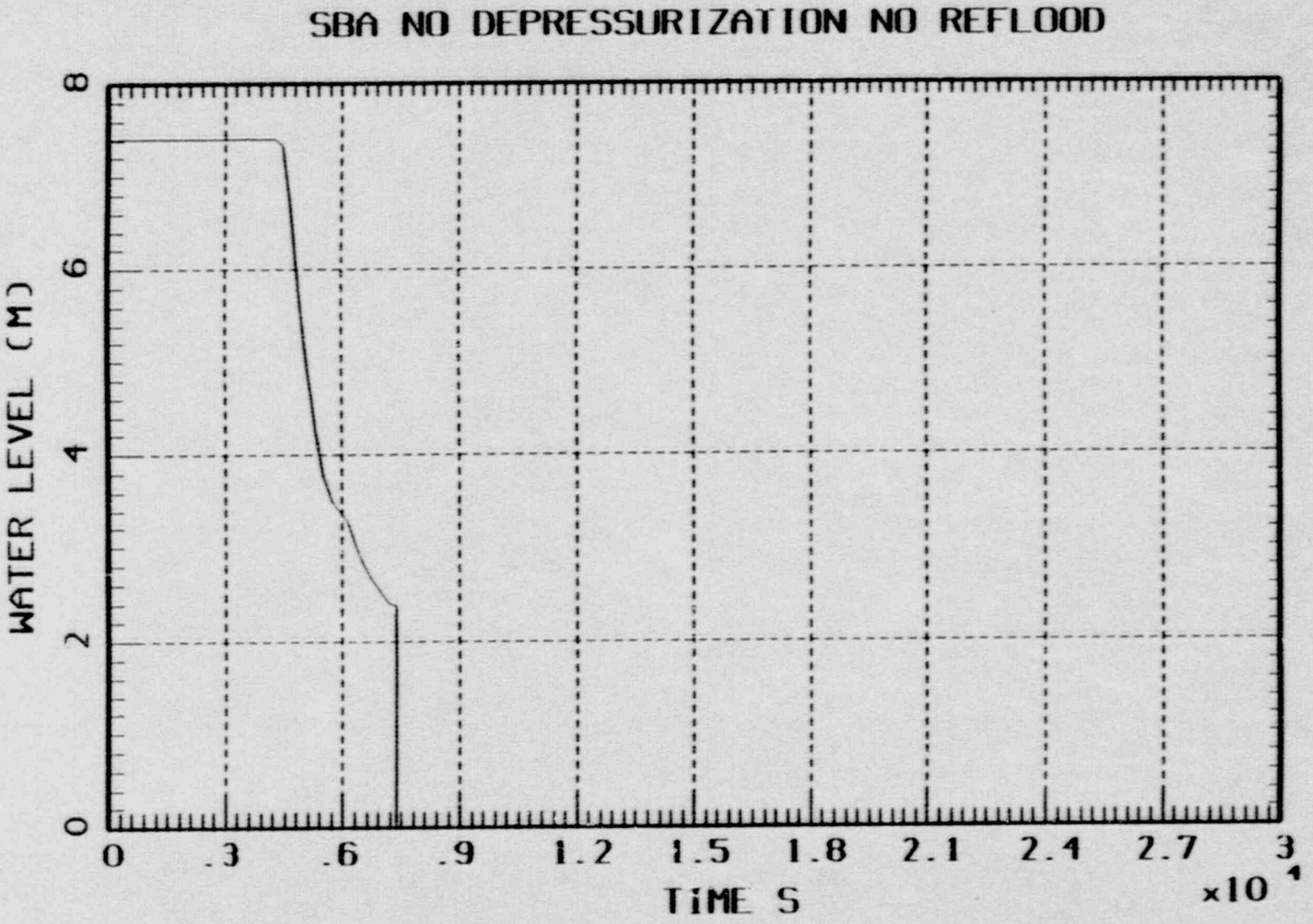

Figure B-7 Water level in reactor vessel for case 5.

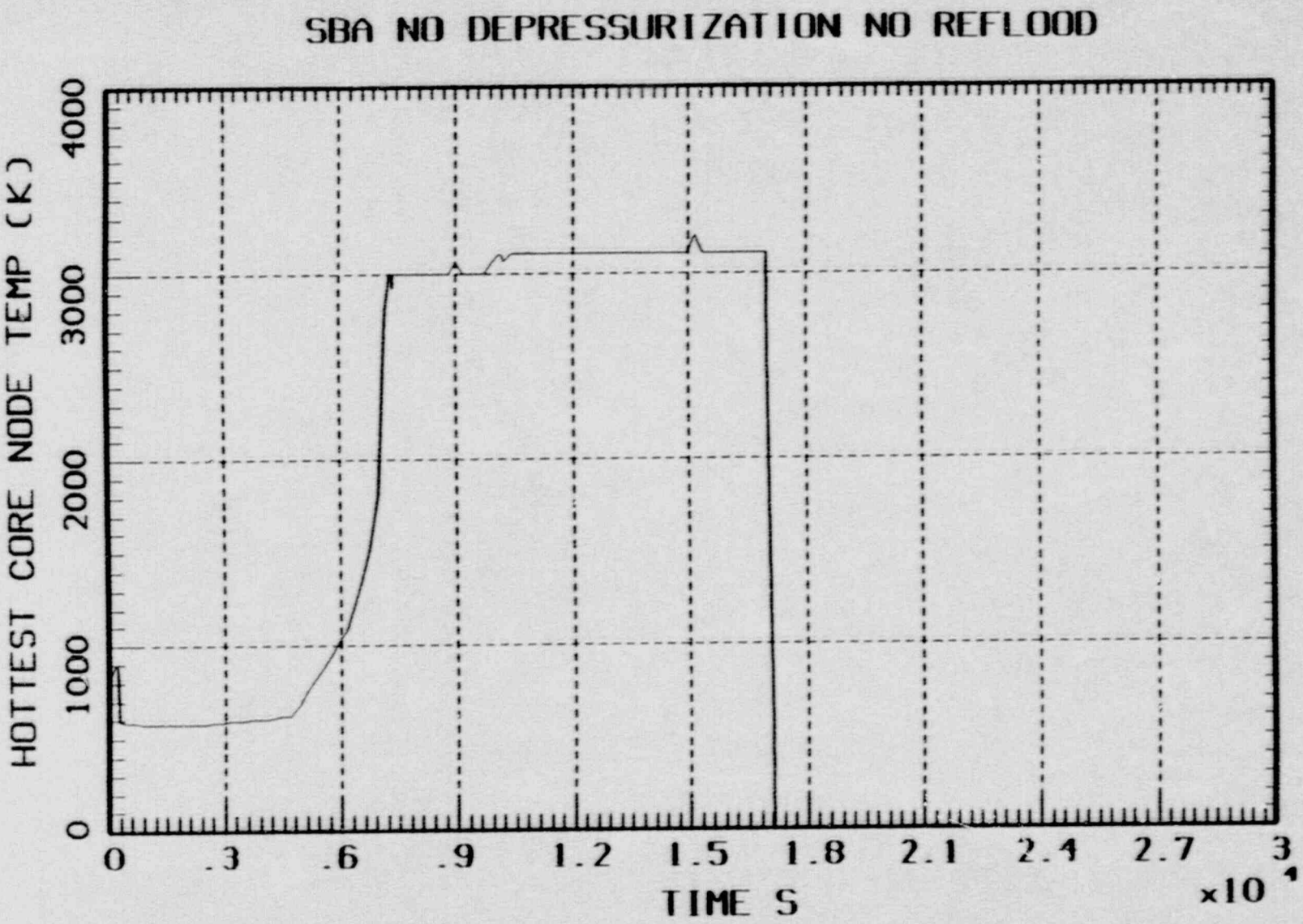

Figure B-8 Hottest core node temperature for case 5.

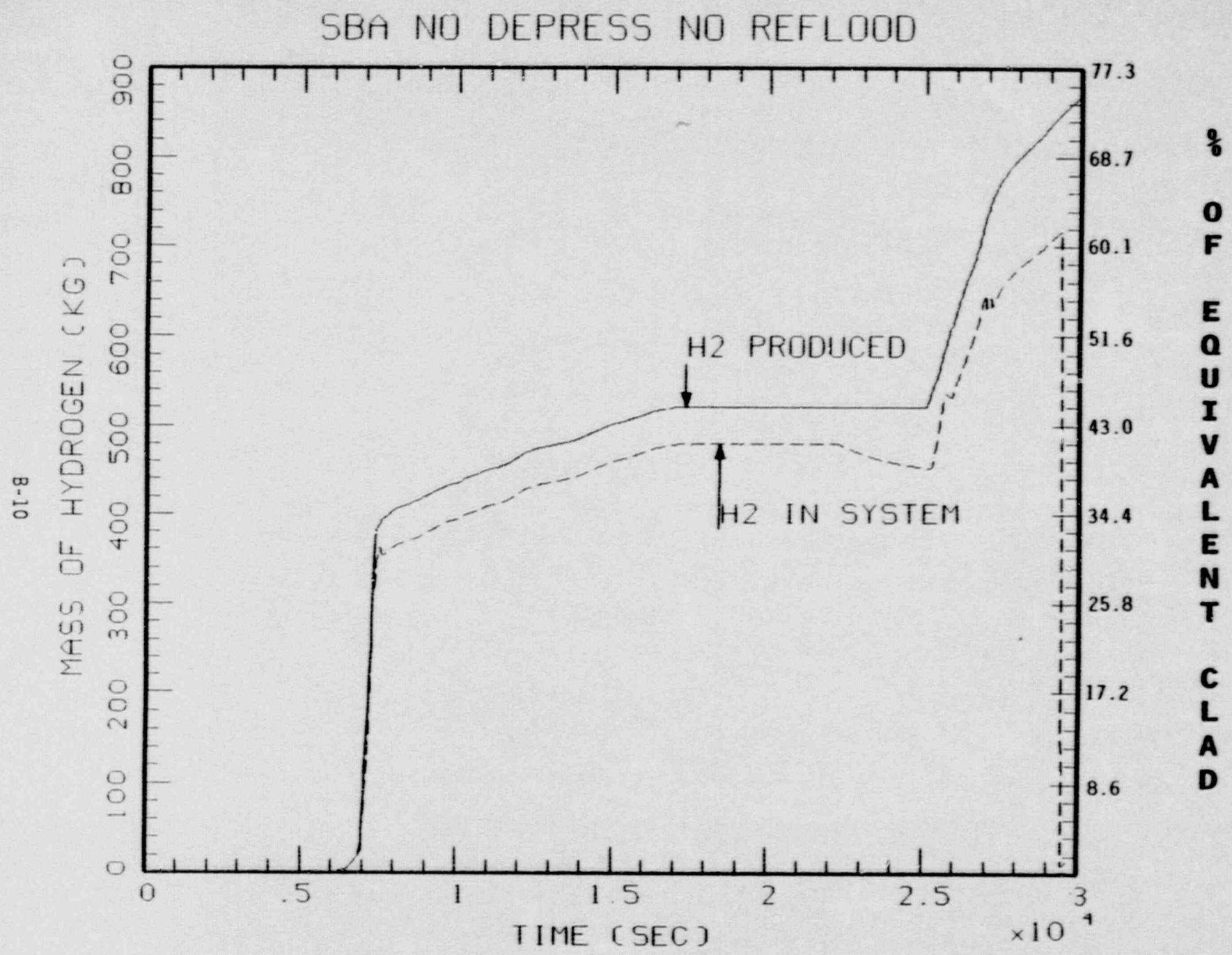

Figure B-9 Hydrogen history for case 5.

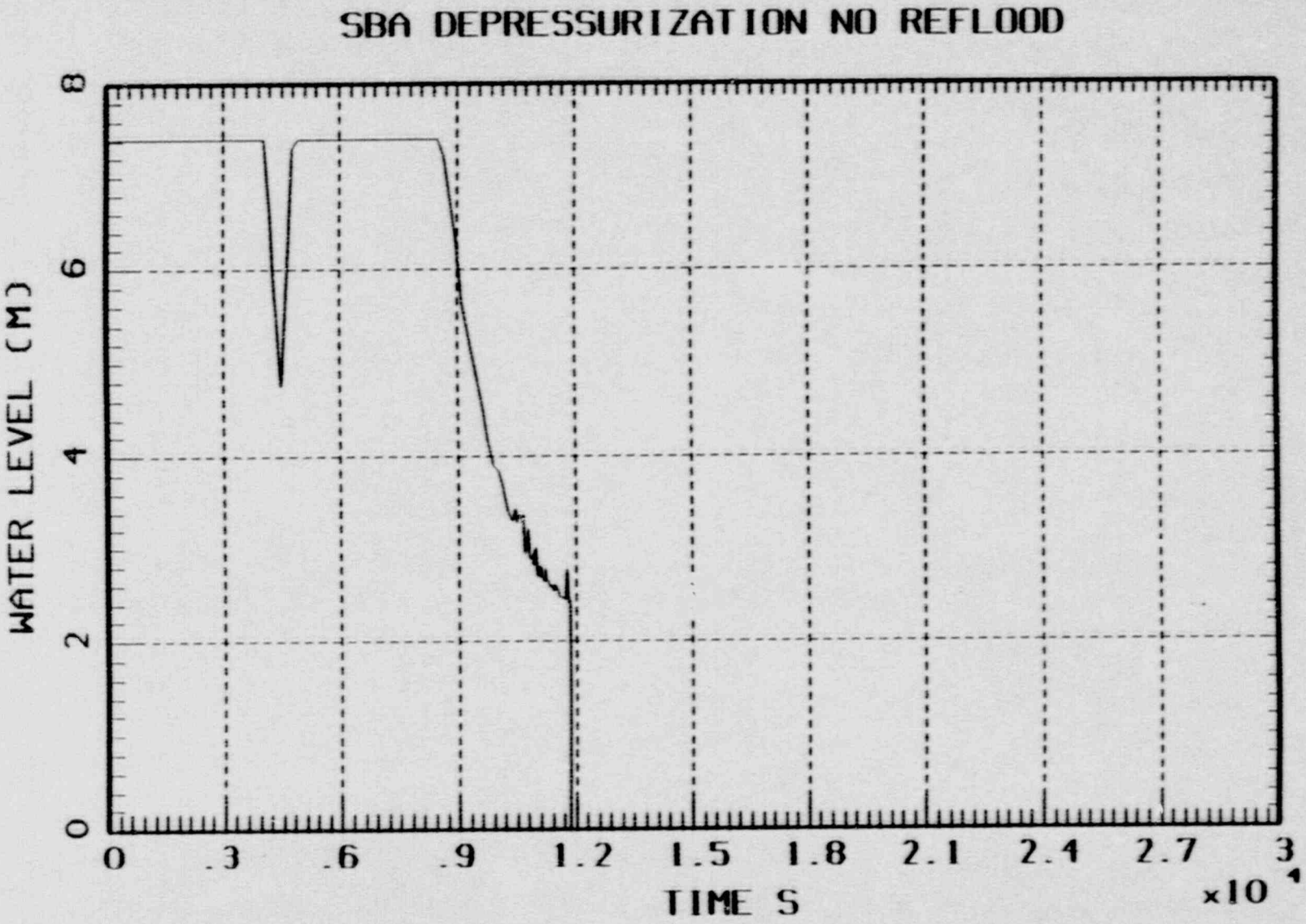

Figure B-10 Water level in reactor vessel for case 7.

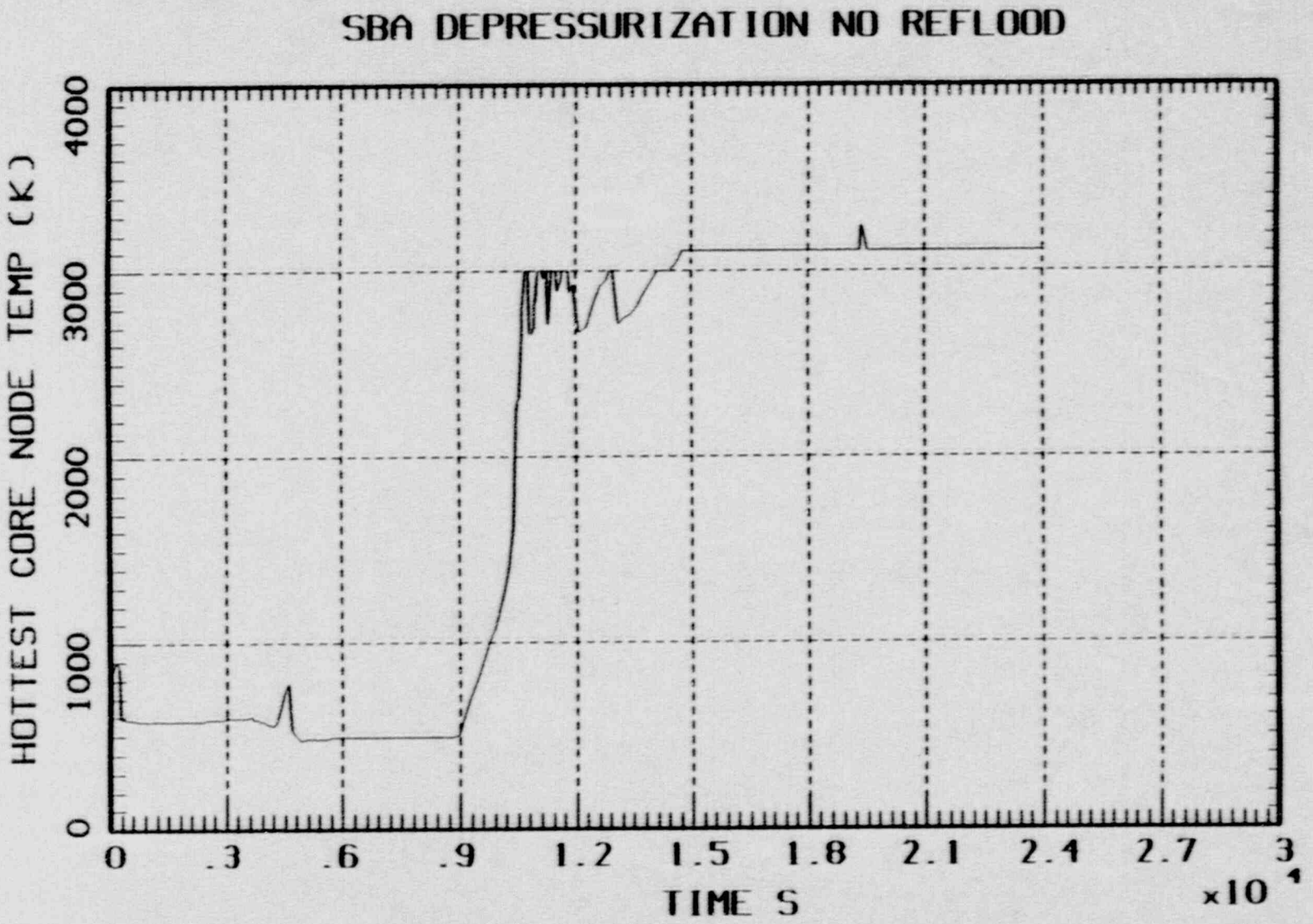

Figure B-11 Hottest core node temperature for case 7.

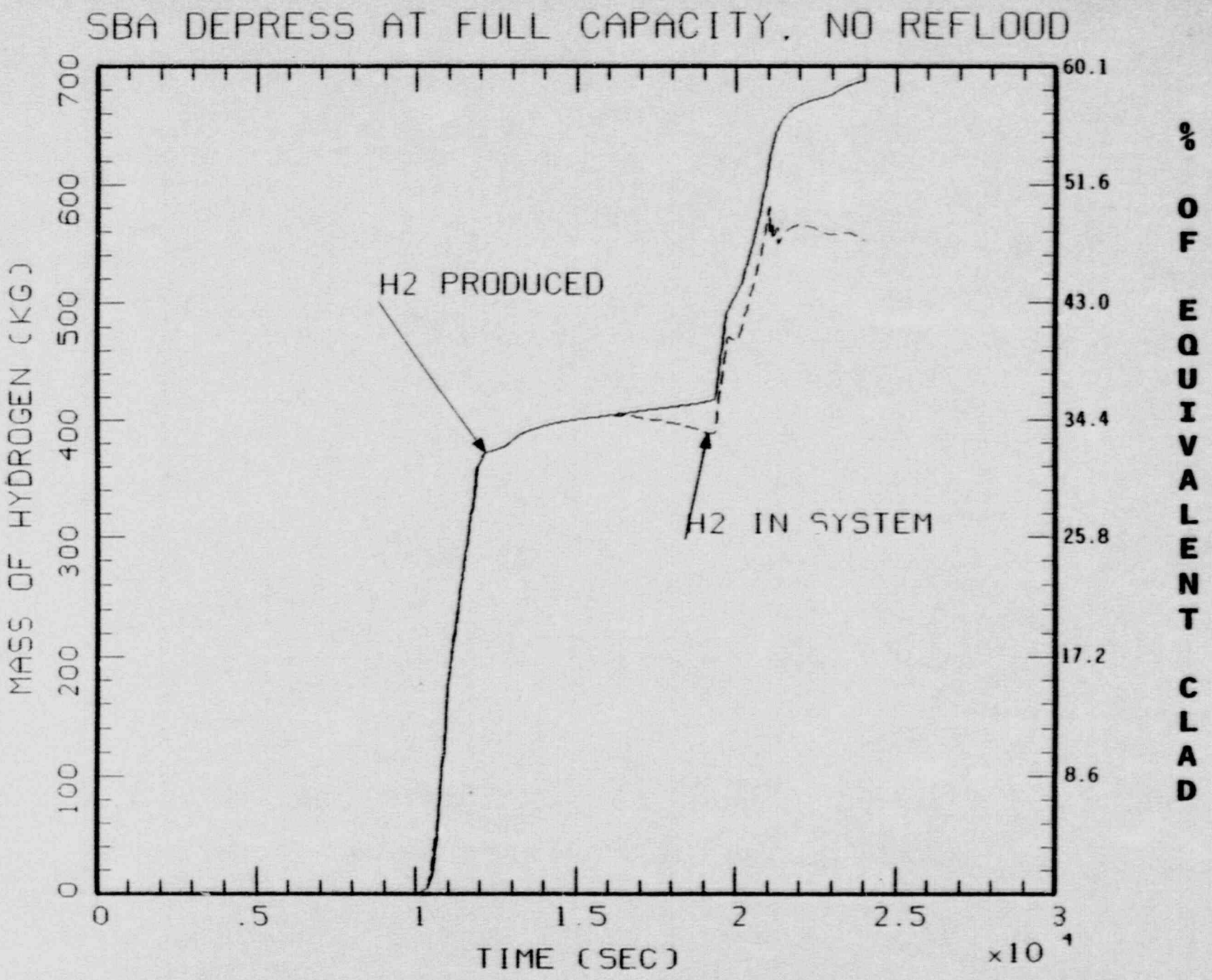

Figure B-12 Hydrogen history for case 7.

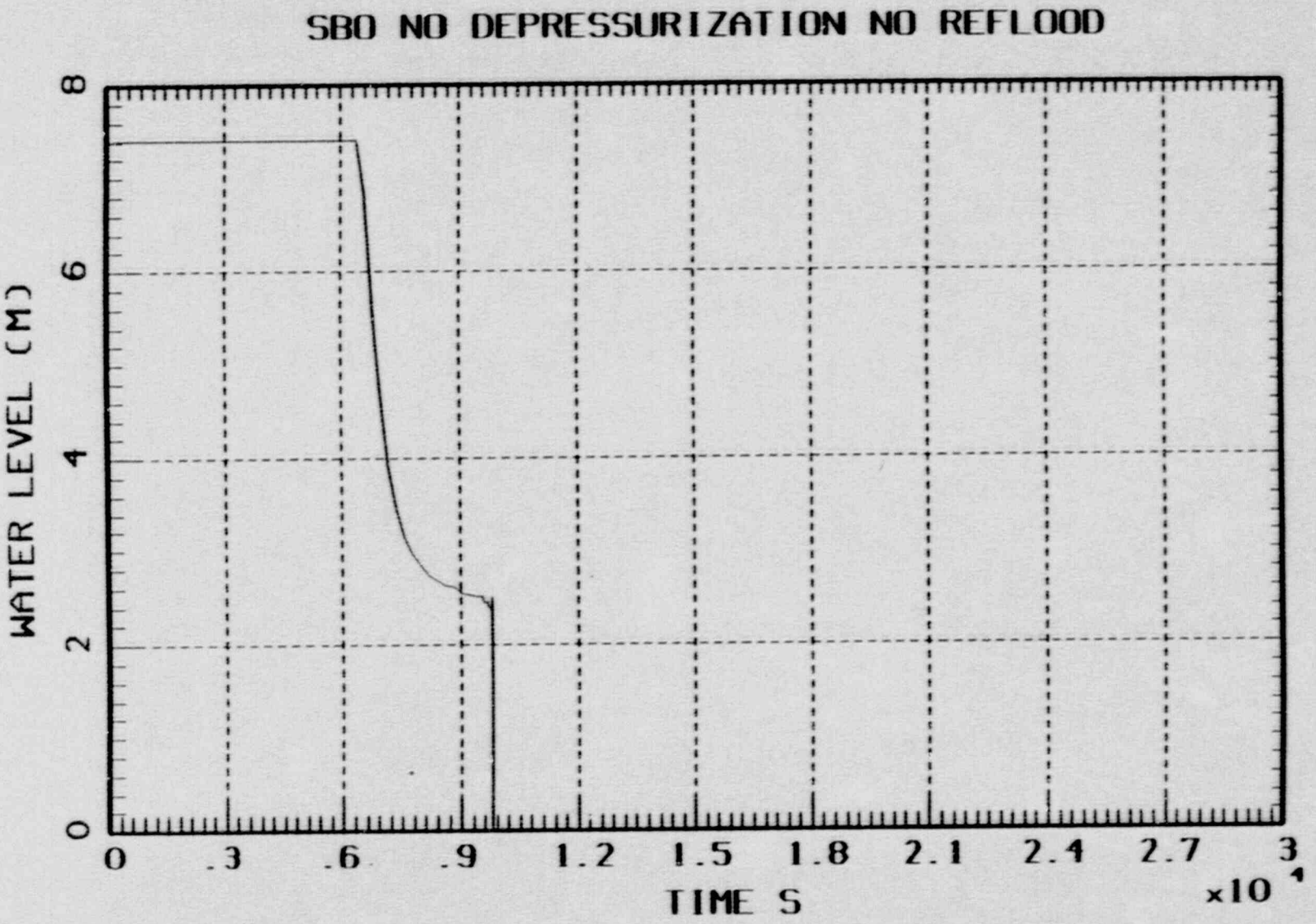

Figure B-13 Water level in reactor vessel for case 12.

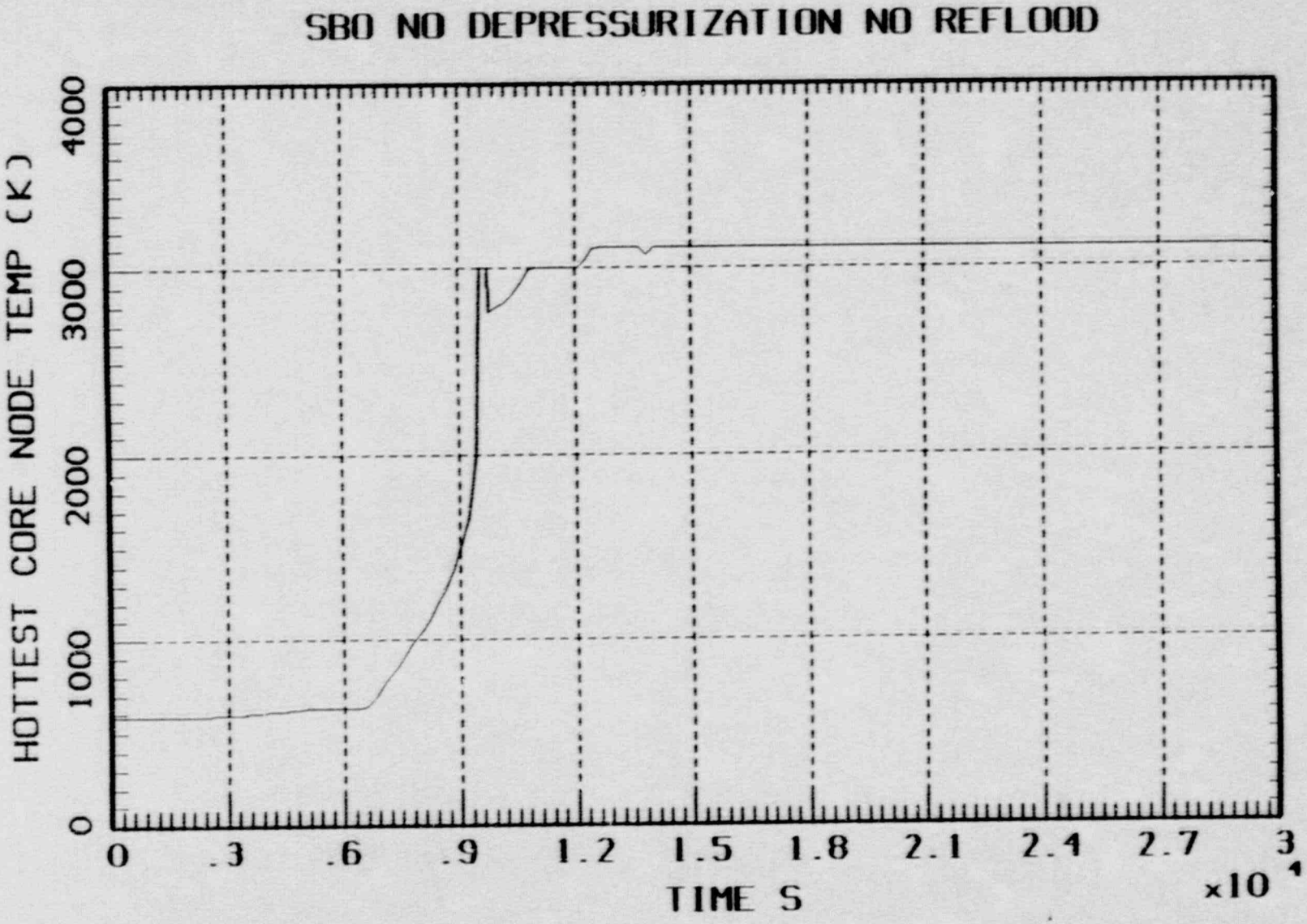

Figure B-14 Hottest core node temperature for case 12.

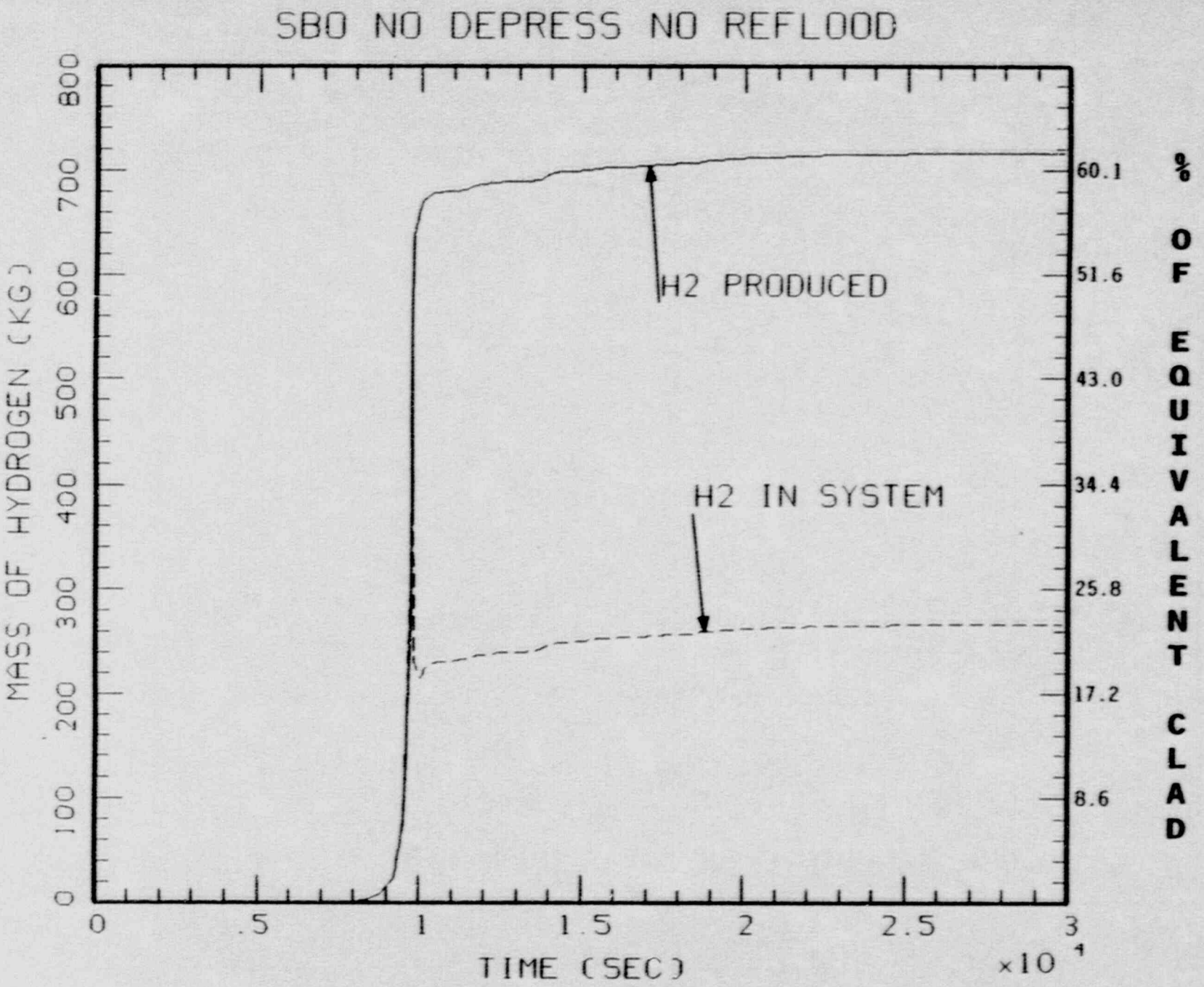

Figure B-15 Hydrogen history for case 12.

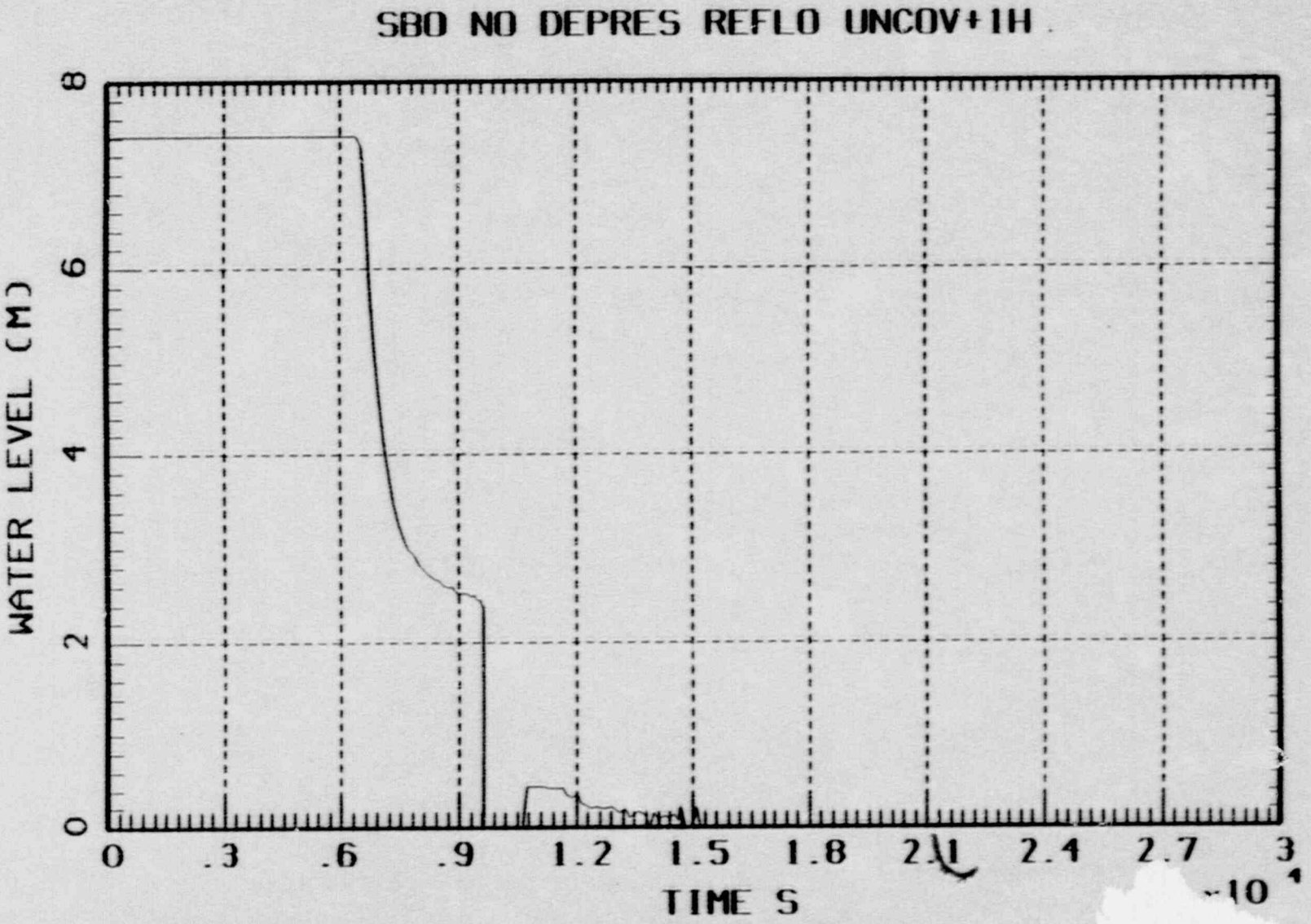

Figure B-16 Water level in reactor vessel for case 14.

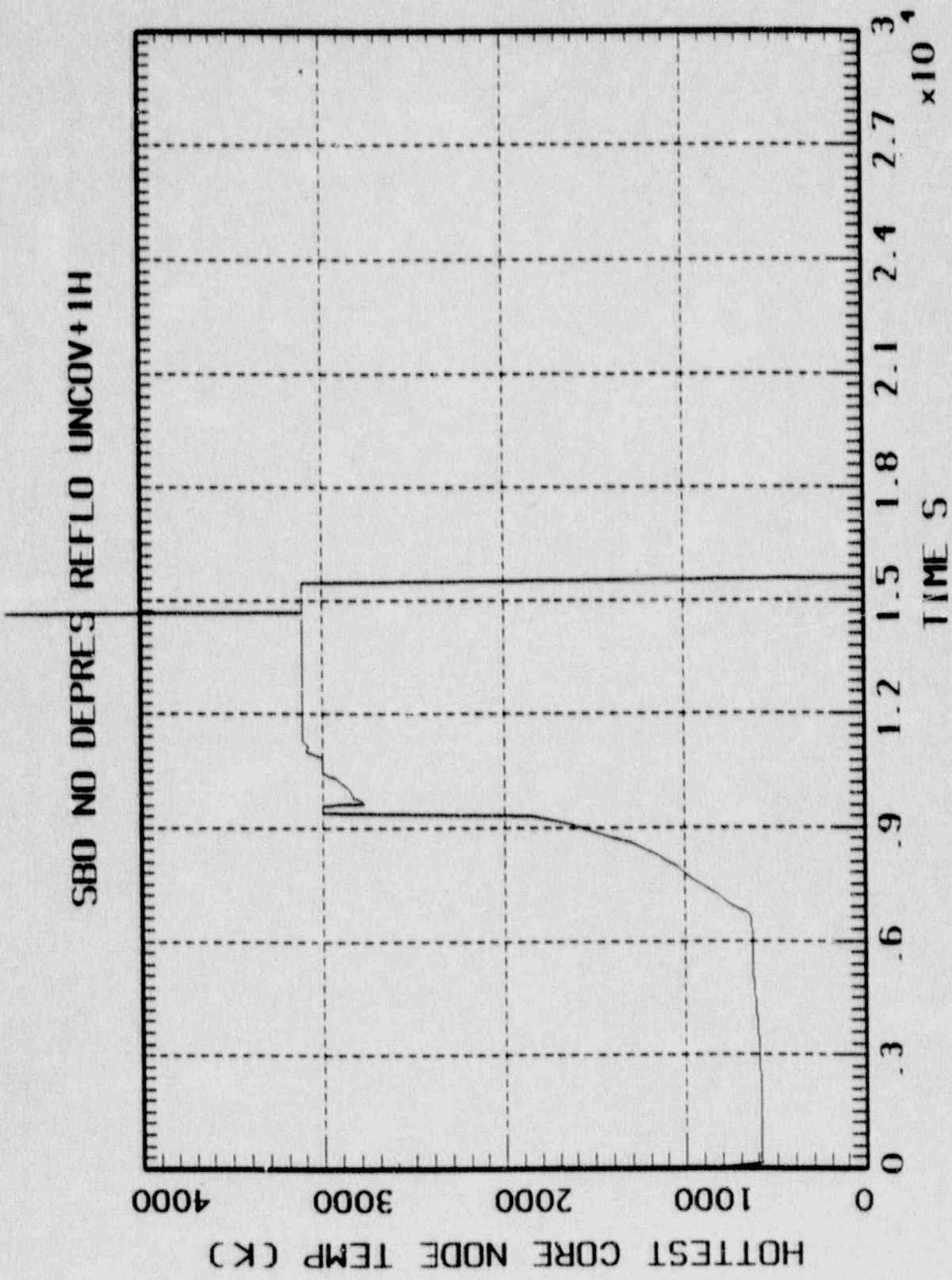

Figure B-17 Hottest core node temperature for case 14.

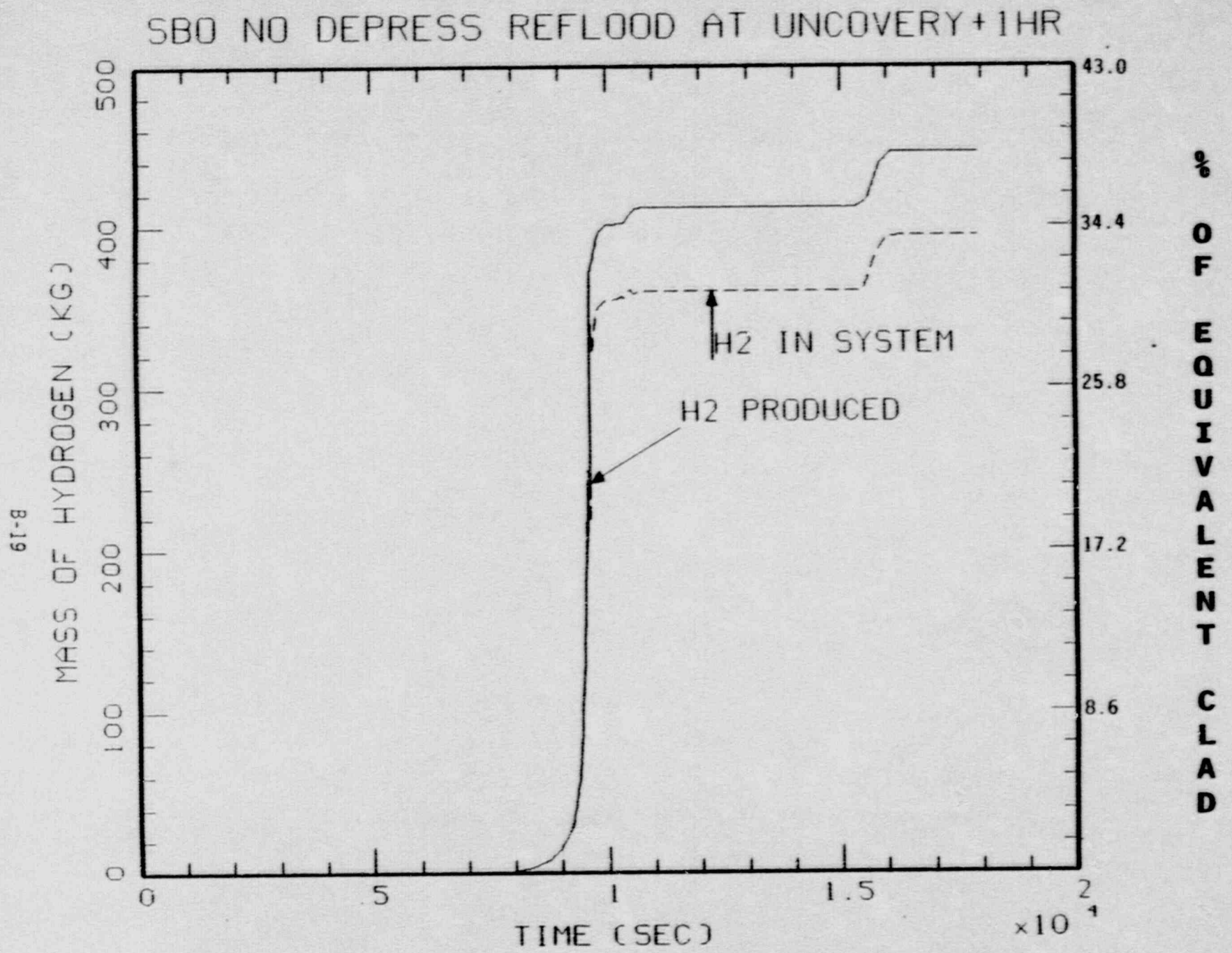

Figure B-18 Hydrogen history for case 14.

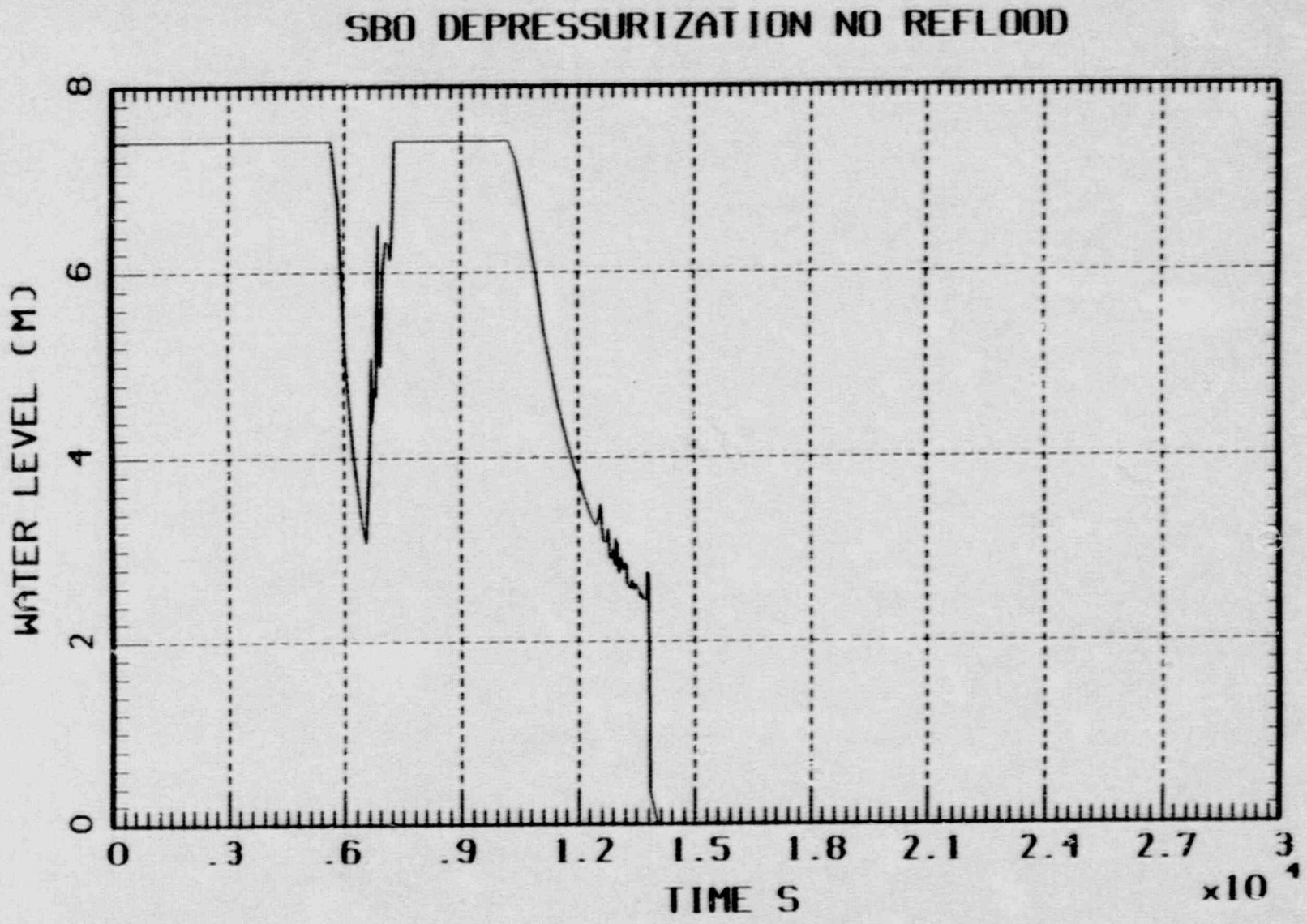

Figure B-19 Water level in reactor vessel for case 15.

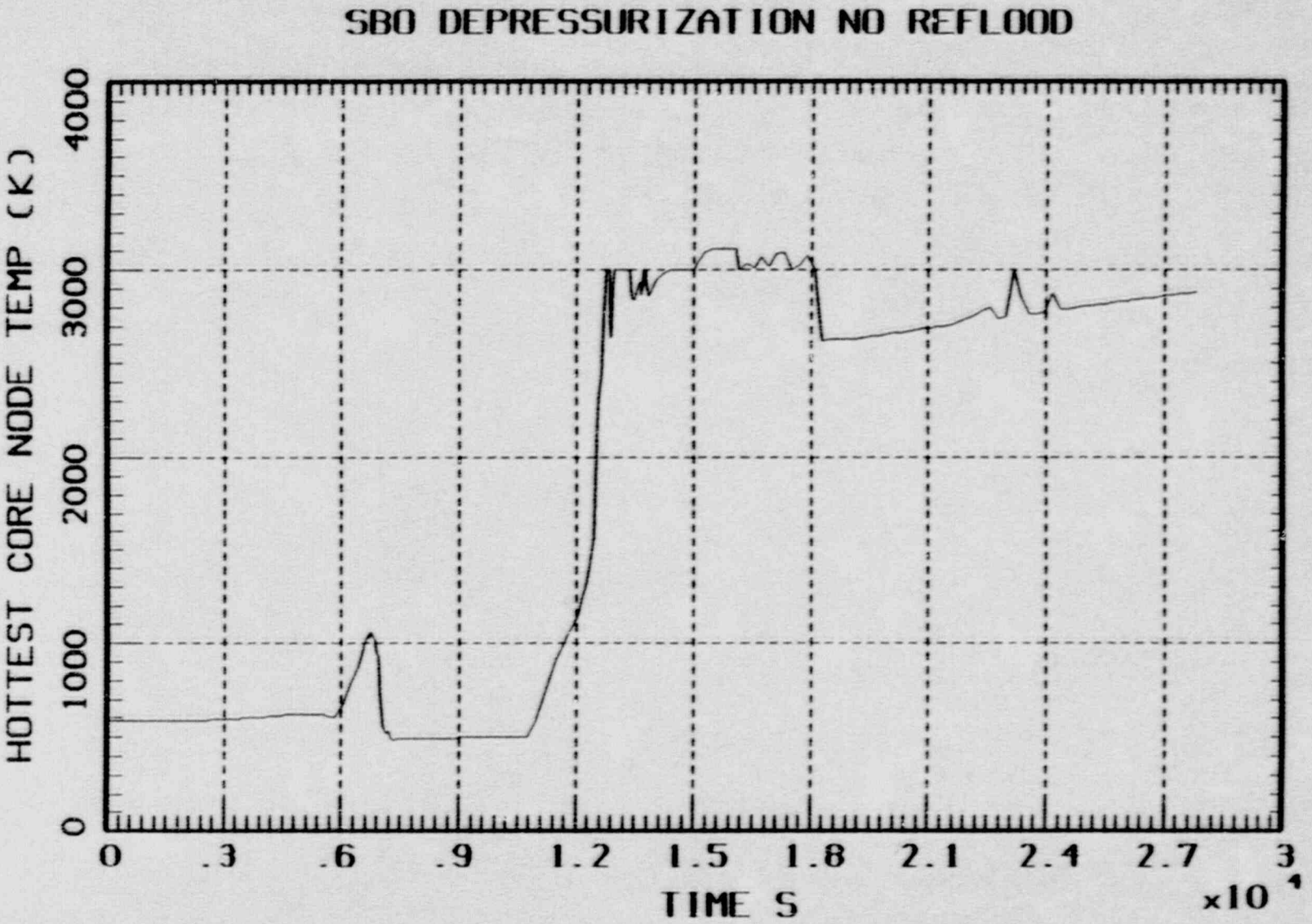

Figure B-20 Hottest core node temperature for case 15.

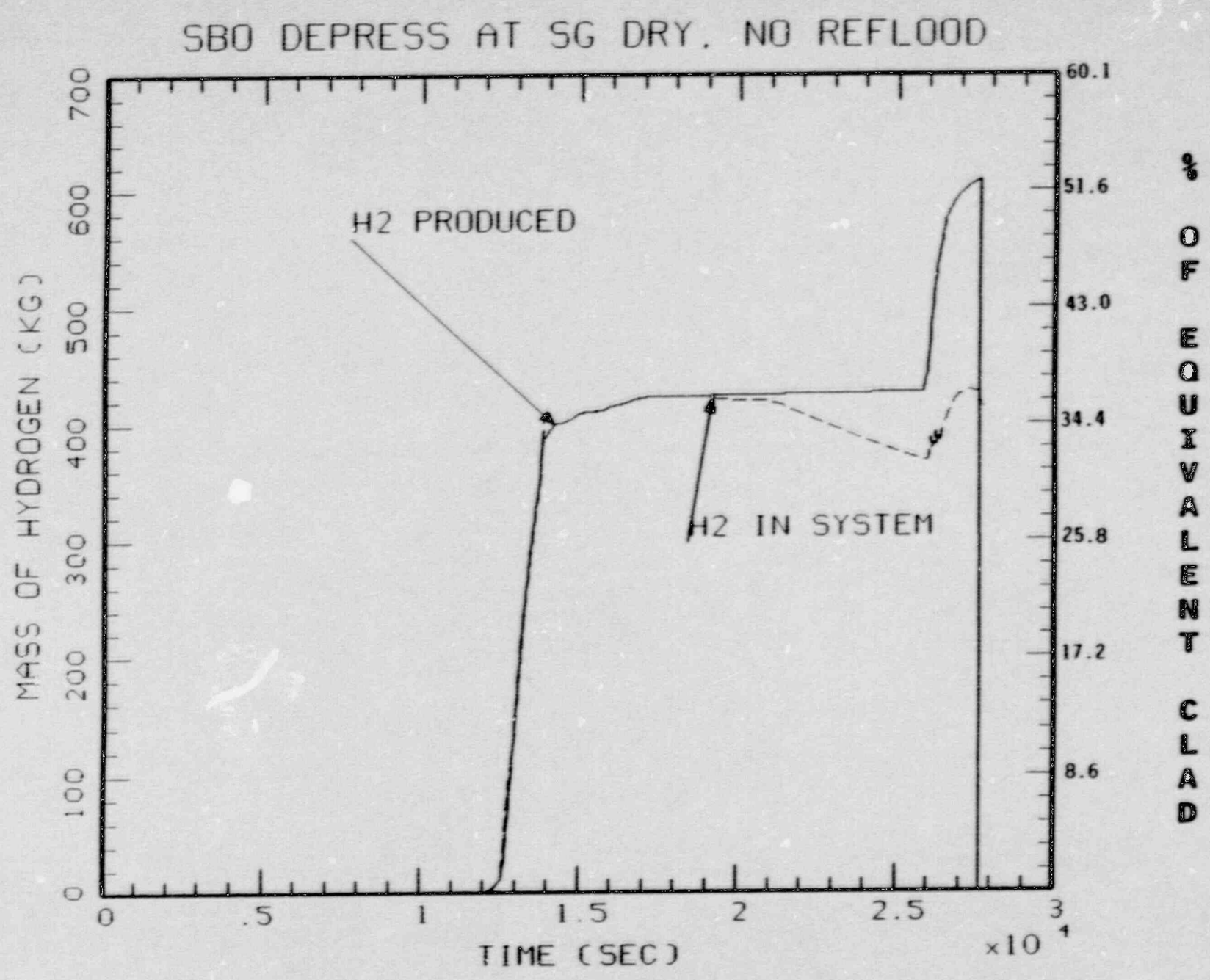

Figure B-21 Hydrogen history for case 15.

APPENDIX C

DEPRESSURIZATION CAPACITY SENSITIVITY STUDY

A sensitivity study was performed to quantify the impact of depressurization capacity on in-vessel hydrogen generation. The results presented in Sections 2.1.4.3 and 3.1 of the main report were all generated by using the full capacity of the depressurization system. This is judged to be the most appropriate value as during feed-and-bleed applications the valves will first be opened at full capacity and then throttled so their normal opening position will be full capacity. During severe accidents when the operator is directed to depressurize the primary system, the procedures will indicate the use of full capacity. Hence, a full capacity depressurization represents the appropriate value to use in the reported best estimate analyses.

In order to gain further insight into the impact of depressurization rates on in-vessel hydrogen generation the following sensitivity study was performed. Depressurization rate directly impacts the timing and ability of both passive (accumulators) and active (ECCS injection) systems to supply water to the core during an accident. Several sequences and a range of depressurization capacities were selected to quantify the performance of the active and passive systems. Table C-1 presents the cases included in this sensitivity study. The only difference between the definitions of these cases and cases 5,6, and 14 (see Section 2.1.4.3) is the depressurization capacity. The balance of the assumptions and sequence descriptions are applicable to the cases presented in this appendix.

The results for case 1 (SBO) are presented in Table C-2. The no depressurization case is an SBO sequence that represents sequences often included in PRAs. The primary system loses inventory through the safety relief valves but remains at a high pressure. The inventory loss leads to core uncovery and heat-up. The heat-up leads to hydrogen generation, core melt, and vessel failure, all at pressures near the safety valve set point. The accumulators do not discharge due to the high vessel pressure. The vessel fails before safety injection is recovered at about 12,000 seconds for

Table C-1. Summary of Cases Included in MAAP-DOE ALWR Depressurization Capacity Sensitivity Study[1]

	Sequence Type	Recovery of Core Injection	
		Yes[3]	No
1.	SBO	X	
2.	Small LOCA[2]		X
3.	Small LOCA[2]	X	

Notes: [1] Six depressurization capabilities were considered for each case in this table. The depressurization capacities (in % of full capacity) used were 0%, 20%, 40%, 60%, 80%, and 100%

[2] Includes loss of all injection

[3] Recovery at approximately one hour after core uncovery

Table C-2. Depressurization Capacity Sensitivity Study: SBO With Recovery

Depressurization Capacity (% of full flow)	Time (sec) Core Uncovery	Time (sec) Vessel Failure	In-Vessel Hydrogen Production (% MWR)
0	6688	9638	20.8
20	6663	9371	30.5
40	6473	8485	26.6
60	6211	23997	73.5
80	6050	None[1]	1
100	5892	None	0

Note: [1]None means no vessel failure.

this case. Similar behavior is exhibited for the 20% and 40% depressurization capacity cases in terms of the amount of hydrogen produced. The details of the sequence progression vary slightly due to the depressurization causing a water inventory loss which changes the core heat-up rate. The heat-up rate and water level dry out rate variations cause the core melt progression to vary. In the 20% case the debris is delivered to the lower vessel at a rate such that it is quenched for a longer period in the lower head. This provides more time for hydrogen generation before vessel failure. In the 40% case the debris is delivered to the lower vessel at a rate that causes earlier vessel failure and, therefore, less in-vessel hydrogen production. The 60% depressurization capacity case produces much more hydrogen. The depressurization rate is high enough to reduce the vessel pressure and allow the accumulators to discharge. The accumulator discharge directs water to the hot core which turns to steam and causes the pressure in the vessel to increase. The pressure increase is large enough to prevent the continued accumulator discharge. This behavior causes a prolonged and intermittent accumulator discharge which provides a long period of core oxidation, larger hydrogen production, and a later vessel failure time. When the depressurization capacity is increased to 80% and 100%, the hydrogen production is very small or totally prevented. For these sequences the primary system pressure is reduced at a faster rate and the accumulators discharge sooner than in the previous runs. The steaming rate is within the relief capacity of the depressurization system for the 80% and 100% runs such that the primary system pressure does not increase and cause the accumulator flow to stop. The core is cooled by the accumulator water. Less or no core damage results and so very little or no hydrogen is produced. The accumulator water keeps the core and vessel pressure low enough such that when the safety injection is recovered it can deliver cooling water to the core. Thus, vessel failure is also prevented for the 80% and 100% depressurization capacity sequences.

The results for case 2 (small LOCA without recovery) are presented in Table C-3. The dependence of hydrogen generation on depressurization capacity is similar to that discussed above for the SBO case. In this case the break provides an additional mechanism for the vessel depressurization so the peak hydrogen generation is predicted at about 40% depressurization

Table C-3. Depressurization Capacity Sensitivity Study: Small LOCA without Recovery

Depressurization Capacity (% of full flow)	Time (sec) Core Uncovery	Time (sec) Vessel Failure	In-Vessel Hydrogen Production (% MWR)
0	4768	7378	32.7
20	4482	18000	60.6
40	4493	20105	73.5
60	4356	12914	38.0
80	4260	13190	45.7
100	4243	11835	29.2

capacity. The same physical phenomena as discussed above explain the results for this case. The variation in hydrogen generation for the 60%, 80%, and 100% depressurization capacity results is due to the details of the core melt progression and the delivery rate and quenching of debris in the lower vessel.

The results for case 3 (small LOCA with recovery) are presented in Table C-4. Again, a similar dependence of hydrogen generation on depressurization capacity is predicted as the same physical phenomena are involved. Case 3 demonstrates the impact of the recovery of safety injection. The safety injection system provides water which quenches the core, reduces hydrogen production, and usually prevents vessel failure. The 20% depressurization case is the one exception regarding the prevention of vessel failure. The increased depressurization rate resulted in a higher rate of loss of water inventory, faster core heat-up, more severe core damage and relocation, and more hydrogen production. The accident had progressed to vessel failure by the time that safety injection was recovered for this sequence. For higher depressurization rates (> 20%) the accumulator discharge is sooner in the accident sequence and limits or prevents core damage until safety injection is recovered.

The results of this sensitivity study demonstrate the dependence of in-vessel hydrogen production on depressurization capacity. The results show that the reactor system response is sequence dependent. The depressurization capacity impacts the rate of delivery of the passive and active emergency cooling water supplies. If the delivery rate is limited for extended periods of time, core damage and hydrogen generation are increased. These results show that hydrogen generation can be increased to the point that the LDB hydrogen limit of 75% MWR is met with no margin. However, vessel failure occurs in all these cases with no margin which means that they would be treated in REB assessments which would be able to accommodate such hydrogen generation. The majority of the runs (16 of 18) with or without vessel failure demonstrate significant margin for the LDB 75% MWR requirement. As stated in Section 3.1, optimizing operation can involve the

Table C-4. Depressurization Capacity Sensitivity Study: Small LOCA with Recovery

Depressurization Capacity (%* of full flow)	Time (sec) Core Uncovery	Time (sec) Vessel Failure	In-Vessel Hydrogen Production (% MWR)
0	4767	None[1]	32.9
20	4469	7353	54.3
40	4478	None	37.6
60	4358	None	0
80	4296	None	0
100	4246	None	0

Note: [1]No vessel failure.

interface between emergency operation procedures and severe accident management actions. The results of this sensitivity study demonstrate that significant and sufficient flexibility in reactor system response exits such that the suggested optimization can be successfully performed.